

**LIGAND BASED AND STRUCTURE BASED STUDIES OF HDAC6  
INHIBITORS**

Submitted by

**CHAYANTA SEN**

EXAMINATION ROLL NO. M4PHC23020

REGISTRATION NO.160248 of 2021-22

UNDER THE GUIDANCE OF

**DR. NILANJAN ADHIKARI**

Assistant Professor

Natural Science Laboratory, Division of Medicinal and Pharmaceutical Chemistry

DEPARTMENT OF PHARMACEUTICAL TECHNOLOGY

Faculty of Engineering and Technology

**JADAVPUR UNIVERSITY**

Thesis submission in partial fulfilment of the requirements for the

**DEGREE OF MASTER OF PHARMACY**

Department of Pharmaceutical Technology

Faculty of Engineering and Technology

**JADAVPUR UNIVERSITY**

Kolkata- 700032

Session: 2021-2023

Declaration of the Originality and Compliance of Academic Ethics

I, Chayanta Sen, a student of M.Pharm, 2nd year, bearing Roll No: 002111402016,

Registration no. 160248 of 2021-22 studying in the Department of Pharmaceutical Technology, Jadavpur University, Kolkata-32, hereby declare that my thesis work titled – “Ligand Based and Structure Based Studies of HDAC6 Inhibitors”, is original and presented following academic rules and ethical conduct and no part of this project work has been submitted for any other degree of mine.

I hereby declare that any mistakes present in the thesis report is solely my own responsibility. All the information and works are true to the best of my sense and knowledge.

Name: Chayanta Sen

Class Roll No.: 002111402016

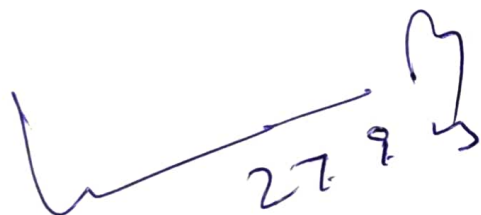
Registration No.: 160248 of 2021-22

Signature with date:

Chayanta Sen  
27.09.2023

## Certificate of Approval

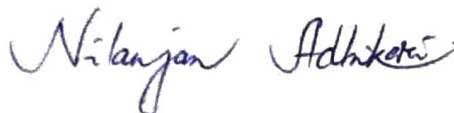
This is to certify that the thesis entitled "Ligand Based and Structure Based Studies of HDAC6 Inhibitors" submitted to Jadavpur University, Kolkata for the partial fulfilment of Master Degree in Pharmacy, is a faithful record of bonafide and original research work carried out by Mr. Chayanta Sen bearing Class Roll No. 002111402016 and Registration No.160248 of 2021-22 of under my supervision and guidance.



Head of the Department

Department of Pharmaceutical  
Technology  
Jadavpur University  
Kolkata - 700032

HEAD  
DEPT. OF PHARMACEUTICAL TECHNOLOGY  
JADAVPUR UNIVERSITY, KOLKATA, INDIA



Supervisor

Assistant Professor

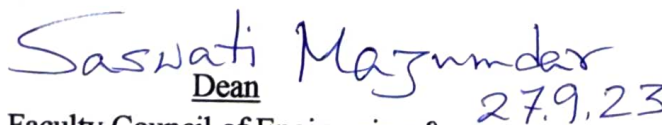
Dept. of Pharmaceutical Technology

Dr. Nilanjan Adhikari

Jadavpur University

Natural Science Laboratory, W.B. India

Department of Pharmaceutical  
Technology  
Jadavpur University  
Kolkata - 700032



Dean

Faculty Council of Engineering &  
Technology (FET)  
Jadavpur University  
Kolkata - 700032



**DEAN**  
Faculty of Engineering & Technology  
JADAVPUR UNIVERSITY  
KOLKATA-700 032

### Acknowledgement

The outcome of this thesis required a lot of guidance and assistance from many people. I am extremely fortunate to have these all along the completion of my work. Whatever I have done is only due to such guidance and assistance and I would not forget to thank them.

I am highly obliged and would like to express my deepest gratitude and profoundness to my mentor Dr. Nilanjan Adhikari of The Department of Pharmaceutical Technology, Jadavpur University, Kolkata for his excellent and constant guidance and help, endless encouragement, thoughtful and freedom, and stupendous cooperation throughout the term paper till its successful completion. I am grateful to his motivation, fruitful suggestions, and inspiration.

I owe my deepest respect to Prof. Tarun Jha, Prof. Sanmoy Karmakar; former Head of the Department and Prof. Amalesh Shamanta; Head of the Department, Prof. Kunal Roy; HOD-in-Charge, Department of Pharmaceutical Technology, Jadavpur University, Kolkata for all the necessary help and encouragement. I would like to convey my sincere gratitude to AICTE and Jadavpur University for their financial and equipment support for my M. Pharm course.

I want to express my thanks to Mr. Sandip Kr. Baidya, and Mr. Suvankar Banerjee, my laboratory colleagues Mr. Rahul Jana, Mr. Jigme Sangay Dorjay Tamang, Mr. Vishal saha, and my juniors Mr. Sandeep Jana and Mr. Tuhin Baran Samoi of the Natural Science Laboratory Department of Pharmaceutical Technology, Jadavpur University, Kolkata-700032

Finally, I would like to express my deep respect to my father Mr. Shyamapada Sen, my mother Mrs. Jayashree Sen, my sister Ms Riya Sen and my friends and relatives for their continuous help, love, encouragement, and moral support throughout my work.

Chayanta Sen

[CHAYANTA SEN]

Date: 27.09.2023

Place: Department of Pharmacy, Jadavpur University, Kolkata.

<b><u>Contents</u></b>	<b><u>Page</u></b>
<b>Chapter 1: Introduction</b>	<b>6-8</b>
<b>Chapter 2: Structure and Pathophysiology of HDAC6</b>	<b>9-38</b>
<b>Chapter 3: Literature Review</b>	<b>39-50</b>
<b>Chapter 4: Rationale Behind Studies</b>	<b>51-52</b>
<b>Chapter 5: Materials &amp; Methods</b>	<b>53-63</b>
<b>Chapter 6: Result and Discussion</b>	<b>64-79</b>
<b>Chapter 7: Conclusion &amp; Future Aspects</b>	<b>80-82</b>
<b>References</b>	<b>83-103</b>

## **Chapter 1: Introduction**

### **1.1 Metalloenzymes:**

A group of enzyme proteins with metal ions as cofactors in the active site are called as metalloenzymes [1]. They are associated with hydrolysis, oxidation/reduction reactions. Metalloenzymes are important for different aspects of physiology, like transcriptional processes, catabolic processes and mitochondrial functions. One-third of all the known enzymes are metalloproteins. Some of the examples are-Superoxide dismutase, carbonic anhydrase, nitrogenase, matrix metalloproteins (MMP), histone deacetylases (HDACs) etc [2].

### **1.2 What is HDAC**

Histone deacetylase (HDACs) are a family of metalloenzymes responsible for alternation status of substrate proteins from side chain lysine (K) residues and thus regulating gene expression. HDACs have opposing effects to histone acetyltransferases (HATs), on the acetylation status of the substrates [3][6]. HDAC enzymes have become a leading drug target in anti-cancer drug and neurodegenerative drug therapy [6][7]

### **1.3 Classification of HDAC Family**

HDAC6 is a member of the zinc dependent HDAC isozymes. Four classes of HDAC are found in humans: class I, class IIa, class IIb, class III, and class IV [5]. HDAC6 belongs to class IIb and deacetylates a range of non-histone proteins including heat shock protein (Hsp90),  $\alpha$ -tubulin, cortactin among many others. Class I, II and IV HDAC isoforms are zinc-dependent as  $Zn^{+2}$  metal ion acts as cofactor. HDAC6 protein contains few major region in its structure in between the N-terminal and C-terminal- these are Nuclear localised signal (NLS), Nuclear export signal (NES1), catalytic domain 1, dynein motor binding region (DMB), catalytic domain2, cytoplasmic retention signal also called SE14, NES2 and the ZnF-UBP domain. The most unique feature of HDAC6 is the presence of two catalytic domains, experimentally the second catalytic domain has proven to be more important for the activity. Due to its structural and functional virtue, HDAC6 is involved in several cellular activities and response systems [5]. Sirtuins or class III are exceptional in their requirement for  $NAD^+$  and not  $Zn^{2+}$  ion. [6] [7].

## **1.4 Epigenetics**

Epigenetics is the process of specific structural modification of histone proteins and although DNA sequence is not altered, gene expressions are influenced [8]. HDAC enzymes influence the acetylation status of several transcription factors and histone proteins and influence their ability to bind to DNA and regulation of gene expression. [4]

Histone modification: Histone modification occurs in two different mechanisms, one involving the nucleosome-nucleosome interaction through covalent bonds. Lysine is positively charged at physiological pH and it attracts to the negatively charged DNA such attraction guides the winding of DNA around histone and a condensed chromatin structure is formed. Acetylation of histones by acetyltransferases removes the positive charge of lysine and as a result, DNA unwinds from histone [8]. HDAC proteins deacetylate histones to influence its acetylation status indirectly [8].

DNA Methylation: Methylation of histone does not change the charged state of lysine or arginine residues so the chromatin structure is not affected directly. DNA methylation is one of the most researched topics in epigenetic alteration. It entails the addition of a methyl group to the DNA's cytosine residues, which frequently takes place in CpG dinucleotides. DNAmethyltransferases (DNMTs) catalyse this alteration. By blocking transcription factors from binding, promoter hypermethylation typically results in the silencing of genes, whereas promoter hypomethylation can increase gene expression [8][9].



## **Chapter 2: Structure and Pathophysiology of HDAC**

## **2.1 HDAC6 Crystal Structure-**

The only significant differences between the active sites of human and zebrafish HDAC6 CD2 are N645M and N530D, respectively. Five domains make up the HDAC6 enzyme sequence: the N-terminal end (amino acid 1–87), CD1 (amino acid:88–447), CD2 (amino acid: 482–800), SE14 (amino acid:884–1022), cytoplasmic retention signal, and zinc finger ubiquitin binding domain (amino acid: 1131–1192). The nuclear-localised signal (NLS; amino acid: 14–59), which is rich in arginine and lysine sequences, and the nuclear export signal (NES1; amino acid:67–76), which is rich in leucine, make up the N-terminal domain, which together controls the nuclear and cytoplasmic shift of HDAC6. Between CD1 and CD2, there is a dynein motor binding area. The similarities between yeast HDAC1 and HDAC6 are limited to the catalytic domains and not the N-terminal residues. It has 1215 amino acid residues, the most of any HDAC isoform. Notably, HDAC6 is the only HDAC in the family to have two extremely conserved catalytic domains, making it structurally distinct. The distinctive ZnF-UBP domain at the C-terminus end participates in ubiquitination, a modification that facilitates aggresome-mediated protein breakdown and clearance [10].

The catalytic domains of HDAC6 were studied in detail by Miyake et al, they found that CD2 may have a more important role than CD1 due to more evolutionary conservation of the active site and its surrounding substrate recognition region. Substrate recognition in CD2 was credited to the flexibility of Trp459 and Asp460, and in the case of CD1, it was Trp78 and Asp79 present in the H1-H2 and H20-H21 loops. H6 and H25  $\alpha$ -helices are crucial for substrate specificity. As replacement of H25 of CD2 by loop H6-H7 of HDAC8 reduced the activity on  $\alpha$ -tubulin but in the case of substitution of CD1 H6 had no impairing effect on  $\alpha$ -tubulin. Inactivating CD2 had a detrimental effect on tubulin deacetylation the same was not observed by inactivating CD1. It was also found that isolated CD2 retained the deacetylation activity in contrast to CD1 which did not have activity, however, the presence of CD1 increased the activity of the CD2 by almost tenfold [11].

## **2.2 Role of HDAC6 in cancer-**

It is well established that HDAC6 has a significant impact on several signalling pathways connected to cancer. In several malignancies, HDAC6 expression is increased or downregulated [23].

### **2.2.1 What is cancer:**

Cancer is a pathological condition in which a few of the body's cells start to grow without any control and spread to other parts of the body. In the millions of cells that make up the human body, cancer can develop in most parts. Human cells divide (via a process known as cell growth and multiplication) to create new cells as per the body's requirement. Older cells are replaced by newly divided cells when they die due to damage stress or ageing. Occasionally, control of the cell cycle fails, causing damaged or aberrant cells to proliferate bypassing all the defensive mechanisms of the body. Tumours, which are an accumulation of tissue masses, develop from these cells. Cancerous or non-cancerous (benign) tumours both can form. Cancerous tumours can metastasize, which is the process by which they migrate to other parts of the body to produce new tumours, and they can also infect surrounding tissues. The term "malignant tumour" can also refer to cancerous growth. While many malignancies become solid tumours, blood-related cancers like leukaemia typically do not. The tissues around a benign tumour are not invaded or disseminated to. While dangerous tumours may come back after removal, benign tumours typically don't. However, sometimes benign tumours can grow to be extremely enormous. Some, like benign brain tumours, might have life-threatening side effects or serious symptoms [3].

### **2.2.2 Cancer Pathology**

The primary factor in cancer mortality is metastasis. The metastatic cascade is a multi-step process that comprises local tumour cell invasion, entrance into the vascular followed by carcinoma cells leaving the bloodstream, and colonisation at remote sites. Early on in the process of successfully disseminating cancer cells, the primary malignancy adapts to the secondary site of tumour colonisation including tumour-stroma crosstalk [4]. Cancer cells' flexibility and migration, as well as the environment's stromal and endothelial cells, are essential. The processes of cell mobility, of which three main types have been described, are therefore crucial for targeted action. Together, in a mesenchymal or an amoeboid manner, or individually, tumour cells can migrate. The ultimate escape mechanism of cancer cells was an amoeboid cell phenotype, which was caused by interfering with collective or mesenchymal cell invasion by targeting integrin expression or metalloproteinase activity, respectively [3]. There are few *in vivo* molecular details that demonstrate how the amoeboid behaviour might be effectively reversed or suppressed [4]. As these many types of movement can coexist and collaborate, future notions of metastasis intervention must concurrently address the

mesenchymal, and amoeboid mechanisms of cell invasion. Beyond focusing on cell mobility, anti-metastatic therapy must pay close attention to how cancer cells adhere to the stroma in heterotypic circulating tumour cell emboli [3].

Local Invasion: Local cancer cell invasion into neighbouring tissues marks the start of the metastatic phase. The extracellular matrix and basement membrane can become permeable to cancer cells, enabling them to infect surrounding tissues [2].

Intravasation: Cancer cells can penetrate lymphatic or blood arteries if they have already infiltrated adjacent tissues (intravasation). At the initial tumour site, intravasation generally happens [2].

Circulation survival: Cancer cells that enter the bloodstream or lymphatic system are transported to far-flung areas of the body as a result of circulation and survival. Because of obstacles including immune surveillance and circulatory shear forces, the majority of cancer cells do not survive this voyage [2].

Extravasation: Some cancer cells escape the bloodstream by clinging to the endothelial cells lining blood arteries or lymphatic vessels and then extravasate and penetrate the surrounding tissue [2].

Micrometastases Formation: Micrometastases are tiny cell clusters that can develop if cancer cells extravasate into a distant region. These clusters could either become macroscopic tumours or lay latent for a while [2].

Angiogenesis at Secondary Sites: Angiogenesis is induced, ensuring a blood supply for the growing metastatic lesion, to support the growth of metastatic tumours at secondary sites [3].

Metastatic Colonisation: Metastatic colonisation is the process by which cancer cells create a microenvironment that promotes tumour growth at secondary sites. The extracellular matrix, immunological cells, and stromal cells are all involved in this [2].

Microenvironmental adaptations: The underlying tumour's molecular properties are frequently distinct from those of metastatic cancer cells, which can adapt to the new milieu. They may be more or less responsive to treatments depending on this adaption.

Immune Evasion: Metastatic tumours can elude the immune system through a variety of ways, such as downregulating immunological checkpoints or secreting immunosuppressive chemicals.

Secondary Tumour Growth: At the secondary site, metastatic lesions are still developing and growing. Depending on the type of disease and individual circumstances, the location and growth rate of metastatic tumours might differ significantly[2][3].

### **2.2.3 Colorectal Cancer (CRC):**

Colorectal cancer (CRC) is the second leading cause of death in cancer-associated mortality. Ricolinostat or ACY-1215 combined with other anticancer agents oxaliplatin and irinotecan exhibited synergism and increased apoptosis, inhibition of AKT and ERK by phosphorylation and by upregulating PDL-1 in the HCT116 and HT29 cells. Apoptosis was induced by upregulating the proapoptotic factors like Bak and decreasing the expressions of the anti-apoptotic molecule Bcl-xL. The results were better in this combined therapy compared to the results previously accomplished by treatment with any individual anti-cancer agent used in this experiment [19].

### **2.2.4 Hepatocellular Carcinoma (HCC):**

Hepatocellular carcinoma (HCC) is the fifth largest cause of cancer in the world. HDAC6 knockdown suppressed cell apoptosis in HCC by improving cell proliferation rate. It also upregulated the level of HIF-1 $\alpha$  and VEGFA factors. HDAC6 promotes angiogenesis in liver cancer cell lines and plays a crucial role in its survival under hypoxia[20]. HDAC6 promotes hepatocellular carcinoma progression by inhibiting P53 transcriptional activity. In Hepatocellular Carcinoma (HCC) HDAC6 regulates the expression of p53. NF-kB, the central immunological transcription factor increases the expression of HDAC6 in HCC tissues. hDAC6 overexpression inhibits the tumour suppressor protein p53. HDAC6 interferes with the interaction of p300 and p53, p300 acetylates p53 and stabilises it. HDAC6 retards the interaction of p53 and coactivator p300 and enhances the interaction of p53 with its negative regulator Mdm2 [21].

### 2.2.5 Breast cancer

HDAC6 regulates estrogen receptor expression, in ER-positive breast cancer the HDAC6 expression is up-regulated by estradiol. In MCF-7 cell line, Selective estrogen modulator tamoxifen (TAM) and anti-estrogen molecule ICI 182,780 (Fluvestrant), structure given in Figure 1. in combination reduced HDAC6 expression and cell motility caused by the deacetylation of  $\alpha$ -tubulin [23].

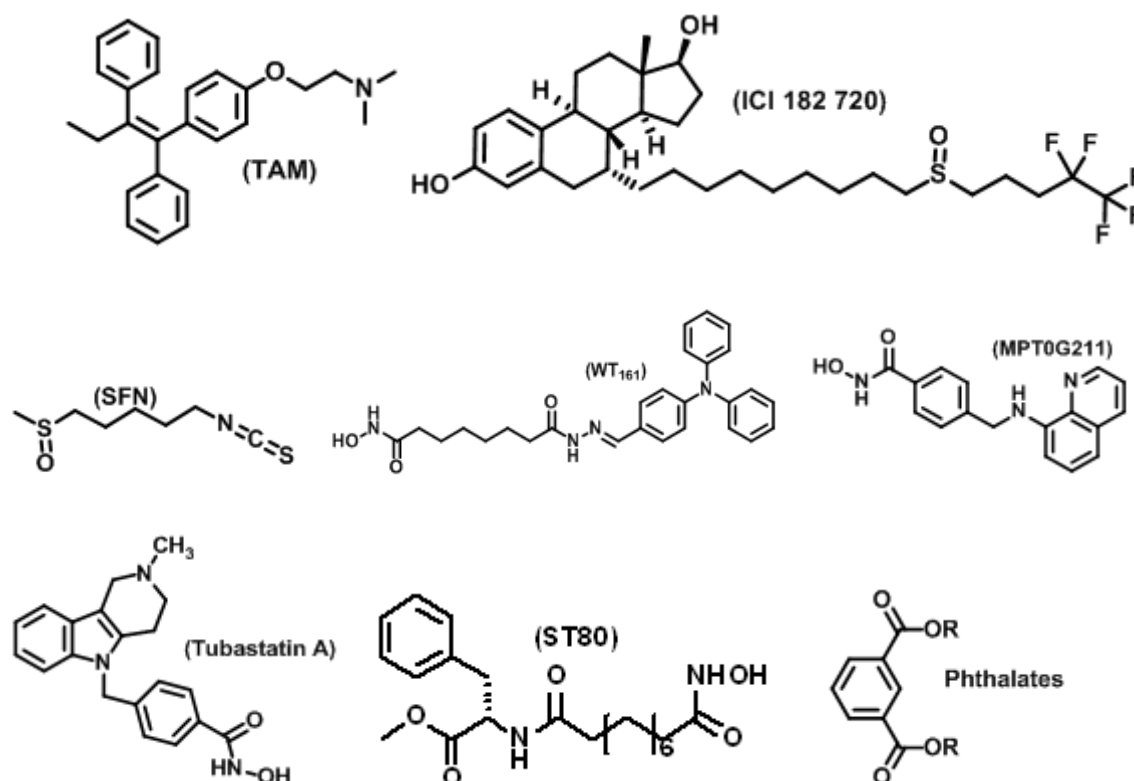


**Figure 1: Structure of Tamoxifen (TAM) and Fluvestrant (ICI 182,720) and Anti-cancer HDAC6 inhibitors**

MST1 was found to be downregulated by HBXIP in breast cancer samples [26]. Mammalian STE20-like kinase 1 (MST1) is a tumoursuppressor and is associated with the Hippo signalling pathway that controls the size of organ and tissue homeostatis [26]. MST1 reduction is associated with breast cancer, prostate cancer, head and neck squamous cell carcinoma, colorectal cancer. MST1 lysine35 residue is responsible for deacetylation by HBXIP, and HDAC6 functions as a deacetylase of MST1 as they colocalised in MCF-7 cells [26]. It was also found that silencing or inhibiting nuclear factor(NF)-kB activates HDAC6

expression transcriptionally in hepatocellular carcinomas. HBXIP activates NF- $\kappa$ B in breast cancer cells and thus indirectly upregulates HDAC6 in breast cancer [26]. HBXIP facilitates cancer cell proliferation and migration by acting as a cofactor for different transcription factors such as transcription factor 4, transcription factor II D, and Sp1. HBXIP downregulated MST1 through its lysine 35 residue by upregulating HDAC6 in breast cancer cell lines [26].

Tumourigenesis is aided by a decrease in or deletion of the tumour-suppressor mammalian STE20-like kinase 1 (MST1) in the Hippo pathway [27]. MST1 is decreased in breast cancer due to the oncoprotein hepatitis B X-interacting protein (HBXIP) [27]. In clinical breast tissue samples, the expression of HBXIP was found to be inversely correlated with that of MST1, according to an immunohistochemical examination of tissue microarrays [27]. In breast cancer cells, it was discovered that HBXIP might post-translationally downregulate MST1. Mechanistically, MST1 may have its lysine 35 residue acetylated in the cells [27]. Surprisingly, the HDAC inhibitor trichostatin A therapy significantly raised the levels of MST1 acetylation and protein in the cells [27]. It's interesting to note that MST1's acetylation could be drastically reduced by the oncoprotein HBXIP. Through deacetylation modification of MST1 in the cells, the HDAC6 might lower the amounts of MST1 in the proteins [27]. Furthermore, data showed that HBXIP activated the transcription factor nuclear factor- $\kappa$ B, upregulating HDAC6 at the mRNA and protein levels [27]. MST1's association with HSC70 in the cells was facilitated by deacetylation, and this connection led to MST1's lysosome-dependent destruction by chaperone-mediated autophagy (CMA) [27]. Functionally, HBXIP-mediated suppression of the tumour suppressor MST1 accelerated the development of breast cancer cells both in vitro and in vivo [27]. Therefore, it was concluded that MST1 is degraded in a CMA manner, which promotes the growth of breast cancer, as a result of the deacetylation of MST1 mediated by HBXIP-enhanced HDAC6 [27].

Sulforaphane (SFN) (Figure 1) is a natural HDAC6 inhibitor and it has antineoplastic activity as it is effective in preventing breast cancer prostate cancer, colon cancer, and skin and urinary bladder cancer [28]. In human triple-negative breast cancer (TNBC) cell lines (MDA-MB-231) a dose of 25  $\mu$ M of SFN induced autophagosome formation, it upregulated protein expression of Beclin1 and LC3-II and expression of p62 decreased [28]. SFN in combination with doxorubicin, the first-line drug of TNBC, significantly decreased the mean tumour weights in nude mice in comparison to mice treated with either SFN or Doxorubicin (DOX)

alone [28]. The SFN and DOX combination shows synergistic effects in a low dose combination, it helps to reduce adverse effects despite SFN being a naturally occurring substance, DOX however has severe side effects and thus is limited in use in advanced breast cancer [28]. The combination therapy thus produces a desirable effect without the danger of severe off-target effects. SFN treatment of TNBC cell lines suppressed HDAC6 expression and increased acetylation of Phosphatase and TENsin homolog on chromosome 10 (PTEN) which subsequently activated PTEN through decreasing phosphorylation of Akt and promoted PTEN translocation [28].

Phthalates or phthalate (Figure 1) esters activate the aryl hydrocarbon receptor (AhR), which is a transcriptional protein of the helix-loop-helix family. AhR is present vastly in ER-negative breast cancer cells MDA-MB-231 [29]. Treatment of such ER-negative breast cancer cell lines with phthalates increased intracellular cAMP levels as a result of AhR inhibition through HDAC6 block, as the outcome remains the same with the treatment of specific AhR siRNA [29]. HDAC6 through nuclear translocation of complex protein facilitates c-Myc expression. Treatment of phthalate promotes the formation of the same protein complex, the B-catenin/LEF1/TCF4 and thus induces both HDAC6 and c-Myc expressions in *in vitro* conditions. The nuclear function of B-catenin increased and contributed to the proliferation of ER-negative breast cancer cell lines [29].

MPT0G211 (Figure 1) is a potent HDAC6 inhibitor, it suppresses the TNBC Cells by HDAC6 inhibition. HDAC6 Inhibition increases acetylation of HSP90 rendering it inactive, which influences aurora-A degradation. Aurora-A upregulates Phosphate Slingshot (SSH1), which mediates actin recognition & polymerization [30]. HDAC6 inhibition contributes to the inhibition of the cortactin- F-actin pathway leading to decreased cell motility. Inflammatory breast cancer (IBC), is the most deadly subtype of breast cancer with a mere survival rate of 5 years. HDAC6 plays a sensitive role in IBC cells [31]. MPT0G211 (Figure 1) in triple negative breast cancer ameliorates the disease by dissociating the aurora-A/Hsp90 complex as HDAC6 inhibition increases the Hsp90 hyperacetylation [32]. Aurora-A promotes cellular migration by increasing the concentration of phosphate slingshot-1 (SSH1) by actin polymerization. MPT0G211 decreases the cell motility by inhibiting in binding of cortactin and F-actin, as acetylation caused by HDAC6 inhibition renders the cortactin ineffective in binding with F-actin [33]. TNBC cell lines showed a significant decrease in



metastatic features in both *in vivo* and *in vitro*. In *in vivo* mouse models MPT0G211 in combination with paclitaxel showed more reduction in the number of tumour nodules [30].

### **2.2.6 Cholangiocarcinoma (CCA) & Liver cancers:**

Cholangiocarcinoma(CCA) is the cancer of cholangiocytes, the inner lining of bile ducts, and it is responsible for 15%-20% of all hepatobiliary malignancies[32]. HDAC6 is overexpressed in CCA, it increased declination, which is directly related to the introduction of malignancy in cholangiocytes [32]. Inhibition of HDAC6 by specific inhibitors like Tubastatin-A(Figure 6) or by shRNAs both restored the primary ciliary expression in cholangiocarcinoma cell lines[32].

It was also found that the decilationprocess involved the MAPK and hedgehog (Hh) pathways. HDAC6 inhibition with Tubastatin-A (Figure 1) reduced the growth of tumours in cholangiocarcinoma, restored the primary cilia,and reduced cell proliferation [32].

To control survivin's acetylation status and its escape from the nucleus and prevent apoptosis, cytoplasmic HDAC6 interacts with survivin upon its entry into the nucleus. To stop the invasion of lung cancer cells, nuclear HDAC6 attaches to and deacetylates NF-kB, upregulating matrix metalloproteinase 2 (MMP2) [33].HDAC6 is associated with EGFR and increase its expression, HDAC6 binds the 3'UTR of the mRNA of EGFR in liver cells and stabilises it [33]. Improvement of EGFR mRNA in liver cancer activates p-AKT/B-catenin signalling. The advancement of liver cancer is led by the accumulation of nuclear B-catenin and deacetylation of p53 [33].

### **2.2.7 Lung Cancer:**

HDACs overexpression, specifically HDAC1, HDAC2, HDAC3 and HDAC6 play an evident role in certain cancers like breast, colon, cervical and prostate cancers [35]. Non small cell lung cancer (NSCLC) accounts for more than 80% of all diagnosed lung cancer with only 16% survival rate [35]. HDAC6 inhibitors sensitised NSCLC towards cisplatin and induced apoptosis. In H292, A549 cell lines activation of the ATR/Chk1 pathway was found to be responsible for the cisplatin-mediated cytotoxicity as a result of HDAC6 depletion or inhibition [35].

Inhibition of HSP90 reduced the expression of transforming growth factor (TGF)- $\beta$ 1, which is present in plenty in tumour microenvironments and plays the role of an inducer in the transition of lung cancer from epithelial to mesenchymal transition (EMT) [34]. TGF- $\beta$  communicates with the NOTCH pathway in NSCLC and eventually, HSP90 is deacetylated through the actions of HDAC6 [34]. Deacetylation of lysine residue 294 of HSP90 is HDAC6-dependent in the cancer cell line of human adenocarcinoma A549 and correlates to the cleavage of Notch1 domain (ICN) and the following nuclear translocation. The NOTCH signalling functions through HEY-1 and HES-1 genes in lung adenocarcinoma in human cell lines [34]. Inhibition of HSP90 with 17-AAG, a geldanamycin analog, inhibited the TGF- $\beta$  induced EMT, demonstrating the role of HDAC6 in lung cancer through deacetylation of substrate HSP90 contributes to signalling networks involved in EMT [34].

### **2.2.8 Pancreatic Cancer**

A point mutation in KRAS gene is present in colon cancers 40%, 90% of pancreatic cancer, and 30% of cases of lung cancers, making it the most commonly, mutated oncogene [36]. Targeting posttranslational acetylation of KRAS has been to show to be effective in cancer. HDAC6 and SIRT2 were found to be responsible for the modulation of the acetylation state of KRAS [36]. Other methods like farnesyltransferase inhibitors failed to be effective against KRAS, thus controlling KRAS acetylation might open a new therapeutic door. The acetylation site for KRAS is lysine 104, in the acetylated state it cannot reload GTP through guanine nucleotide exchange factor (GEF) and fails to maintain activated state which results in decreased activity [36]. To sum it up HDAC6 and SIRT2 positively regulate KRAS while acetylation negatively regulates the same [36].

A novel hydroxamate derivative HDAC6 inhibitor ST80 (Figure 5) was found to be effective in leukemia cell lines HL60 and NB-4. ST80 decreased the expression of HDAC6 protein in these cell lines and it was hypothesised the mechanism induced acetylated  $\alpha$ -tubulin expression [37]. It affects the centriole duplication during cell division and thus stalls the G1-S stage progression [37].

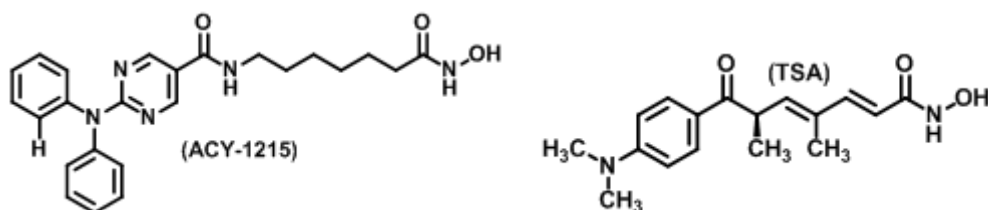


**Figure 2: Structure of TSA and ACY-1215**

In inhibition with TSA (Figure 2), Tubastatin-A does not inhibit HDAC6 from associating with interphase microtubules in MCF-7 cancer cell lines and provides stability toward nocodazole-induced depolymerisation [38]. Two end-tracking proteins EB1 and Arp1 might help HDAC6 to localise towards the end of microtubules and form a cap-like structure. An inactive HDAC6 has more prominent capping activity than an active HDAC6, and remains bound to the microtubule end for a much longer period, it was hypothesized that a conformational change in inactive HDAC6 might be a contributing factor. It was observed a genetic knockdown that is complete depletion of HDAC6 did not provide the same result that is increased microtubule stability it was only achieved with pharmacological inhibition of HDAC6 and thus acting as a Microtubule Associated Protein (MAP) [38].

### **2.2.9 Ovarian Cancer:**

AT-rich interacting domain-containing protein 1A (ARID1A) is a cancer suppressor gene, its mutations are responsible for 40-67% of epithelial ovarian cancer (EOC) [39]. ARID1A is an epigenetic regulator gene with the highest rate of mutation in all kinds of cancer as such it controls the expression of HDAC6. ARID1A interacts with the SWI/SNF complex and interrupts its stability, binds to E4F1, the complex-induced HDAC6 expression, and produces IL-10 by mediation of GATA3 and subsequent mobilization and affects polarization of M2 macrophage [39]. HDAC6 inhibitor vorinostat reduces the level of HDAC6, and IL-10; these events resulted in a reduction of M2 macrophage polarisation and inhibited tumour information [39]. Mutation of ARID1A occurs in more than half of the cases of ovarian clear cell carcinomas (OCCC). ACY1215 activates CD4 and CD8 T cells to boost anti-tumour immunity and in addition suppress ARID1A mutated tumours [40].

### **2.2.10 Glioblastoma& Neuroblastoma:**

HDAC6 inhibition or knockdown is beneficial in glioblastoma tissues and cell lines. HDAC6 promotes spheroid formation in the glioblastoma cells and their proliferation. Resistance to temozolomide (TMZ) in cases of glioblastoma may be overcome by HDAC6 inhibition. HDAC6 stabilises EGFR which confers resistance of glioblastoma cells to TMZ [41].ACY-1215 (Figure 2) has been effective in several types of cancer; in glioblastoma, it inhibits tumour growth by the transformation of growth factor B receptor and subsequent phosphorylation of SMDA2 and upregulation of P21 expressions [42].

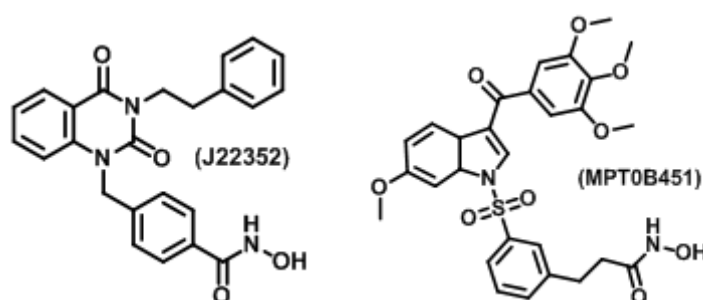


**Figure 3: Structure of HDAC6 Inhibitor J22353 and MPT0B451**

The most lethal primary brain cancer is glioblastoma, and glioblastoma treatments available today are insufficient. Glioblastoma has an overexpression of HDAC6, and siRNA-mediated reduction of HDAC6 prevents the proliferation of glioma cells. J22352 (Figure 3) is a high-selective HDAC6 inhibitor that has PROTAC (proteolysis-targeting chimeras)-like properties [43]. J22352 caused p62 accumulation and proteasomal degradation, which in turn caused abnormally overexpressed HDAC6 in glioblastoma to be proteolyzed [43]. As a result of J22352's effect on HDAC6 expression, cancer cells died more frequently by autophagy, and tumour growth was significantly inhibited. Notably, J22352 restored host anti-tumour activity by reducing the immunosuppressive action of PD-L1 [43]. These findings show that J22352 inhibits autophagy and triggers the anti-tumour immune response in glioblastoma, which enhances the degradation of HDAC6 and generates anticancer effects [43]. Wang et al found HDAC6 was overexpressed in glioblastoma cells, and conferred resistance to temozolomide(TMZ) [44]. HDAC6 stabilised the EGFR, which is responsible for TMZ resistance in glioblastoma [44]. Inhibition of HDAC6 destabilises EGRF pathway and results in TMZ-induced proliferation inhibition, and apoptosis induction [41].

Endoplasmic reticulum stress tolerance (ERST) is responsible for resistance to Temozolomide (TMZ) in glioblastoma multiforme (GBM). HDAC6 and p97/VCP concentration are directly responsible for the TMZ resistance in glioma cells. HDAC6 inhibition confers a positive effect to overcome the TMZ resistance, TMZ when used with HDAC6 inhibitor Tubastatin A (TUB), overcame ERST. HDAC6 inhibition reduces the binding of dynein to HDAC6 and the expression of Dynein-Dynactin complex is reduced, this motor complex is involved in the clearance of ubiquitinated proteins mediated by HDAC6-p97/VCP. TUB promoted the UPS pathway promoted by p97/VCP and reduced the aggresome-autophagy pathway for clearance of ubiquitinated proteins. Hyperacetylation of heat shock proteins by TUB is responsible for the reversal of ERST-induced resistance by modulation of the balance of HDAC6 and p97/VCP [45].

Ku70, another direct HDAC6 deacetylation substrate, in case of acetylation it loses the ability to bind with Bax. Neuroblastoma(NB) is a form of cancer in children formed during the embryogenesis during development, after birth in the adrenal gland sympathoadrenal stem cells. Through acetylation of this substrate Ku70, pan HDAC6 inhibitor SAHA was able to induce cell death in N-type NB. The hypothesis was confirmed by HDAC6 knockdown in SH-SY5Y cells [46].

### **2.2.11 Adenocarcinoma and Esophageal Squamous Cell Carcinoma**

Ricolinostat (ACY-1215) (Figure 6) arrests the G2/M phase of cell division by decreasing the cycle regulatory proteins like survivin, cyclin A2, CDC2, and P-P53, and shows therapeutic effect in esophageal squamous cell carcinoma (ESCC) by apoptosis [48]. ACY-1215 inhibits signalling pathways like PI3K/AKT/mTOR and ERK and triggers apoptosis [47]. Adenocarcinoma is a subtype of carcinoma and accounts for 38.5% of all lung cancer cases. CAY10603, a selective HDAC6 inhibitor suppresses the adenocarcinoma cell growth and proliferation rate by inducing apoptosis. HDAC6 have shown to increase gefitinib resistance, inhibition of the former synergises gefitinib-induced apoptosis by destabilization of EGFR and its subsequent inactivation [48].

### **2.2.12 Lymphoma**

c-Myc is a gene involved in protein biosynthesis and cancer metabolism, in the lymphoma microenvironment it recruited a histone methyltransferase, EZH2, and HDAC3 to the

promoter region of miR-29, miR-15a/16 to downregulate miRNA expressions [49]. c-Myc/miR-548m feed-forward circuit influences stroma-mediated c-Myc activation and downregulation of miR-548m in microenvironments of lymphoma cells. miRNAs are downregulated in MCL and B cell lymphomas as a result of the adhesion of lymphoma cells to lymph node stromal cells and induces the HDAC6 expression, these particular conditions when met are responsible for drug resistance [49]. HDAC6 inhibition suppressed lymphoma growth, stroma mediated clonogenic growth of lymphoma cells in case of cellular adhesion [49].

### **2.2.13 Leukemia**

Wen Wu et al synthesised a compound named MPT0B451 (Figure 7) from 1-benzyl-indoles, which is effective against HDAC6 and facilitates microtubule dimerization [50]. It binds with the colchicine binding site with the S1 substructure which contains four methoxy groups, this substructure is an inhibitor cap. HDAC6 binding is not hindered by the theS1 substructure. The N-hydroxyformamide moiety of substructure S2 interacts with the zinc ion of HADC6 [50]. Substructure S2 stabilises HDAC6 binding site with the styrene linker. MPT0B451 inhibits both microtubule assembly and HDAC6 activities [50]. This dual inhibition activates phosphorylated MPM2, the M phase marker, and arrests the cell cycle in the M phase. The caspase-dependent pathway is activated in prostate and acute myeloid leukemia [50].

Heat shock proteins(HSPs) are regulated by the heat shock factor1 (HSF1) [50]. Curcumin downregulates HDAC6, HSP (27, 70, and 90), and HSF1 in leukemia cell lines via the reduction of ROS [51]. The role of HDAC6, HSF1, and HSPs in tumour survival and proliferation is a therapeutic challenge. Curcumin downregulated these tumourogeneand also sensitised the cancer cells towards cytotoxic drugs like imatinib, and cytarabine, thus reducing the dose of these cytotoxic drugs and cutting down adverse effects [52]. HSPs regulate the functions of several apoptotic proteins, the net result of that regulation is the upscaling of antiapoptotic proteins such as Bcl-2 and downscaling of pro-apoptotic proteins such as Bax, Bid [51] [52].

### **2.2.14 Multiple Myeloma:**

In multiple myeloma (MM) combining HDAC6 selective inhibitor with proteasome inhibitors targets both aggresomal and proteasomal protein degradation systems and it induces

apoptosis cascades by the accumulation of ubiquitinated proteins and imparts cytotoxicity [53]. Adherence of multiple myeloma (MM) cells and stromal cells of bone marrow induces resistance to anticancer treatment. HDAC6 inhibitor tubacin and bortezomib overcome the resistance and induced cytotoxicity. Tubacin synergizes with bortezomib via the activation of JNK phosphorylation followed by caspase/PARP cleavage [54].

In multiple myeloma (MM) it targets the acetylation of histone H3 and Histone H4 lysine residues; K9 and K8 respectively. In MM ACY-1215 with bortezomib activates endoplasmic reticulum (ER) stress, it triggers apoptosis. In combination with bendamustine, it inactivates the AKT pathway in lymphoma cells [42].

WT161 (Figure 1) a specific HDAC6 inhibitor was designed to bind with the lipophilic pocket of the HDAC6 with a triphenylamine motif. WT161 can enhance the effect of BTZ and CFZ in multiple myeloma. It can help to overcome BTZ resistance in MM. WT161 with BTZ induces a large accumulation of polyubiquitinated proteins and cellular stress leading up to caspase activation and induction of apoptosis [55].

#### **2.2.15 HDAC6 in Autophagy and Apoptosis**

HR23B a prominent biomarker of HDAC inhibitors may induce apoptosis or autophagy depending upon the higher or lower expression level in the cells, respectively [56]. The BUZ domain of HDAC6 interacts with HR23B, it was identified that HDAC6 downregulates HR23B through HSP90, as the treatment with HSP90 inhibitor 17-AAG suppressed the regulation of HR23B [56]. Tumours use autophagy to evade cell death, HR23B, on the other hand, sensitizes the tumours to apoptosis. HDAC6 by its ability to downregulate HR23B becomes a therapeutic target to increase the apoptosis of tumours and reduce their susceptibility towards autophagy [56].

Cylindromatosis (CYLD) is a tumour suppressor gene that regulates cell proliferation, survival, and inflammatory disease responses through inhibition of NF- $\kappa$ B and JNK signalling with a deubiquitinating product. The product enzyme removes polyubiquitin chains linked with lysine 48 or lysine 63 through the C-terminal hydrolase domain (UCH) [57]. It removes the lysine 63 ubiquitin chain from Bcl-3 and inhibits translocation and activity [57]. Bcl-3 translocated to the nucleus to form a complex with NF- $\kappa$ B p50 and p52 isoforms and results in the activation of cell cycle promoter cyclin-D1 which leads to tumour growth and

proliferation [57]. The three CAP-Gly domains of CYLD are present at the N-terminal are present in various microtubule (MT) binding proteins however their exact purpose is not known. The first and second CAP-Gly domains bind to MTs to inhibit tubulin deacetylation and the third domain activated TNF-receptor mediated NF- $\kappa$ B through a proline sequence-rich pseudokinase named NEMO/IKK $\gamma$  [57]. CYLD can delay the G1/S phase of the cell cycle through its effect on MTs, they are colocalised with acetylated MTs. Inhibition of HDAC6 with TSA-induced translocation of CYLD results in perinuclear association with acetylated MTs [57]. The N terminal domain of CYLD binds MTs and inhibits HDAC6 activity and reduces the rate of cytokinesis during cell division by regulating the perinuclear localisation of CYLD [57]. CYLD was found to be reducing the cell cycle progression in mouse keratinocytes and human melanoma cells [57].

Oncogenes in the simian virus 40 induced the rearrangement, increased entanglement, and increased width of vimentin intermediate filaments (IF)[Ref]. Vimentin IF takes part in cellular motility invasion. HDAC6 inhibitor tubacin blocked SV40T and subsequently induced vimentin reorganisation. IF plays the most important role in the mechanical properties of MT in cells. Cellular stiffness is higher in cancer cells than in normal cells. SV40T oncogene increased the stiffness and invasive properties [58].

Transformation of oncogene RAS leads to the induction of HDAC6 expression. HDAC6 plays a crucial role in oncogene-induced transformation since HDAC6-deficient fibroblasts are more resistant to both oncogenic Ras and ErbB2-dependent transformation [59]. This is corroborated by the fact that inhibiting HDAC6 in several cancer cell lines decreases anchorage-independent growth and the capacity to produce tumours in mice [59]. Increased anoikis, deficiencies in AKT, and extracellular signal-regulated kinase activation upon loss of adhesion are all related to the loss of anchorage-independent growth. Finally, HDAC6-null animals had higher resistance to cutaneous cancers brought on by chemical carcinogens [59].

Compared to differentiated cancer cells, cancer stem-like cells (CSCs), a tiny population of pluripotent cells found inside heterogeneous tumour mass, continue to be extremely resistant to multiple chemotherapies. It is believed that CSCs have special molecular defences that protect them against therapeutic attacks, such as autophagic homeostasis. Here, it is shown that, when compared to differentiated cancer cells, CSCs exhibit a distinct modulation of macroautophagy and autophagy due to HDAC6 inhibition [60]. It was demonstrated that the inhibition of HDAC6 or its knockdown (KD) reduces CSC pluripotency through



downregulation of key pluripotency factors POU5F1, NANOG, and SOX2 using different human and murine CSC models and differentiated cells. Due to the increased ACTB, TUBB3, and CSN2 expression and apoptosis-independent promotion of differentiation in CSCs, HDAC6 expression is lowered [60]. In CSCs, HDAC6 knockdown decreases pluripotency by increasing autophagy, whereas POU5F1, ATG7, and ATG12 knockdown decrease HDAC6 expression and encourage differentiation when pluripotency is inhibited by retinoic acid therapy [60]. Interestingly, the autophagy inducers Tat-Beclin 1 and rapamycin significantly increase the effect of HDAC6 KD-mediated CSC growth suppression. HDAC6 knockdown in differentiated breast cancer cells enhances apoptosis by downregulating autophagy, the opposite of what was seen in CSCs [60]. Additionally, following HDAC6 KD, CSCs are differentially regulated from differentiated cancer cells in terms of the autophagy regulator p-MTOR, upstream negative regulators of p-MTOR (TSC1 and TSC2), and downstream effectors of p-MTOR (p-RPS6KB and p-EIF4EBP1) [60]. The distinct chemosusceptibility of CSCs and differentiated cancer cells can be attributed to the unequal control of autophagy, which serves as a molecular connection [60].

### **2.3 Role of HDAC6 in Neurodegenerative Diseases-**

Protein aggregates are linked to neurodegenerative diseases (NDs), including Alzheimer's disease, Huntington's disease, Parkinson's disease, and Charcot-Marie-Tooth disease. HDAC6 is crucial for the removal of misfolded proteins by altering the UPS (ubiquitin and proteasome system) and enhancing autophagy. The dynamic balance between fusion and fission maintains mitochondrial connectivity. HDAC6, under glucose deficit condition, can activate adaptive mitochondrial fusion. Membrane-bound GTPases regulate mitochondrial fusion, for example, Mitofusion 1 (MFN1) and Mitofusion 2 (MFN2). Under hypoxic conditions, HDAC6 inhibited the degradation of MFN2 through interaction. MARCH5, a mitochondrial ubiquitin ligase that promotes MFN2 degradation under similar conditions, was found to be increased in HDAC6 deficit cells and associated with neurodegenerative disorders [61].

In the neurodegenerative disease, Parkinson's disease (PD), Lewy body aggregates form, and dopaminergic neuron depletion occur selectively. The substantia nigra part of the human brain is affected. Alpha-synuclein ( $\alpha$ -syn) accumulation in the form of Lewy bodies is a key

pathological characteristic of PD. UPS, along with chaperones and autophagy-lysosome pathway clears the abnormal proteins [62].

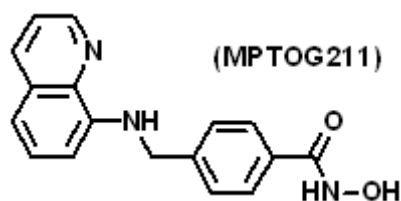


**Figure 4: Structure of HDAC6 inhibitor MPTOG211**

Novel HDAC6 inhibitor, MPTOG211 (Nhydroxy-4-((quinolin-8-ylamino)methyl)benzamide) (Figure 4) treatment attenuated the amount of tau phosphorylation in the hippocampal CA1 region of AD *vivo* models. Phosphorylation on tau residue Ser396, and Ser404 decreased HDAC6/Hsp90 binding is halted causing degradation of polyubiquitinated proteins [63].

In experiments on oligodendroglial cell lines (OLN-t40 and OLN-t44) with inhibitor tubastatin A, the microtubule activities of tau were decreased. HDAC6 inhibition and accompanying effects on tau hyperacetylation as well as phosphorylation in oligodendrocytes could have protective effects in neurodegenerative diseases as cellular acetylation in a protection mechanism of cells under severe stress situations [64].

HDAC6 mRNA and HDAC6 protein were detected mainly in the hippocampus and cortical regions of the adult mouse brain and a lower level was detected in the cerebellum [65]. A $\beta$  peptides found in Alzheimer's disease, cause cytoskeletal abnormalities mainly by impairing intracellular transport and mitochondrial trafficking thus impairing neural function [65]. Loss of HDAC6 was found not to be detrimental in the normal brain activities of the mice model, it was however, protective against the impairment of mitochondrial trafficking in the hippocampal region caused by A $\beta$  peptides in *in vitro* and as well as *in vivo* [65]. An increase in the level of  $\alpha$ -tubulin acetylated at the lysine 40 (K40ac) was also observed following the knockout of HDAC6 (Hdac6<sup>-/-</sup> mice), it has a great impact on intracellular transport [65].

HDAC6 localised at the distal region of the axon and was responsible for axon elongation and initial growth through the deacetylase domain. In the hippocampal region inhibition of HDAC6 slowed down the axonal growth as tubulin acetylation increased and modified the distribution of axon growth protein KIF5C. HDAC6 activity is necessary for the polarisation of localised proteins in the hippocampal axon initial segment (AIS) [66].

In Alzheimer's pathology, A $\beta$ -induced ROS and excessive Ca<sup>2+</sup> contributed to neuronal cell death and impaired mitochondrial axonal transport [67]. HDAC6 inhibitors have reduced the level of excessive ROS and Ca<sup>2+</sup> elevated by A $\beta$  [67]. Prx1 acetylation plays an important role in the recovery of axonal transport in AD. HDAC6 deacetylation of  $\alpha$ -tubulin contributed to the pathology of AD in terms of impaired axonal transport, however, the role of Prx1 is more important [67]. Since antioxidant characteristics of Prx1 reduce the level of ROS and Ca<sup>2+</sup> and acetylation of Prx1 at K197 [67].

Carboxy terminus of HSP-70 interacting protein (CHIP) is part of the protein triage for clearance of protein tau, it targets the phosphorylated tau. CHIP is reducing the expression of HDAC6, by binding and ubiquitinating the same. HDAC6 undergoes proteasomal degradation mediated by CHIP [68]. Upon binding of CHIP with Hsp90, p23 is released, which shifts the refolding function of Hsp90 to the degradation function of their client proteins. A decrease of HDAC6 promotes Hsp90 acetylation, it favours tau degradation [68].

Neuronal polarity maintenance and control of cytoskeleton dynamics are essential in the development, and synaptic activity of neural networks. Through the activation of RhoA and the inhibition of HDAC6 in hippocampal neurons, soluble  $\beta$  amyloid (A $\beta$ ) alters the dynamics of actin and microtubules (MT). A $\beta$ 's interaction with the extracellular membrane facilitates RhoA activation, which causes growth cone collapse and neurite retraction and may be the cause of impaired neuronal migration and pathfinding in Alzheimer's disease (AD). A $\beta$  raises the levels of heterodimeric acetylated tubulin and acetylated tau, both of which have been observed to be changed in AD, via inhibition HDAC6. Loss of HDAC6 activity compromises the integrity of the axon initial segment (AIS), leading to ankyrin G mislocalisation, increased MT instability, loss of tau polarised location, and impaired action potential firing [69].

The presence of ZnF UBP domain is a unique feature of the HDAC6, it promotes nuclear localization of ApoE and modulates Tau phosphorylation in AD. HDAC ZnF UBP reorganises the cytoskeleton structure through actin dynamics and localization of tubulin. Podosome formation, and neuritic extension formation have also been associated with this domain [70].

Tau-induced defects in the microtubules in tauopathies were reversed by HDAC6b mutation in the drosophila model. Tubacin, being a Tubulin-specific deacetylase also rescued the Tau-

induced defects in MT. The loss of HDAC6 activity proved to be effective in opposing the abnormalities caused by Tau in MT stability and structure [71].

Charcot-Marie-Tooth (CMT) disease is an inherited disorder in the peripheral nervous system. It occurs due to mutation of the small heat shock protein gene (HSPB1) of 27-kDa, as a result, axonal CMT or distal hereditary motor neuropathy (HMN) occurs. In mice models with S135F mutation, symptoms of CMT2 and distal HMN similar to humans were observed. It was observed the mutated HSPB1 autonomously attenuated the acetylated  $\alpha$ -tubulin levels and affected the axonal transport. Inhibition of HDAC6 reversed the acetylation status of the  $\alpha$ -tubulin, and the axonal transport was also restored [72].

HDAC6 is present in plenty of serotonin neurons. The selective HDAC6 depletion in mouse models in raphe neurons controls hyperacetylation of Hsp90 and affects the assembly of glucocorticoid receptors (GR). Both genetic and pharmacological inhibition of HDAC6 showed the interference with GR signalling and modulation of stress and hormone-induced GR translocation. HSP 90-GR heterocomplex dynamics play a vulnerable role in post-traumatic stress disorder (PTSD) and behavioural disorders. HDAC6 does not play any developmental role in serotonin (5-HT) neurons thus depletion does not have any impact on the number, and morphology of the serotonin neurons. Moreover, HDAC6 depletion in 5-HT neurons showed antidepressant characteristics, it protected the mice from hypoexcitability and somatodendritic hypertrophy after exposure to chronic stress and repeated social defeat. The modulation of GR chaperones through HDAC6 might provide new insights and a novel approach to pro-resilience interventions in mood disorders [73].

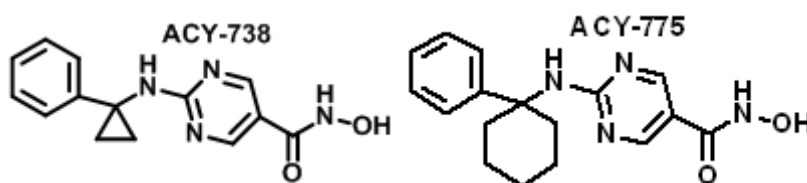


**Figure 5: Structure of HDAC6 inhibitors ACY-738 and ACY-775**

Novel pyrimidine hydroxyl amide molecules ACY-738 & ACY-775 (Figure 5) show specific inhibition of HDAC6. These molecules show antidepressant properties similar to HDAC inhibitor SAHA, MS-275 in mice models. ACY-775 & ACY-738, upon systemic administration, showed good brain bioavailability [74].

Abnormal tau species are commonly found in neurodegenerative diseases. Aggresomes are enriched with abnormal tau species, hyperphosphorylated, and misfolded tau proteins. HDAC6 takes up a composite role in the management of abnormal tau proteins. It helps to clear insoluble tau through aggresome formation [75].

HDAC inhibitors show benefits in brain disorders like ischemic stroke. HDAC6 inhibitor TubA promoted  $\alpha$ -tubulin acetylation and increased the neuroprotective protein FGF-21 and its transport. The FGF-21 mRNA transcript is also increased via Akt activation and inhibition of GSK-3 $\beta$  [76].

Treatment with HDAC1 and HDAC6 inhibitors MS-275 and TBA, respectively improved larvae metabolic activity and recovered the MPP<sup>+</sup>-induced reduction of dopaminergic neurons in diencephalon homologue to mammalian substantia nigra, Tubastatin also improved head-reflex [77].

## **2.4 Role of HDAC6 in cardiovascular diseases**

HDACs show opposite functions in the pathology of the heart to either inhibit or induce cardiac hypertrophy. Where class I HADCs induce pathological hypertrophy the class II HADCs are known to block the same. Cardiac hypertrophy and fibrosis were reversed by sodium alphonate, a known HADC inhibitor in DOCA-salt hypertensive rats. Markers of fibrosis such as collagen, and fibronectin decreased by Valproate treatment. Levels of fibronectin mRNA, and fibrotic mediator connective tissue growth factor (CTGF) also decreased significantly [78].

In hypoxia-ischemia (HI) of the spinal cord, reactive oxygen species (ROS) have been reported to be generated. Chaperone Mediated Autophagy (CMA) is one of the three types of autophagy of mammalian cells, that resist ROS-induced motorneural death. HDAC6 plays an important role in regenerating the ROS, thus knocking it down may have neuroprotective roles as apoptosis ensues. HSC70 and LAMP-2a two markers of CMA, increased significantly in HI-induced cells. The CMA pathway is partly responsible for the accumulation of abnormal, damaged proteins due to oxidative stress. HSP90 stabilises LAMP-2a protein by binding with the lysosomal membrane. Inhibition or knockdown of HDAC6 promote reversible hyperacetylation of HSP90, thus affecting the interaction with

LAMP-2a, which in turn interferes with the CMA pathway. HDAC6 inhibition promotes ROS generation and in response cell apoptosis under HI conditions [79].

Smooth muscle cells and endothelial cells in the pulmonary artery proliferate due to pulmonary vascular resistance in pulmonary arterial hypertension (PAH). Ku70 is a DNA repair factor. Ku70 acetylation contributes to mitochondrial-dependent apoptosis. HDAC6 inhibits the acetylation of Ku 70 and thus enhances k70bax binding as a result stress-induced apoptosis is prevented [80].

HDAC6 inhibitors such as tubastatin A improved the ejection volume of the heart in mice model, HDAC6 contributes to the cardiac dysfunction caused by ANG-II signalling. HDAC6 depletion has shown favourable effect on myofibril force generation. HDAC6 is a potential candidate for heart failure by improving cardiac dysfunction and muscle wasting associated with the pathology. HDAC6 control of myofibril and subsequently sarcomere protein acetylation could be a possible route for such therapeutic findings. In some works, HDAC6 is an important factor in atrial fibrillation and skeletal muscle sepsis [81].

Cathepsin S (CatS) participates in stem cell development through its role in epigenetics. Vascular injury in mice increased the CatS expression, in the absence of CatS in the injured arteries the formation of neointima was reduced. CatS gene through the p38MAPK/Akt signalling pathway regulates HDAC6 phosphorylation. Inhibition of HDAC6 or CatS reduced VSMC migration and proliferation. CatS modulates the injury-related vascular repair in mice through its interaction via TLR2 moderated p38MAPK/Akt-HDAC6 signalling pathway. It has been suggested that CatS suppression reduced HDAC6 phosphorylation through PDGF and HDAC6 activities in VSMC proliferation and migration. CatS controls vascular repair and formation of neointima through the phosphorylation of p38MAPK and Akt pathways. HDAC6 is a potential drug target in restenosis and maladaptive vascular remodelling altered cardiovascular diseases [82].

HDAC6 was found to be upregulated in PASMCs isolated from the PAH patients. HDAC6 opposed apoptosis in PAH-PASMCs by keeping the Ku70 in the hyperacetylated state as the latter interacts with bax to inhibit its translocation to mitochondria to initiate apoptosis. Ku70, a substrate of HDAC6 is associated with sequestering Bax from mitochondria and suppressing apoptosis. Acetylation of Ku-70 disrupts the interaction with Bax and gives rise to cytoplasmic CBP [83]. Bax-inhibition peptide (BIP) called V5 was designed from Ku70's

Bax inhibiting domain and was used in PAH\_PASMCs cells treated with HDAC6 selective inhibitor and it was found to rescue cells from apoptosis [84].

## **2.5 Role of HDAC6 in HIV:**

Human immunodeficiency virus type 1 (HIV-1) overcame immune barriers inside of a preying organism through a sophisticated strategy by its use of the protein viral infectivity factor (Vif). Vif promotes ubiquitination and degradation of apolipoprotein B mRNA-editing enzyme catalytic polypeptide-like 3G (A3G). The A3G is degraded by the proteasome and subsequently evades its restriction activity against HIV-1. Human HDAC6 has a protective action against the activity of vif and thus it restricts the activity of HIV-1. HDAC6 interacts with A3G or Vif through the BUZ domain. HDAC6 can form a ternary complex with A3G and Vif, however, the BUZ domain may not be the absolute requirement for this complex formation. HDAC6 competes for the A3G-Vif interaction and is instrumental in protecting A3G from Vif-mediated degradation. The data from this experiment also confirmed the existence of Vif-independent HDAC6/A3G interaction and complex formation. HDAC6 with its BUZ domain protects A3G from Vif-mediated ubiquitination and proteasome degradation. HDAC6 demonstrated anti-HIV-1 activity by directly promoting Vif degradation and the deacetylase activity cleared Vif through autophagy. HDAC6 and the HDAC6/A3G complex may prove to be a good antiviral drug target [85].

## **2.6 Role of HDAC6 in Inflammation:**

HDAC6 interacts with the Nucleotide-binding domain, leucine-rich-containing family, and pyrin domain-containing-3 (NLRP3) on the lysosomal membrane enhancing the interaction between NLRP3 and Lamtor1 and increases the activation of NLRP3 inflammasome. Inhibition of HDAC6 interrupted inflammasome activation and thus could serve as a potential target for NLRP3 inflammasome-related diseases [86].

Psychiatric and neurological diseases are associated with inflammation of the central nervous system (CNS). HDAC6 differs not just structurally but functionally from other HDACs as it targets acetyltubulin as its substrate and is predominantly cytosolic. HDAC6 inhibition increases tolerance towards bacterial lipopolysaccharides (LPS) induced IL-6 production and activation of glycogen synthase kinase-3 (GSK3) in astrocytes. HDAC6 through actin network and cellular signalling might affect the inflammatory signalling network, however,

the exact mechanics of inflammatory tolerance is unknown. Protection of neurons in astrocytes is done by inhibition of HDAC6 or activation of GSK3. GSK3, through its inhibition of HDAC6, counteracted the tolerance, it was evident that inhibition of GSK3 with lithium promoted not only tolerance but also decreased the amount of acetyl-tubulin in the presence of LPS treatment. Since HDAC6 is directly associated with neurodegenerative diseases, another role of HDAC6 is the Protection from irreversible damage of CNS from inflammatory mediators by the enhancement of the endogenous process of inflammatory tolerance. Tubacin induced HDAC6 inhibition and reduced the LPS tolerance in microglia as the production of inflammatory agent IL-6 production was reduced [87].

HDAC6 recruits and activates signal transducer and activator of transcription 3 (STAT3) to regulate to control the expression of programmed cell death ligand 1 (PD-L1). In t-cells Inhibitory regulatory pathway, PD-1 is activated by the expression of PD-L1. The same group has reported that in the IL-10 promoter, the same region is used for the recruitment of both HDAC6 and STAT3 [88].

HDAC6 is overexpressed in inflammatory diseases in macrophages and enhances pro-inflammatory cytokines, such as TNF- $\alpha$ , IL-1 $\beta$ , and IL-6 along with a reduction in acetylated  $\alpha$ -tubulin. Overexpression of HDAC6 during inflammatory diseases contributes to the elevated generation of ROS through activated macrophages; signalling pathways such as MAPK, NF- $\kappa$ B, and activator protein-1 (AP-1) participate in the pro-inflammatory response. HDAC6 transcriptionally regulates the pro-inflammatory genes. ROS is produced by Nox-2 based NADPH oxidase in phagocytes. HDAC6 overexpression upregulates the transcriptional expression of gp91<sup>phox</sup>/Nox2 and p22<sup>phox</sup> [89].

Activated macrophages are differentiated into two types- activated macrophages M1 and M2, this classification depends upon prototypical activating stimuli. M1 is induced by bacterial lipopolysaccharide (LPS) and interferon  $\gamma$  (IFN- $\gamma$ ); a T helper type I (Th1) cytokine to produce pro-inflammatory cytokines T helper type II (Th2) cytokines such as interleukin 1b (IL-1b). IL-4, and IL-13 TGF- $\beta$  induce M2 phenotype to produce anti-inflammatory cytokines to take part in tissue repair and protection from parasites. The balance between M2 and M1 is vital in the regulation of inflammatory diseases. LPS through a toll-like receptor 4 (TLR4) signalling induced macrophage activation to differentiate it towards M1, this process involves cytoskeletal reorganisation. HDAC6 targets to deacetylate several cellular cytoskeleton-associated proteins such as Hsp90, cortactin, end binding protein I (EBI),



microtubule-associated protein 7 domain-containing protein 3 (Mdp3), protein farbesyltransferase and cytoplasmic linker protein 170 (CLIP-170). Inhibition of HDAC6 through Tubacin or gene knockout showed a decrease in M1 markers like pro-inflammatory cytokines such as IL-6, TNF- $\alpha$  but LPS-induced IL-10 (M2 marker) level remained unaltered. The interaction between F actin and Cortactin remained unhinged [90].

Tumour cells suppress immunity by downregulating MHC and upregulating the ligand blocking immune checkpoints and inflammatory cytokines. Targeting HDAC6 in melanoma shows immunomodulatory effects, by upregulation anti-tumour antigens, MHC class I like CD4<sup>+</sup> CD8<sup>+</sup>, these effects together with the arrest of G1 phase which induces apoptosis, decreased melanoma. Antigen-dependent CD4<sup>+</sup> T cell activation is impacted by HDAC6. It was proven that HDAC6 helps CD8<sup>+</sup> T lymphocytes perform their cytotoxic activity. Studies on immunisation have shown that when HDAC6 is absent, cytotoxic action *in vivo* is defective. Adoptive transfer of Hdac6<sup>-/-</sup> or wild-type CD8<sup>+</sup> T cells to Rag1<sup>-/-</sup> mice revealed a particular reduction in CD8<sup>+</sup> T cell responses against vaccinia infection [91].

*In vitro* cytolytic activity of HDAC6-deficient cytotoxic T lymphocytes (CTLs) were impaired due to altered dynamics of lytic granules, inhibited kinesin-1-dynactin-mediated terminal transport of lytic granules to the immune synapse, and impaired exocytosis but not target cell recognition, TCR activation, or interferon (IFN) $\gamma$  production. HDAC6 affects the kinetics, transport, and secretion of lytic granules by CTLs as an effector of the immune cytotoxic response. Kinesin-1 and HDAC6 work together to control lytic granule delivery and mobility at the immunological synapses. Using a biochemical method, it was discovered that HDAC6 and kinesin-1 light chain (KLC1) formed a complex after being activated by anti-CD3 and anti-CD28 monoclonal antibodies. Furthermore, Hdac6 knockdown animals had reduced p50-dynamin (also known as DCTN2) and p150-glued (also known as DCTN1) interaction in the kinesin-activator complex. HDAC6 plays a unique function in the exocytosis of lytic mediators as well as their intracellular location. Therefore, HDAC6 is a viable candidate that might be targeted to modulate CTLs in particular disorders because of the catalytic and scaffold activities of HDAC6 that may function at various levels in the control of cytotoxic-related pathways [92].

## **2.7 Role of HDAC6 in Miscellaneous Diseases:**

HDAC6 is overexpressed in Cystic Cholangiocytes and its inhibition reduced Cystogenesis. Polycystic liver disease (PLD), a member of the cholangiopathies is caused by a mutation in *Sec63* and *PKRCSH* (protein kinase C substrate 80K-H) genes. It has been found that HDAC6 is overexpressed in liver tissues of PCK rats and ADPKD and ARPKD patients, specifically in hepatic cysts. HDAC6-specific inhibitors such as Tubastatin-A, and ACY-1215 decreased cholangiocyte proliferation and cystic growth in vitro models. The amount of acetylated  $\alpha$ -tubulin was found to be increased while the  $\beta$ -catenin level decreased, both proteins related to cystogenesis. Which might be the mechanism behind the decreased cyst growth after HDAC6 inhibitor treatment.  $\beta$ -catenin is accumulated due to abnormal activity of the Wnt/ $\beta$ -catenin pathway and characteristic features in kidney polycysts.  $\beta$ -catenin nuclear localisation is regulated by HDAC6 in colon cancer cell line [93].

Autosomal dominant polycystic kidney disease (ADPKD) is a progressive genetic disease characterised by the growth of cystic lesions in the renal parenchyma, it is caused by the genetic mutation of *PKD1* or *PKD2*. HDAC6 being a versatile protein controls the degradation of EGFR in intracellular renal epithelial cells along with its trafficking through  $\alpha$ -tubulin acetylation [94].

Protein turnover and aggregation are governed by the tubulin deacetylase histone deacetylase 6 (HDAC6). Cu/Zn superoxide dismutase (*SOD1*) mutations associated with familial amyotrophic lateral sclerosis (ALS) result in a propensity for protein aggregation. HDAC6's contribution to mutant *SOD1* aggregation and the aetiology of ALS remains unclear, though. It was found that mutant *SOD1* aggregation in cultured cells was induced by HDAC6 knockdown. HDAC6 is primarily associated with mutant *SOD1* via two motifs like the *SOD1* mutant interaction region (SMIR) was discovered in p62/sequestosome 1, in contrast to its known function in promoting the degradation of poly-ubiquitinated proteins. The acetylation-mimicking K40Q -tubulin mutant boosted mutant *SOD1* aggregation, while expression of the aggregation-prone mutant *SOD1* increased -tubulin acetylation. Findings imply that ALS-linked mutant *SOD1* can influence HDAC6 activity and boost tubulin acetylation, which in turn promotes mutant *SOD1* aggregation that is dependent on microtubules and retrograde transport. Impairment of HDAC6 may be a characteristic of many ALS subgroups [95].

During platelet activation a change in microtubule organisation takes place. HDAC6 is found to deacetylate tubulin which is followed by microtubule reacylation [96].

Death inducer obliterator (Dido3) distributed in the centrosome of the cells controls cilium size by regulating the HDAC6 present in the centrosome. The distribution of HDAC6 at the subcellular level indicates control mechanism based on the kinase dependent activation, the change in concentration regulates the cilium length [97].

## **2.8 HDAC6 and Misfolded Proteins:**

HDAC6 belongs to the IIb histone deacetylase family and is mainly located in the cytosol of the cell. HDAC6 is a master regulator, performing protective cellular response to the accumulation of cytotoxic bioproducts. It responds to damaged mitochondrial damage and protein aggregation. Chaperones correct the misfolded polypeptides. However, when their capacity is exceeded toxic protein aggregates are formed. Then autophagy pathways eliminate the intracellular protein aggregates accumulated through misfolded proteins. HDAC6 is an essential component of the aggresome. The absence of HDAC6 produces the Endoplasmic reticulum stress (EnR) which in turn triggers the unfolded protein response (UPR). In this absence of HDAC6, IBC cells commit themselves to apoptosis [98]. HDAC6 inhibition in oligodendrocytes increases autophagosome formation and accumulation in the cellular cytoplasm. HDAC6 controls the autophagosome by linking autophagy and UPS. Autophagy functions as the alternative degradation system in case the UPS is impaired [99]. HDAC6 regulates the actin membrane, and F actin polymerisation to assist in the autophagosome-lysosome fusion. Actin is found in the autophagosome in abundance and in very low amounts in lysosome. In a HDAC6-dependent manner, autophagosomes are assembled at autophagic substrates into an F-actin network [101]. Heat shock protein 5 (HSPA5) or GRP78/BiP regulates UPR in the Endoplasmic reticulum (ER). GRP78, a member of the E3 ligase family takes part in ubiquitination and misfolded protein degradation. It targets cancer-promoting agents such as CYP3A4, hydroxymethylglutaryl CoA reductase and, apo B lipoprotein. GRP78 through the C terminal promotes HSPA5 ubiquitination and subsequent degradation. HDAC6 knockdown promoted HSPA5 acetylation at K353, it reduced the ubiquitination of HSPA5 at K447 as a consequence the cell migration and invasion increased [22]. HDAC6 through its ubiquitin binding domain, controls auto-phagosome maturation and aggresome formation. Selective HDAC6 inhibitor A452 (Figure 6) increases p53 level through destabilisation of murine double minute-2

(MDM2). A452 hinders the deacetylation of p53 at lysine 381 and 382 (lys381/382). p53 is a tumour suppressor gene, mutated in most malignancies. Over 50% tumours in humans have a mutation in the TP53 gene, which encodes the p53 transcription factor [102].

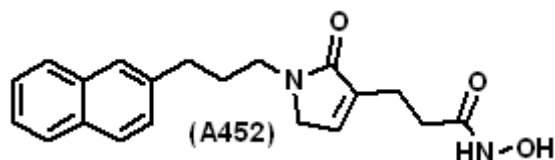


**Figure 6: Structure of HDAC6 inhibitor A452**

Proteasomal damage causes the impaired or misfolded protein to aggregate at the perinuclear space. RanBPM (Ran-binding protein M) promotes aggresome formation and activation of apoptosis. It is a ubiquitous, nucleocytoplasmic protein with several conserved domains. Among the domains LisH/CTLH domain (Lossencephaly type-1 like homology/carboxy-terminal to LisH) interacts with HDAC6 and colocalises with the same in aggresome formation to inhibit HDAC6 activity. Due to the negative regulation of HDAC6 by RanBPM, the level of acetylated  $\alpha$ -tubulin is also depleted, and it has been established that RanBPM directly interacts with microtubules [100].

HDAC6 binds mono and polyubiquitin, this induces the upregulation of expressions of HSP genes. HDAC6-ubiquitin binding acts as a sensor for misfolded protein accumulation and subsequently activates transcription factor HSF1 via Hsp90 involvement. HSPs are activated by the ubiquitin binding and dissociation of the HSP90-HSF1 complex [103].

The concentration and balance of HDAC6 and p97/VCP determine the protein degradation. p97/VCP facilitates the degradation of ubiquitinated protein whereas HDAC6 opposes that function and promotes the accumulation of the same protein [104].

Tripartite Motif Containing 50 (TRIM50) gene, functions as an aggresome precursor, and participates in recruiting polyubiquitinated proteins into aggresome, these proteins are its substrates. TRIM50 interacts with p62, an adaptor protein involved in TRIM50- p62 interaction via the LC3-Interacting region (LIR) domain. TRIM50 activity is HDAC6 dependent, HDAC6 inhibition promotes aggresome formation through TRIM50 bodies [105].

## **2.9 Role of HDAC6 in Mitochondrial Transport:**

Mitochondria is delivered in association with microtubules in the axon. A $\beta$  alters the microtubule stability to interrupt vesicular and axonal transport. Motor proteins Kinesin is responsible for anterograde transport and dynein for retrograde transport of mitochondrial axon transport. Kinesin connects adaptor proteins such as Miro and Milton to mitochondria. Most scientist groups have reported that A $\beta$  impairs mitochondrial transport in both directions. Dynein affects the mitochondrial morphology, Inhibition of HDAC6 was found to influence mitochondrial length. Inhibitor TBA even in the presence of A $\beta$  restored the amount of acetylated  $\alpha$ -tubulin to regulate bidirectional mitochondrial transport [106].

## **2.10 HDAC6 &GRK2:**

G protein-coupled receptor kinase 2 (GRK2) directly stimulates the phosphorylation of HDAC6 to increase  $\alpha$ -tubulin deacetylation in epithelial and fibroblasts, it gains the ability by getting phosphorylated at the S670 regulatory site. GRK2 phosphorylation sites are located in between the region of DD2 and the ubiquitin binding domain of HDAC6. The second catalytic domain is involved in  $\alpha$ -tubulin deacetylase activity and interacts with the specific HDAC6 inhibitors to impair tubulin deacetylase (TDAC) activity. GRK2 enhances the extent and the kinetics of TDAC activity is mediated by HDAC6. GRK2 and HDAC6 both colocalise at the periphery of wound-edged pseudopodia induced by chemoattractant, it functions as a key step in the dynamic modulation of the microtubule during chemotactic migration of epithelial cells and fibroblasts [107].

## **2.11 HDAC6 &Peroxiredoxin (Prx):**

HDAC6 deacetylated the peroxiredoxin(Prx) I and II, two redox regulatory proteins. These two proteins regulate the amount of ROS in several cancer cells and in normal cells too. ROS regulation of Prx I and II have implications in cancer and several neurodegenerative diseases. acetylation of Prx enhanced its reduction activity of H<sub>2</sub>O<sub>2</sub> and the cellular stress associated with it [108].

Diabetes patients are more prone to myocardial ischemia/reperfusion (MI/R) injury, which is linked to increased ROS production and diminished antioxidant defence. A regulator of the antioxidant protein peroxiredoxin 1 (Prdx1), histone deacetylase 6 (HDAC6) is linked to

several degenerative disorders in the cardiovascular system. Heart MI/R damage was more likely to occur in diabetic hearts with elevated HDAC6 activity and lower acetylated-Prdx1 levels. In diabetic MI/R rats, Tub A therapy significantly enhanced acetylated-Prdx1 levels, decreased ROS generation, decreased myocardial infarction, and improved cardiac function. An in vitro investigation employing H9c2 cells further supported these findings. TubA only marginally reduced H/R-induced cell death and ROS generation in K197R-transfected H9c2 cells exposed to high glucose (HG), but these differences were not statistically significant, according to a study employing Prdx1 acetyl-silencing mutants (K197R). Together, our results indicate that HDAC6 inhibition alters Prdx1 acetylation at K197, which lowers ROS production and gives protection against MI/R or H/R injury [109]

### **Chapter 3: Literature Review**

HDAC inhibitors are being developed to be used in conjugation with other cytotoxic drugs. Gene expression silencing of HDACs has supported the fact that it is indeed the presence of HDACs in cancer cells that cause the disease progression. Inhibition of HDAC6 and several other HDAC enzymes induce cell apoptosis. HDAC6 interacts with  $\alpha$ -tubulin, HSP 90, GRK2, Dysferlin, HSP 90, P97, TRIM50, EGFR, Tax and several other substrates [4][5]. HDAC6 changes the acetylation status of  $\alpha$ -tubulin and microtubule cytoskeleton structure [3]. Modifying the size of the linker group improves protein binding as reported by the docking and NMR studies. Several HDAC inhibitors have been approved for use in different cancer treatments. Selective HDAC inhibitors have much less adverse effects compared to the pan HDAC inhibitor candidates. HDAC6 has proven to be a novel target for the treatment of several types of cancer, and neurodegenerative diseases. The structure of HDAC6 is unique owing to the presence of two catalytic binding domains and being the largest member of the HDAC family. HDAC inhibitors have three regions, a zinc binding group, a linker, and a cap region [4][6].

In  $\text{Zn}^{+2}$  dependent HDAC inhibitors; A zinc-binding group (ZBG) function as a chelating group, a cap group takes part in surface recognition, and a linker joins the ZBG and cap portion that make up the main pharmacophore components. The potency, stability, and selectivity of the HDAC inhibitors have been significantly changed as a result of modifications made to any one of these three areas, i.e., the cap group, the linker, or the ZBG. HDAC inhibitors have so far been prescribed, including vorinostat, romidepsin, belinostat, panobinostat, chidamide, and pracinostat (Table 1). The majority of them are pan-HDACis with a variety of toxicities and unfavourable side effects. As a result, highly isoform-specific HDAC inhibitors are necessary for both the targeted therapy and a further discovery and understanding of the function of individual members of HDACs [110].

The hydroxamate moiety serves as the ZBG in tubacin's (7, Figure 13) bulky structural design, which has six lipophilic rings in the form of four phenyl rings, one 1, 3-dioxane ring, and one oxazolidine ring that interact with the HDAC6 surface.



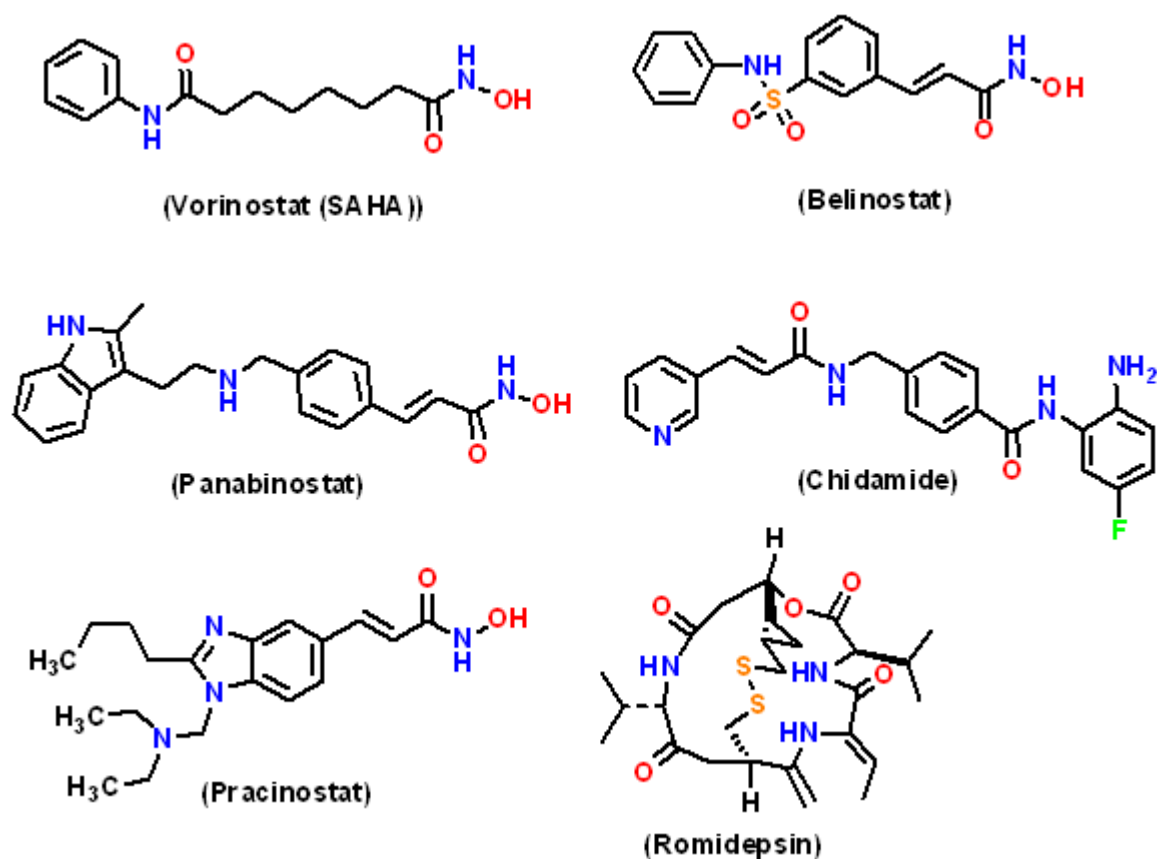


Figure 12: FDA approved HDAC6 inhibitors

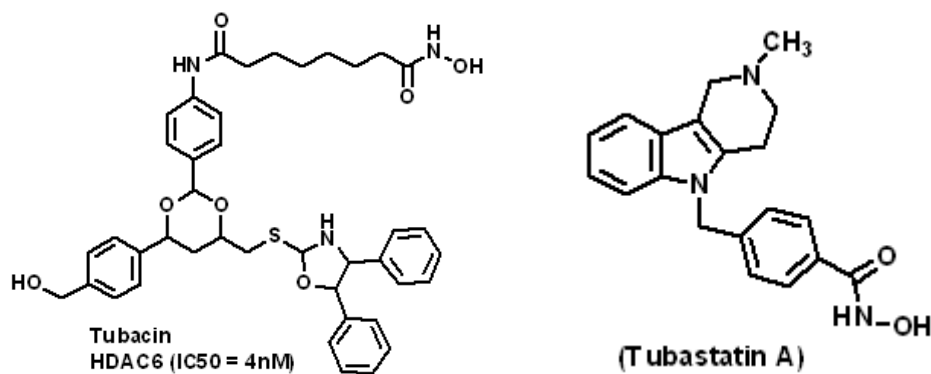
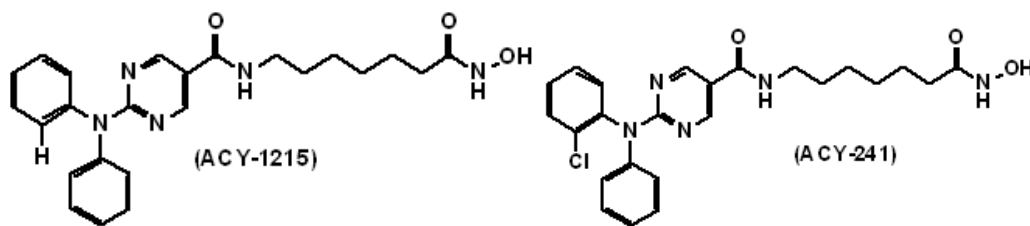


Figure 7: Structure of HDAC6 Inhibitors Tubacin and Tubastatin A

Tubacin in Figure 7, has a reputation for reducing cell motility while having minimal impact on the stability of the microtubule and cell cycle. It is a very potent HDAC6i with an IC<sub>50</sub> of 4 nM. Tetrahydro- $\gamma$ -carboline serves as the cap group, benzyl serves as the linker, and the hydroxamate function serves as the ZBG in tubastatin A (Tub A). Structure-based drug design

revealed it as a powerful and selective HDAC6i. The IC<sub>50</sub> for Tub A against HDAC6 is 15 nM. In comparison to HDAC1, it is around 1000 times more selective, and it is extremely selective against other HDACs. In primary cortical neuron cultures, Tub A selectively increased the amounts of acetylated  $\alpha$ -tubulin over histone and also demonstrated dose-dependent protection against oxidative stress brought on by glutathione depletion. At the same concentration, it was discovered to be non-toxic to neuronal cells. It was therefore noted as a possible agent in neurodegenerative diseases. According to research, it may act as an agent in neurodegenerative diseases. In numerous animal models of neurological, autoimmune, and cardiovascular illnesses, it is well recognised to exhibit significant efficacy. The monodentate coordination of the hydroxamate moiety to  $Zn^{+2}$  was disclosed by the drHDAC6-CD2/Tub A complex, while the apex of the linker's phenyl function is located between the side chain amino acid residues (F583, F643, and H614). The L1-loop amino acids create a hydrophobic groove where indole activity is centered around.

In addition, the methylpiperidine group is surrounded by neighbouring five water molecules and van der Waals forces are found in interaction with the residues F643 and L712. It was established the functional capacity of Tub A is to acetylated levels of  $\alpha$ -tubulin *in vitro* and *in vivo*, and these values were associated with ADMET profiles of plasma and brain. In psychiatric illnesses, the therapeutic potential of Tub A has been investigated. Additionally, reports claimed that Tub A has anti-inflammatory, anti-rheumatic, and anti-hepatitis C properties [111]. In rat models of MCAO (Middle Cerebral Artery Occlusion), it was recently revealed that post-ischemic Tub A therapy reduced brain infarction and neuronal cell death. As a result, there was an increase of the acetylated tubulin and FGF-21. The hypertensive stress-induced fibrosis-associated genes were found to be suppressed by Tub A activity and HDAC6 knockdown, pointing to a regulatory mechanism involving histone (H4) modification and phosphorylation of Smad 2/3 binding activity in fibrosis-related gene promoters. As demonstrated in HDAC6 mutant mice, Tub A was also said to target the TGF $\beta$ -PI3K-Akt pathway independently of the HDAC6 involvement, alleviating bleomycin-induced lung fibrosis. Palladium nanoparticles and tub A were discovered to increase apoptosis in human breast cancer cell lines, indicating a useful anticancer therapy [112] [113].



**Figure 8: Structure of HDAC6 Inhibitors**

For the first time, Santo et al. used the HDAC6-specific inhibitor ACY-1215 (Figure 8), and proteasome inhibitor bortezomib when used together in therapy demonstrated an HDAC6 IC<sub>50</sub> of 4.7 nM. HDAC6 specificity was demonstrated by ACY-1215 (Figure 8) via acetylating  $\alpha$ -tubulin even at 0.62 nM without affecting the acetylation status of histones. In xenograft mice models, bortezomib inhibited the aggresome and proteasome pathways, respectively, and this resulted in synergistic anti-MM action [114]. ACY-1215 (Figure 8) resembles the pan-HDACi SAHA as it too possesses a long-chain aliphatic linker and a ZBG for bidentate coordination, but it differs significantly from it in terms of its big cap group, which binds in the gap between HDAC6's L1 and L7 loops and is responsible for HDAC6 selectivity. When combined with carfilzomib, ricolinostat/ACY 1215 (Figure 8) was also reported to accelerate the mortality of multiple myeloma cells by inhibiting aggresome activity. Additionally, ricolinostat (Figure 8) and bendamustine have been investigated as potential anti-lymphoma agents. ACY-1215 (Figure 8) resembles the pan-HDACi SAHA in terms of its long-chain aliphatic linker and a bidentate ZBG, but it differs significantly from it in terms of its big cap group, which binds in the gap between HDAC6's L1 and L7 loops and causes a 12-fold selectivity towards HDAC6. With an IC<sub>50</sub> of 2.6 nM against HDAC6 and an almost 18-fold diminished effectiveness against the Class I HDACs, HDAC6i is more powerful than ricolinostat (in Figure 8). The HDAC6 inhibitory potency and selectivity of both of these compounds may be attributed to their 2-(diphenylamino) pyrimidine-5-carboxamide cap groups. It may be concluded from a comparison of these compounds that ACY-241 (Figure 8), which has an electron-withdrawing chloro atom as a substitution at one of the phenyl rings, is slightly more active than ACY-1215 (Figure 8). Clinical trials included a multiple myeloma phase Ib clinical trial [115] in solid tumours, ACY-241 (Figure 8) plus paclitaxel boosted the antiproliferative activity and hence increased cell death. [116].

For the treatment of various symptoms of chemotherapy-induced disorders such as peripheral neuropathy and cognitive impairment peripheral with ACY-1083 (Figure 9), the first brain penetrating HDAC6i [117].

The monodentate coordination that occurs in between  $\text{Zn}^{+2}$  to the hydroxamate ZBG was shown by the powerful HDAC6i ACY-1083 (Figure 9), which has an  $\text{IC}_{50}$  value of 3 nM. Between the F583 and F643 residues, the linker's aromatic pyrimidine ring is grooved. The chair conformation of the difluorocyclohexyl cap group and the hydroxyl side chain of the S531 residue present on the L2 loop are joined by a hydrogen bond by the secondary amino group. The fluorine atom interacts with the edge of residue F643. Van der Waals forces are responsible for phenyl group interaction with P464 and F583 respectively [118].

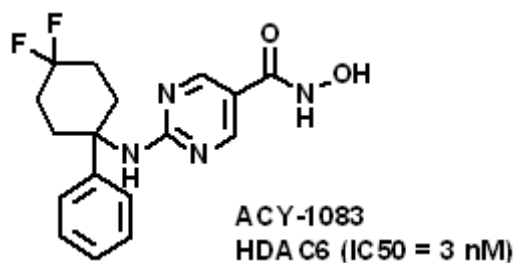


**Figure 9: Structure of HDAC6 Inhibitors**

Several new, physiologically active hydroxamic acids based on bicyclic imidazo[1,2- $\alpha$ ]pyridine was synthesised, and tested as very powerful and selective HDAC6i. ACY-1083 or (MAIP-032) (Figure 9) has high HDAC6 inhibitory properties it has 38 times more selectivity towards HDAC6 in comparison to HDAC1. By producing apoptotic activity at 1 nM, it demonstrated a potential anticancer activity with  $\text{IC}_{50}$  of 3.87 nM. The monodentate binding form of hydroxamate to  $\text{Zn}^{+2}$  was discovered by closely examining the ligand-receptor interaction of 60. ZBG's aromatic ring fit tightly into the aromatic groove that was created by the F583 and F643 residues. The para-substituted secondary amide group created hydrogen bonds with the S531 residue on the L2 loop and it increases HDAC6 selectivity.

For Alzheimer's disease, a group of chemicals with quinazoline-4-one as a cap and hydroxamate moiety (as ZBG) have been described as selective HDAC6i. As illustrated in Table 1, several compounds 15-33 were created and produced using various linkers or ZBG replacements in various places. The SAR investigation showed that the respective phenyl analogues (21-24) were less effective and less selective than the phenethyl or substituted phenethyl analogues (19-28). However, when the ZBG was linked to phenyl analogues, the

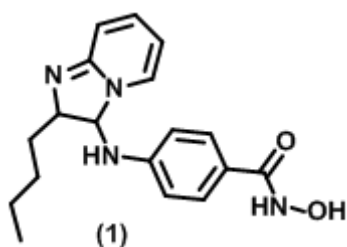
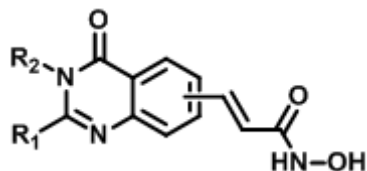


**Figure 10: Structure of HDAC6 Inhibitor**

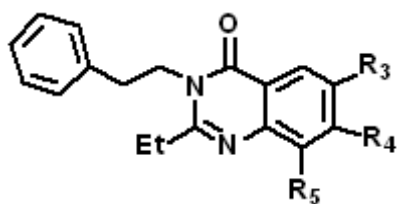
activity was shown to be strongest at the sixth position (2 vs. 1, 3, and 4). The alkyl groups of smaller sizes were effective for all of these highly potent HDAC6 inhibitors (11-2). To create some useful HDAC6 inhibitors (2-18, Table 2), the ZBG group was changed while preserving the ethyl and phenethyl groups at the R1 and R2 positions. Other substituents were added at the R3, R4, and R5 sites. Smaller electron withdrawing groups, like fluorine (atomic numbers 134–135), were shown to be advantageous in the R3 and R4 positions, whereas larger electron-withdrawing groups, like chlorine (atomic numbers 136), were completely unfavourable. However, the benzyl-hydroxamate group was shown to be advantageous at the R3 and R4 positions but unfavourable at the R5 position for HDAC6 inhibition and selectivity. With an IC<sub>50</sub> of 8 nM, compound 23 was the strongest HDAC inhibitor. With an HDAC6 IC<sub>50</sub> of 29 nM, compound 20 was discovered to be the most effective therapeutic candidate. *In vivo* investigations in mice models indicated a considerable improvement in hippocampal lesions induced by  $\beta$ -amyloid with compound 23. A novel series of quinazoline-2,4-dione core-based HDAC6 inhibitors were created using the scaffold hopping technique from quinazoline-4-one derivatives. With modified caps that improved functionality, the ZBG and linker were kept. The quinazoline-2,4-dione scaffold's N-1 position was changed to a linker that contained benzyl. Among all the derivatives, compound 21 (Figure 11) with a non-functionalized core had the highest efficacy (IC<sub>50</sub>= 4 nM) and selectivity for HDAC6 over HDAC1. Similar to 20, 21 (Figure 11) showed low activity against HDAC8 and an HDAC6 inhibitory value of 5.3 nM. Any changes to the core with new substituents or the addition of heterocycles to the ZBG significantly decreased the potency and had a detrimental impact on selectivity. Additionally, 20 showed a modest level of activity against non-small cell lung cancer (NSCLC) cells in *in vitro* experiments (IC<sub>50</sub>= 7.87 M), and it also showed anticancer efficacy when combined with paclitaxel. When used in conjunction with paclitaxel, compound 35 decreased the expression of PD-L1 in LL2 cells. When used in conjunction with paclitaxel, the *in vivo* experiments in the NSCLC mouse model

demonstrated significant tumour growth suppression. When compared to ACY-1215 and HDAC6i, compound 20 showed higher penetration in the mouse lung [119] [120].

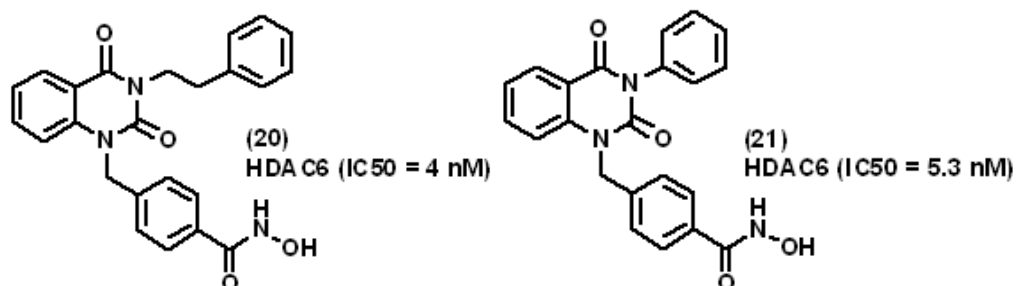
**Table 1: Structure of HDAC6 Inhibitors**



Compound	R1	R2	Linker (n)	HDAC6 IC50 (nM)
2	-CH3	Ph	5	1920
3	-CH3	Ph	6	22
4	-CH3	Ph	7	88
5	-CH3	Ph	8	690
6	-CH3	Ph(CH <sub>2</sub> )	7	24
7	-CH3	Ph(CH) <sub>2</sub>	7	29
8	-CH3	3-indolylethyl	7	15
9	-H	Ph(CH) <sub>2</sub>	7	35
10	-Et	Ph(CH) <sub>2</sub>	7	11
11	-Et	Ph(CH) <sub>3</sub>	7	33
12	c-Pr	Ph(CH) <sub>2</sub>	7	41
13	i-Pr	Ph(CH) <sub>2</sub>	7	13
14	-Et	4-CH <sub>3</sub> O- Ph(CH) <sub>2</sub>	7	41
15	-Et	4-F- Ph(CH) <sub>2</sub>	7	43

**Table 2: Structure of HDAC6 Inhibitors**

Compound	R1	R2	Linker (n)	HDAC6 IC <sub>50</sub> (nM)
16		Cl	H	747
17		H	H	11
18	H		H	9
19	H	H		79

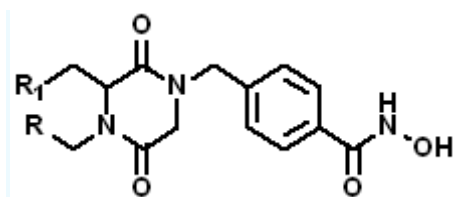
**Figure 11: Structure of HDAC6 Inhibitors**

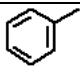
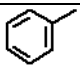
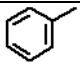
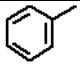
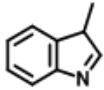
By using a rational drug design technique, further research of compound 20 (J22352) resulted in the identification of 21 (J27820) (Fig.11) as a highly selective HDAC6i. Compound 21, an analogue of 20, was created by the replacement of the 3-position of the phenylethyl group with a phenyl group to increase water solubility. It had an HDAC6 inhibitory value of 5.3 nM and was nearly 4 times less selective than compound 20 over other HDACs. A dose-dependent suppression was seen in the in vitro antiproliferative activity of 20 against U87MG glioma cells, with an IC<sub>50</sub> of 1.56 M, which was around 2.2-fold higher than that of SAHA.

Among a group of novel 2,5-diketopiperazine (DKP) compounds 22-26 (Table 3), it was made with cyclisation of two neighbouring peptide bonds and phenyl group attached to the N1 of DKP skeleton as ZBG. 26 was the most active HDAC6i and displayed selectivity over

Class I HDACs, HDAC11, and other Class II HDACs, compound 26 with an IC<sub>50</sub> value of 0.73 nM was the most selective HDAC6i. Due to its lipophilic character, which facilitates penetration into the cell membrane, compound 135 (IC<sub>50</sub> = 9.83 nM) demonstrated better efficacy than compound 26 in antiproliferative activities against hematological tumour cell lines. Compounds 23, 24, and 25) demonstrated superior antiproliferative activity against multiple myeloma cells in comparison to ACY-1215 with low micromolar IC<sub>50</sub> values. [121].

**Table 3: Structure of HDAC6 Inhibitors**



Compound	R	R1	Isomer	HDAC6 IC <sub>50</sub> (nM)
22	H		S	17.50
23	Ph		R	9.83
24	2-Cl-Ph		R	10.10
25	3-Cl-Ph		R	10.50
26	H		R	0.73

To overcome the genotoxicity linked to hydroxamates, a set of non-hydroxamate-based HDAC6 inhibitors were created with better selectivity from a previous set of HDAC6-selective inhibitors with the presence of mercaptoacetamide functioning as ZBG. As cap group 8-aminoquinoline and 1,2,3,4-tetrahydroquinoline were present and methylene chain with 4-7 atom length as a linker, their earlier studies discovered a molecule called MF-2-30 with low HDAC6 IC<sub>50</sub> value of 1.3 nM (Figure 12). It was discovered that MF-2-30 (27 in Figure 12) prefers HDAC6 by >3000 times more than HDAC1 [122].



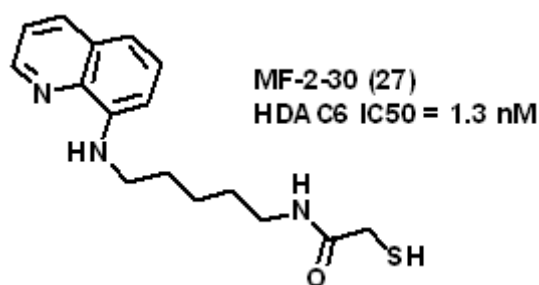
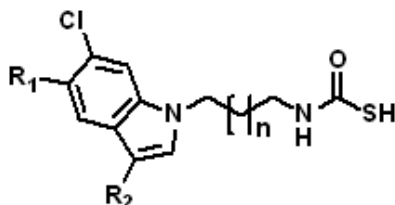


**Figure 12: Structure of HDAC6 Inhibitors**

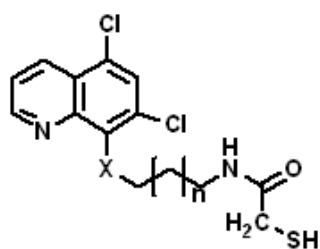
Lv and coworkers synthesised compounds substituted with halogen atoms into the quinoline indole cap-based mercaptoacetamide inhibitors (28, 29) to further improve its lipophilicity and blood-brain barrier (BBB) penetration capabilities. Compounds 28 and 29 from the series, which include quinoline or indole cap groups, respectively, have proven to be more potent and selective for HDAC6 than for HDAC1 and HDAC8. High Log BBB values of these compounds (Table 4) compared to MF-2-30 (Log BB = -0.27) showed greater BBB penetration capacities. Porter and coworkers presented the X-ray crystal structure of drHDAC6 CD2 and their interactions in the active site of CD2 drHDAC6 to explore the structure activity relationship of the mercaptoacetamide compounds. The phenyl rings present on residues F583 and F643 were closely linked with the aliphatic linker [123]. The indole cap group occupied the L1 loop pocket, which contributed to its HDAC6 selectivity. The substituted chlorine atoms on the indole cap group were present and interacted with the side chains of the H463 and P464 residues. The ZBG's thiol group underwent a negative charge change to become a thiolate, which is connected with the  $\text{Zn}^{2+}$  ion and caused the complex's distorted tetrahedral geometry. Additionally, the differences in their interactions were observed in the active site with the tandem histidine pair and chemical differences between the binding of hydroxamates and mercaptoacetamides to HDAC6 and HDAC8. HDAC6 and HDAC8 both had the same interactions with the -NH group for the histidine pair when it came to hydroxamates. The interaction of  $-\text{NH}_2$  with the second histidine of both HDAC6 and HDAC8 in the case of mercaptoacetamides, however, varied. It was found that the -NH group accepts H-bonds to HDAC6 and HDAC8's H573 and H141, respectively. Although the second histidine H574 of HDAC6 receives a donation from the -NH group, H142/143 of HDAC8 did not exhibit an H-bonding contact, highlighting the significance of these interactions in the increased specificity of mercaptoacetamides as compared to hydroxamates. The difference in the second histidine's basicity has been shown to have a significant impact

on the inhibitor's binding and catalysis, which can be used to take advantage of the mercaptoacetamide's preference for HDAC6 over class I HDACs like HDAC8 [124].

**Table 4: Structure of HDAC6 Inhibitors**



Compound	R1	R2	n	HDAC6 IC50 (nM)
28	Cl	H	3	11.4



Compound	X	n	Log-BB	HDAC6 IC50 (nM)
29	NH	2	0.17	11.4

## **Chapter 4: Rationale Behind Studies**

HDAC6 inhibitors have shown therapeutic activity in non-small cell lung cancer, triple-negative breast cancer, prostate cancer, ovarian cancer glioblastoma, melanoma, lymphoma, and several other forms of cancer [36]. HDAC 6 has an important role in several neurodegenerative diseases as it regulates aggresome formation, clearance of tau protein, abnormal protein folding. HDAC6 controls apoptosis and immune response to misfolded proteins and tumour formation. HDAC6 is the most unique structural aspect of the HDAC family, with two catalytic domains. One domain is more active than the other domain, however, it is dependent upon the less active domain to impart activity. The crystal structure of human HDAC6 has only been published a few years ago, showcasing some important conservation across species and thus proving its significance in evolution. Owing to its structural features and diverse presence across biochemical pathways it has been assumed by the scientific community to be a groundbreaking drug target in the treatment of not just different forms of cancer and neurodegenerative diseases but also in several other disorders and to understand the process of epigenetics even further. Five pan HDAC inhibitors are at present approved for the treatment of different forms of cancer; panobinostat, romidepsin, belinostat, vorinostat, and chidamide. Each inhibitors includes three parts - zinc chelating moiety, a hydrophobic linker group and a capping group mainly responsible for isoform selectivity. Several selective HDAC6 inhibitors are under trial in phase I & II for anticancer therapy, in most cases in combination with another anticancer drug. The motivation and ideas behind the studies is to find some structural properties of ligand molecule responsible for HDAC6 inhibition through several model-building and validation steps [41] [60].

## **Chapter 5: Materials and Methods**

## **5.1 What is Ligand Based QSAR:**

A computational technique called QSAR can be used to measure the relationship between a certain chemical or biological process and a set of substances' chemical structures. A single compound or a group of compounds that are known to be effective against a target is the starting point for ligand based drug development. Based on an understanding of structure activity relationships (SAR), the potency and other key features are then improved by creating suitable analogues. The techniques for using data from a drug target's existing ligands are described by ligand based approaches [126].

The step-by-step procedure of the model development are described in the following parts.

### **5.1.1 Dataset preparation**

A dataset of 105 molecules with HDAC6 inhibitory activity were collected from the literature. These are dual PDE5/ HDAC6 inhibitors have shown good activity against HDAC6, these molecules contain a sildenafil or tadalafil moiety core [3] [125-129]. The structures of the compounds of the dataset are given in the SMILES format in the supplementary section. The molecular structures were drawn using the ChemDraw Ultra 3.0. Afterward the structures were converted into their respective 3D structures by minimising energy in the ChemDraw 3D [130]. All of these 3D structures were further prepared in Discovery Studio using the 'Prepare Ligands for QSAR' protocol [131] to check for any duplicate structures present in the dataset. The complete dataset was converted into a single SDF file. The PaDEL descriptors software [132] was used to calculate the descriptors of the dataset using the SDF file format. A total of 6828 fingerprint descriptors (PubChem fingerprinter, KlekotaRoth fingerprinter, Substructuref ingerprinter and AtomPair2Dfingerprinter) were calculated. The HDAC6 inhibitory value ( $IC_{50}$ ) of the dataset was converted to their respective negative logarithm [ $pIC_{50} = -\log(IC_{50}/10^6)$ ]. The dataset is given in Table 5.

**Table 5:** Details SMILES of all the 105 compounds of the dataset

Cpd no	SMILES	<i>pIC<sub>50</sub></i>
1	<chem>CCCC1nn(C)c2C(=O)NC(=Nc12)c3cc(ccc3OCC)S(=O)(=O)N4CCN(CCC(=O)NO)CC4</chem>	5.627

2	<chem>CCCC1nn(C)c2C(=O)NC(=Nc12)c3ccc(ccc3OCC)S(=O)(=O)N4CCN(CCCC(=O)NO)CC4</chem>	6.444
3	<chem>CCCC1nn(C)c2C(=O)NC(=Nc12)c3ccc(ccc3OCC)S(=O)(=O)N4CCN(CC4)c5ncc(en5)C(=O)NO</chem>	6.572
4	<chem>CCCC1nn(C)c2C(=O)NC(=Nc12)c3ccc(ccc3OCC)S(=O)(=O)N4CCN(Cc5ccc(\C=C\C(=O)NO)cc5)CC4</chem>	7.051
5	<chem>CCCC1nn(C)c2C(=O)NC(=Nc12)c3ccc(ccc3OCC)S(=O)(=O)N4CCC(CCC(=O)NO)CC4</chem>	7.060
6	<chem>CCCC1nn(C)c2C(=O)NC(=Nc12)c3ccc(ccc3OCC)S(=O)(=O)NC4CCN(CC4)c5ncc(en5)C(=O)NO</chem>	7.229
7	<chem>CCCC1nn(C)c2C(=O)NC(=Nc12)c3ccc(ccc3OCC)S(=O)(=O)Nc4ccc(\C=C\C(=O)NO)cc4</chem>	7.076
8	<chem>CCCC1nn(C)c2C(=O)NC(=Nc12)c3ccc(NCCC(=O)NO)ccc3OCC</chem>	4.983
9	<chem>CCCC1nn(C)c2C(=O)NC(=Nc12)c3cc(N[C@@H]4CC[C@H](CC4)C(=O)NO)ccc3OCC</chem>	4.896
10	<chem>CCCC1nn(C)c2C(=O)NC(=Nc12)c3cc(NC4CCN(CC4)c5ccc(cc5)C(=O)NO)ccc3OCC</chem>	5.796
11	<chem>CCCC1nn(C)c2C(=O)NC(=Nc12)c3cc(NC4CCN(CC4)c5ncc(en5)C(=O)NO)ccc3OCC</chem>	6.356
12	<chem>CCCC1nn(C)c2C(=O)NC(=Nc12)c3cc(NCC4CCN(CC4)c5ncc(en5)C(=O)NO)ccc3OCC</chem>	6.149
13	<chem>CCCC1nn(C)c2C(=O)NC(=Nc12)c3ccc(ccc3OCC)N(C)C4CCN(CC4)c5ncc(en5)C(=O)NO</chem>	6.234
14	<chem>CCCC1nn(C)c2C(=O)NC(=Nc12)c3ccc(ccc3OCC)N4CCC(CC(=O)NO)CC4</chem>	5.963
15	<chem>CCCC1nn(C)c2C(=O)NC(=Nc12)c3ccc(ccc3OCC)N4CCC(CCC(=O)NO)CC4</chem>	5.975
16	<chem>CCCC1nn(C)c2C(=O)NC(=Nc12)c3ccc(ccc3OCC)N4CCCC(CC[C@H](C5)C(=O)NO)CC4</chem>	5.363
17	<chem>CCCC1nn(C)c2C(=O)NC(=Nc12)c3ccc(ccc3OCC)N4CCC[C@@]5(CC[C@H](CC5)C(=O)NO)C4</chem>	4.996
18	<chem>CCCC1nn(C)c2C(=O)NC(=Nc12)c3ccc(ccc3OCC)N4CCCC(CCN(CC5)c6ncc(en6)C(=O)NO)C4</chem>	5.721
19	<chem>CCCC1nn(C)c2C(=O)NC(=Nc12)c3cc(O[C@@H]4CC[C@H](CC4)C(=O)NO)ccc3OCC</chem>	5.633
20	<chem>CCCC1nn(C)c2C(=O)NC(=Nc12)c3ccc(Oc4ccc(cc4)C(=O)NO)ccc3OCC</chem>	6.708
21	<chem>CCCC1nn(C)c2C(=O)NC(=Nc12)c3cc(OC4CCN(CC4)c5ncc(en5)C(=O)NO)ccc3OCC</chem>	6.428
22	<chem>CCCC1nn(C)c2C(=O)NC(=Nc12)c3ccc(CCC(=O)NO)ccc3OCC</chem>	5.674
23	<chem>CCCC1nn(C)c2C(=O)NC(=Nc12)c3ccc(Cc4ccc(CCC(=O)NO)cc4)ccc3OCC</chem>	5.629
24	<chem>CCCC1nn(C)c2C(=O)NC(=Nc12)c3ccc(Cc4ccc(\C=C\C(=O)NO)cc4)ccc3OCC</chem>	5.747
25	<chem>CCCC1nn(C)c2C(=O)NC(=Nc12)c3cc(CN4CCN(CC4)c5ncc(en5)C(=O)NO)ccc3OCC</chem>	6.421
26	<chem>CCCC1nn(C)c2C(=O)NC(=Nc12)c3cc(CC4CCN(CC4)c5ncc(en5)C(=O)NO)ccc3OCC</chem>	5.903
27	<chem>CCCC1nn(C)c2C(=O)NC(=Nc12)c3cc(CC4CCN(CC4)c5ccc(en5)C(=O)NO)ccc3OCC</chem>	6.403
28	<chem>CCCC1nn(C)c2C(=O)NC(=Nc12)c3cc(C[C@@H]4CC[C@H](CC(=O)NO)CC4)ccc3OCC</chem>	6.463
29	<chem>CCCC1nn(C)c2C(=O)NC(=Nc12)c3cc(C[C@@H]4CC[C@H](CC4)C(=O)NO)ccc3OCC</chem>	6.288
30	<chem>CCCC1nn(C)c2C(=O)NC(=Nc12)c3cc(C[C@@H]4CC[C@H](CC4)C(=O)NO)ccc3OCC</chem>	7.244
31	<chem>CCCC1nn(C)c2C(=O)NC(=Nc12)c3cc(C[C@H]4CC[C@@H](C4)C(=O)NO)ccc3OCC</chem>	6.381
32	<chem>CCCC1nn(C)c2C(=O)NC(=Nc12)c3cc(C[C@@H]4C[C@@H](C4)C(=O)NO)ccc3OCC</chem>	6.845
33	<chem>CCCC1nn(C)c2C(=O)NC(=Nc12)c3cc(C[C@@H]4C[C@H](C4)C(=O)NO)ccc3OCC</chem>	6.900
34	<chem>CCCC1nn(C)c2C(=O)NC(=Nc12)c3cc(C[C@@H]4C[C@@H]4C(=O)NO)ccc3OCC</chem>	5.717
35	<chem>CCCC1nn(C)c2C(=O)NC(=Nc12)c3cc(CN4CCC(CC4)C(=O)NO)ccc3OCC</chem>	5.016
36	<chem>CCCC1nn(C)c2C(=O)NC(=Nc12)c3ccc(ccc3OCC)[C@@H]4C[C@H](C4)C(=O)NO</chem>	6.886
37	<chem>CCCC1nn(C)c2C(=O)NC(=Nc12)c3ccc(ccc3OCC)[C@@H]4C[C@H]4C(=O)NO</chem>	5.270
38	<chem>CCCC1nn(C)c2C(=O)NC(=Nc12)c3ccc(ccc3OCC)[C@@H]4CC[C@@H](CC(=O)NO)CC4</chem>	5.290
39	<chem>CCCC1nn(C)c2C(=O)NC(=Nc12)c3ccc(ccc3OCC)c4ccc(en4)C(=O)NO</chem>	7.102
40	<chem>CCCC1nn(C)c2C(=O)NC(=Nc12)c3ccc(ccc3OCC)c4ccc(nc4)C(=O)NO</chem>	6.065
41	<chem>CCCC1nn(C)c2C(=O)NC(=Nc12)c3ccc(ccc3OCC)c4oc(cc4)C(=O)NO</chem>	5.254
42	<chem>CCCC1nc(C)c2C(=O)NC(=Nn12)c3ccc(ccc3OCC)S(=O)(=O)N4CCN(CCCC(=O)NO)CC4</chem>	6.462
43	<chem>CCCC1nc(C)c2C(=O)NC(=Nn12)c3ccc(ccc3OCC)S(=O)(=O)N4CCN(CC4)c5ncc(en5)C(=O)NO</chem>	7.721
44	<chem>CCCC1nc(C)c2C(=O)NC(=Nn12)c3ccc(ccc3OCC)S(=O)(=O)N4CCN(Cc5ccc(\C=C\C(=O)NO)cc5)CC4</chem>	5.979
45	<chem>CCCC1nc(C)c2C(=O)NC(=Nn12)c3ccc(ccc3OCC)S(=O)(=O)Nc4ccc(\C=C\C(=O)NO)cc4</chem>	6.955
46	<chem>CCCC1nc(C)c2C(=O)NC(=Nn12)c3ccc(Cc4ccc(\C=C\C(=O)NO)cc4)ccc3OCC</chem>	6.312
47	<chem>CCCC1nc(C)c2C(=O)NC(=Nn12)c3cc(C[C@@H]4C[C@@H](C4)C(=O)NO)ccc3OCC</chem>	6.959
48	<chem>CCCC1nc(C)c2C(=O)NC(=Nn12)c3cc(ccc3OCC)[C@@H]4CC[C@H](CC4)C(=O)NO</chem>	5.007
49	<chem>ONC(=O)CCCN1CCC(CC1)N2CC(=O)N3[C@H](Cc4c([nH]c5ccccc45)[C@H]3c6ccc7OCOc7c6)C2=O</chem>	5.599
50	<chem>ONC(=O)c1cnc(nc1)N2CCC(CC2)N3CC(=O)N4[C@H](Cc5c([nH]c6ccccc56)[C@H]4c7ccc8OCOc8c7)C3=O</chem>	6.622
51	<chem>ONC(=O)\C=C\c1ccc(CN2CCC(CC2)N3CC(=O)N4[C@H](Cc5c([nH]c6ccccc56)[C@H]4c7ccc8OCOc8c7)C3=O)cc1</chem>	6.616
52	<chem>ONC(=O)c1cnc(nc1)N2CCC(CN3CC(=O)N4[C@H](Cc5c([nH]c6ccccc56)[C@H]4c7ccc8OCOc8c7)C3=O)CC2</chem>	7.114
53	<chem>CCCC1nn(C)c2C(=O)NC(=Nc12)c3cc(Cc4ccc(cc4)C(=O)NO)ccc3OCC</chem>	7.208
54	<chem>CCCC1nn(C)c2C(=O)NC(=Nc12)c3cc(Cc4ccc(CCC(=O)NO)cc4)ccc3OCC</chem>	6.790
55	<chem>CCCC1nn(C)c2C(=O)NC(=Nc12)c3cc(Cc4ccc(C(=O)NO)c(F)c4)ccc3OCC</chem>	6.848
56	<chem>CCCC1nn(C)c2C(=O)NC(=Nc12)c3cc(Cc4ccc(cc4F)C(=O)NO)ccc3OCC</chem>	7.060

57	CCc1nn(C)c2C(=O)NC(=Nc12)c3cc(ccc3OCC)[C@@H](O)c4ccc(cc4)C(=O)NO	7.051
58	CCc1nn(C)c2C(=O)NC(=Nc12)c3cc(ccc3OCC)[C@H](OC)c4ccc(cc4)C(=O)NO	7.114
59	CCc1nn(C)c2C(=O)NC(=Nc12)c3cc(Nc4ccc(cc4)C(=O)NO)ccc3OCC	7.180
60	CCc1nn(C)c2C(=O)NC(=Nc12)c3cc(OCc4ccc(cc4)C(=O)NO)ccc3OCC	7.481
61	CCc1nn(C)c2C(=O)NC(=Nc12)c3cc(Cc4oc(cc4)C(=O)NO)ccc3OCC	6.775
62	CCc1nn(C)c2C(=O)NC(=Nc12)c3cc(Cc4ccc(s4)C(=O)NO)ccc3OCC	7.824
63	CCc1nn(C)c2C(=O)NC(=Nc12)c3cc(ccc3OCC)C(=O)c4ccc(s4)C(=O)NO	6.717
64	CCc1nn(C)c2C(=O)NC(=Nc12)c3cc(ccc3OCC)c4ccc(cc4)C(=O)NO	7.377
65	CCc1nn(C)c2C(=O)NC(=Nc12)c3cc(ccc3OCC)c4ccc(CC(=O)NO)cc4	6.089
66	CCc1nn(C)c2C(=O)NC(=Nc12)c3cc(ccc3OCC)c4ccc(s4)C(=O)NO	7.432
67	CCc1nn(C)c2C(=O)NC(=Nc12)c3cc(ccc3OCC)C4=CC[C@H](CC4)C(=O)NO	6.469
68	CCc1nn(C)c2C(=O)NC(=Nc12)c3cc(ccc3OCC)C4=CC[C@H](CC(=O)NO)CC4	6.664
69	CCc1nn(C)c2C(=O)NC(=Nc12)c3cc(ccc3OCC)[C@H]4CC[C@H](CC4)C(=O)NO	5.264
70	CCc1nn(C)c2C(=O)NC(=Nc12)c3cc(ccc3OCC)N4CCC(CC4)C(=O)NO	5.928
71	CCc1nc(C)c2C(=O)NC(=Nn12)c3cc(Cc4ccc(cc4)C(=O)NO)ccc3OCC	6.592
72	CCc1nc(C)c2C(=O)NC(=Nn12)c3cc(Cc4ccc(s4)C(=O)NO)ccc3OCC	7.009
73	CCc1nc(C)c2C(=O)NC(=Nn12)c3cc(ccc3OCC)c4ccc(cc4)C(=O)NO	6.487
74	CCc1nn(C)c2C(=O)NC(=Nc12)c3cc(ccc3OCC)C(=O)CSC4=NC(=CC(=O)N4)O	5.115
75	C[C@H]1CN(C[C@H]2C[C@H](C2)C(=O)NO)C[C@H]1C3=Nc4c(cnn4C5CCCC5)C(=O)N3	6.652
76	C[C@H]1CN(Cc2ccc(cc2)C(=O)NO)C[C@H]1C3=Nc4c(cnn4C5CCCC5)C(=O)N3	7.398
77	C[C@H]1CN(Cc2ccc(cc2F)C(=O)NO)C[C@H]1C3=Nc4c(cnn4C5CCCC5)C(=O)N3	7.208
78	C[C@H]1CN(Cc2ccc(C(=O)NO)c(F)c2)C[C@H]1C3=Nc4c(cnn4C5CCCC5)C(=O)N3	6.772
79	C[C@H]1CN(Cc2ccc(s2)C(=O)NO)C[C@H]1C3=Nc4c(cnn4C5CCCC5)C(=O)N3	7.143
80	C[C@H]1CN(Cc2ncc(en2)C(=O)NO)C[C@H]1C3=Nc4c(cnn4C5CCCC5)C(=O)N3	7.319
81	C[C@H]1CN(Cc2ccc(en2)C(=O)NO)C[C@H]1C3=Nc4c(cnn4C5CCCC5)C(=O)N3	6.845
82	C[C@H]1CN(Cc2ccc(nc2)C(=O)NO)C[C@H]1C3=Nc4c(cnn4C5CCCC5)C(=O)N3	6.063
83	C[C@H]1N1CC(C1)Oc2ccc(cc2)C(=O)NO)C3=Nc4c(cnn4C5CCCC5)C(=O)N3	6.476
84	C[C@H]1N1CC(Cc2ccc(cc2)C(=O)NO)C1)C3=Nc4c(cnn4C5CCCC5)C(=O)N3	6.866
85	C[C@H]1N1CC(Cc2ccc(s2)C(=O)NO)C1)C3=Nc4c(cnn4C5CCCC5)C(=O)N3	7.377
86	C[C@H]1N1CC(C1)c2ccc(cc2)C(=O)NO)C3=Nc4c(cnn4C5CCCC5)C(=O)N3	7.161
87	C[C@H]1N1CC2(CC(CC(=O)NO)C2)C1)C3=Nc4c(cnn4C5CCCC5)C(=O)N3	6.564
88	C[C@H]1CN(Cc2ccc(\C=C\C(=O)NO)cc2)C[C@H]1C3=Nc4c(cnn4C5CCOCC5)C(=O)N3	6.294
89	C[C@H]1CN(C[C@H]2C[C@H](C2)C(=O)NO)C[C@H]1C3=Nc4c(cnn4C5CCOCC5)C(=O)N3	6.192
90	C[C@H]1CN(Cc2ncc(en2)c3ccc(cc3)C(=O)NO)C[C@H]1C4=Nc5c(cnn5C6CCOCC6)C(=O)N4	6.818
91	C[C@H]1CN(Cc2ccc(cc2)C(=O)NO)C[C@H]1C3=Nc4c(cnn4C5CCOCC5)C(=O)N3	6.719
92	C[C@H]1CN(Cc2ccc(s2)C(=O)NO)C[C@H]1C3=Nc4c(cnn4C5CCOCC5)C(=O)N3	6.824
93	C[C@H]1CN(Cc2ncc(en2)N3CCC(CC3)C(=O)NO)C[C@H]1C4=Nc5c(cnn5C6CCOCC6)C(=O)N4	5.818
94	C[C@H]1CN(C[C@H]1C2=Nc3c(cnn3C4CCOCC4)C(=O)N2)c5ccc(cc5)C(=O)NO	6.900
95	C[C@H]1CN(C[C@H]1C2=Nc3c(cnn3C4CCOCC4)C(=O)N2)[C@H]5C[C@H](C5)C(=O)NO	5.854
96	C[C@H]1CN(CC2CCN(CC2)c3ncc(en3)C(=O)NO)C[C@H]1C4=Nc5c(cnn5C6CCOCC6)C(=O)N4	6.305
97	C[C@H]1N1CC(C1)Oc2ccc(cc2)C(=O)NO)C3=Nc4c(cnn4C5CCOCC5)C(=O)N3	6.577
98	C[C@H]1N1CC(C1)Oc2ccc(\C=C\C(=O)NO)cc2)C3=Nc4c(cnn4C5CCOCC5)C(=O)N3	6.815
99	C[C@H]1N1CC(C1)Oc2ccc(cc2)N3CCC(CC3)C(=O)NO)C4=Nc5c(cnn5C6CCOCC6)C(=O)N4	5.071
100	C[C@H]1N1CC(C1)O[C@H]2C[C@H](C2)C(=O)NO)C3=Nc4c(cnn4C5CCOCC5)C(=O)N3	5.759
101	C[C@H]1N1CC(C1)N[C@H]2C[C@H](C2)C(=O)NO)C3=Nc4c(cnn4C5CCOCC5)C(=O)N3	4.959
102	C[C@H]1N1CC(Cc2ccc(cc2)C(=O)NO)C1)C3=Nc4c(cnn4C5CCOCC5)C(=O)N3	6.752
103	C[C@H]1N1CC(Cc2ccc(s2)C(=O)NO)C1)C3=Nc4c(cnn4C5CCOCC5)C(=O)N3	5.996
104	C[C@H]1N1CC(C1)Oc2ccc(cc2)c3ccc(cc3)C(=O)NO)C4=Nc5c(cnn5C6CCOCC6)C(=O)N4	6.620
105	C[C@H]1N1CC(C1)OC2CCN(CC2)c3ncc(en3)C(=O)NO)C4=Nc5c(cnn5C6CCOCC6)C(=O)N4	6.587

### 5.1.2 Data pre-treatment:

The descriptors files were then treated with software packages from the DTC lab for data pre-treatment, the variance cut-off was taken as 0.001 to remove the descriptors with constant



value, and the threshold cut-off was taken as 0.90 to remove the highly correlated descriptors [133].

### **5.1.3 Dataset Division:**

The dataset was divided into training and test set in a ratio of 4:1 with the help of the software protocol of Discovery Studio, the division was done based on the basis of the random per cluster method.

### **5.1.4 Model Development:**

Four different kinds of ligand based QSAR/SAR models were developed for the HDAC6 inhibitors.

### **5.1.5 SARpy Analysis:**

SARpy (SAR in Python) is a free, open-source, python-based analysis tool which uses a recursive algorithm. Structural Alerts (SA) are chemical substructures with known toxicological and biological properties. The following three steps are followed:

Fragmentation- A simple fragmentation algorithm is applied to recursively identify and detect the chemical substructures. The recursive algorithm checks for every possible combination of bond breakages directly through the SMILES string of the molecules.

Evaluation- Each substructure generated is validated on the training set as a potential SA. Each substructure is considered as either 'positive' or 'negative' based on the experimental activity label. The aim is to search for potential SAs with positive activity [134].

Likelihood ratio =  $(TP / FP) * (\text{negatives/positives})$

Rule set extraction- A reduced set of rules are obtained from a huge set of rule set. It is extracted in the manner 'IF contains <SA> THEN <apply label>' [135][136].

For our dataset the SARpy analysis was done by setting up the structural alert option in the W-SARpy; the minimum and maximum atom numbers as 2 and 18, respectively, and the minimum occurrence value of 3.

#### **5.1.6 Linear Discriminant Analysis (LDA):**

LDA was performed as a part of the classification based modelling to separate the higher active molecules from the lower active ones in a binary fashion. A *pIC*50 value of 6.30 was taken as a threshold value, molecules above this value were considered to be active and a value below 6.30 was considered to be inactive. For our dataset, the Linear discriminant analysis classification was computed using STATISTICA 7 software. A tolerance level of 0.001 is the basis of Fisher-Snedecor parameter (F) (F=4.0 inclusion and F= 3.9 for exclusion) [137]. The final descriptors were sorted out in the forward stepwise method, in which the software considers all the variables present in the dataset and chooses the contributing variables which represent the most discrimination between groups. Wilk's parameter ( $\lambda$ ) was used for initial statistical validation. In addition to that other statistical parameters such as squared Mahalanobis distance (d), chi-square ( $\chi^2$ ), MCC, Sensitivity (Se), Specificity (Sp), Accuracy (Ac), Precision (Pr), balanced accuracy (AUC<sub>b</sub>), F measure (F1), Youden's index ( $\gamma$ ), etc. were calculated by the formulas given in the supplementary material [138][139].

#### **5.1.7 Bayesian Classification:**

The Bayesian classification model is based on the naive Bayes theory given by the following equation:

$$P(c|x) = \frac{P(x|c)P(c)}{P(x)}$$

Where, c indicates the hypothesis of the model; P(c|x) is the posterior probability; P(x|c)

is the likelihood (probability of the data x if the hypothesis c is true); P(c) is the prior belief and P(x) is the evidenced data.

In this calculation certain descriptors to build the model- AlogP, Molecular Weight, Number of H donors, Number of H acceptors, Number of Rotable Bonds, Molecular Fractional Surface Area, and function class fingerprints of maximum diameter 6 (ECFP\_6) along with topological descriptors. The developed model was validated with a test set consisting of 20 compounds. The ECFP\_6 selected good fingerprints which are favourable for inhibition of HDAC6 activity, with the same descriptor bad fingerprints were also identified which are poor for HDAC6 inhibition activity.

### **5.1.8 Recursive Partitioning (RP):**

It is a multivariable analysis method. In this method a decision tree is constructed that classifies members of the population under consideration based on contrariety dependent variable Y (inhibition class) and independent variables X (molecular properties and molecular fingerprints) [140]. RP uses a set of hierarchical rules to classify the data and split it into smaller subsets based on the cut-off value of a particular descriptor. Every subsample is called a node. RP oversplits the data and then backtracks the tree [141]. The depth of the decision tree determines the performance of the RP model. However, a large depth of the tree increases the chance of overfitting [142].

## **5.2 What Is Structure Based Drug Discovery:**

Designing and refining a chemical structure to find a substance appropriate for clinical testing that is a therapeutic candidate—is known as structure-based drug design. It is predicated on understanding the three-dimensional structure of the drug and how its shape and charge interact with its biological target to ultimately provide a therapeutic effect [151].

### **5.2.1 Molecular Docking:**

Zinc is an essential part of the HDAC family of enzymes, they are known as zinc metalloproteins, a large group of enzymes containing zinc atoms bound to specific polypeptide chains. The zinc atom functions as a metal ion cofactor, taking part in several biological activities. Most force fields use a nonbonded model of Stote and Karplus to describe the metal coordination, here columb and lennard-jones interactions are used to describe the model. It fails to explain the pervasiveness of histidine and cysteine as the most common zinc coordinating amino acid residues over amino acids like glutamate, and aspartate with a more electronegative carboxylate group [143]. Bonded models are not ideal to describe the tetrahedral geometry of zinc atoms through which most of the ligands form explicit bonds, the tetrahedral zinc coordination is the most common orientation in biological systems [144]. With a standard Autodock force field, the placement of nitrogen hydrogen bond acceptor (NA) was found very close to the ideal position in the zinc coordination, however, Oxygen (OA), Sulfur (SA), and nitrogen non-hydrogen bond acceptor (N) deviated further deviated from the ideal coordination position. In the new Autodock4 Zn forcefield the columbic electrostatic potential was set as zero and replaced by a new potential energy term for OA,SA, and n atom types. A new directional tetrahedral potential  $V_{TZ,NA}$  was split into

two parts. One was the attractive component represented by the new pseudoatom TZ and the repulsive component was arbitrated by the zinc atom. The pseudo atom only interacts with NA, no other types of interaction is permitted. The zinc-hydrogen pairwise interaction was also discarded to prevent clashes that would interfere with the interactions between other groups such as amino-sulfonamide or hydroxyl-zinc.

Autodock Vina 1.2.3 version was used to implement the Autodock4ZN force field with exhaustiveness and the number of modes set as 20 in both cases [145][146]. The exhaustiveness is the number of random independent montecarlo searches. The docking was done with the compound 62 of the dataset (HDAC6 IC<sub>50</sub> = 15 nM) and chain A of catalytic domain 2 of HDAC6 (PDB ID: 5EDU) [156].

### **5.2.2 Molecular Dynamics:**

Protein flexibility plays a crucial role in interaction with the ligand. The cost and time-consuming nature of producing them has prompted to look for computational methods that can forecast protein movements. Unfortunately, even the finest supercomputers frequently struggle to handle the sophisticated calculations needed to explain the complicated quantum-mechanical motions and chemical reactions of huge molecular systems. The purpose of molecular dynamics (MD) simulations is to get beyond this restriction by simulating atomic motions with straightforward Newtonian approximations that are less computationally challenging. The molecular system is first computer-modelled using information from nuclear magnetic resonance (NMR), crystallography, or homology modelling [147].

In brief, the forces from interactions between bonded and unbound atoms are involved. Simple virtual springs are used to simulate chemical bonds and atomic angles, to simulate dihedral angles (rotations about bonds) a sinusoidal function is implemented, it represents the energy differences between eclipsed and staggered conformations. Coulomb's law, and van der Waals interactions are used to model Non-bonded forces resulting from charged (electrostatic) interactions, the Lennard-Jones 6-12 potential is also used. These energy parameters and terms are parameterised to fit quantum-mechanical calculations and experimental data to simulate the actual behaviour of real molecules in motion. This parameterisation entails choosing the best partial atomic charges for computing electrostatic interaction energies, choosing the appropriate van der Waals atomic radii, etc. The springs that describe chemical bonding and atomic angles should have the ideal stiffness and lengths. Due to the way they describe the contributions of the numerous atomic forces that control

molecular dynamics, these parameters are collectively referred to as a "force field." AMBER, CHARMM, and GROMOS are a few force fields that are frequently employed in molecular dynamics simulations. These are similar in general but differ primarily in how they are parameterized. Following the calculation of the forces acting on each of the system's atoms, the locations of these atoms are changed in accordance with Newton's equations of motion[158].

The Root-Mean-Square-Deviation (RMSD) and the Root-Mean-Square-Fluctuations (RMSF) are the two most popular metrics for structural fluctuations. The average displacement of the atoms at a simulation instant about a reference structure—typically the simulation's first frame or the crystallographic structure is known as the RMSD. The RMSF is an averaged measure of the displacement of a specific atom, or group of atoms, with respect to the reference structure. The investigation of the structure's time-dependent motions can benefit from the RMSD. The rigid-body alignment of the structures to reference coordinates in each frame of the simulation is a necessary step in the typical RMSD or RMSF computations for proteins. The existence of subsets of the structure with large conformational variations has a significant impact on rigid-body alignment. High RMSDs or RMSFs may signify that the entire structure fluctuates or they may just represent significant displacements of a tiny structural subset within a rigid overall structure. It is more typical to observe significant RMSDs associated with huge fluctuations of structural subsets that do not reflect the structural fluctuations of the macromolecule as a whole in larger-scale structures examined using MD simulations. As a result, alignment techniques that aid in differentiating between flexible and rigid structural subgroups will become more crucial for the interpretation of MD simulations [149].

Free energy calculations frequently use computational techniques like Molecular Mechanics/Poisson-Boltzmann Surface Area (MM/PBSA) and Molecular Mechanics/Generalized Born Surface Area (MM/GBSA), which integrate molecular mechanics energy and implicit solvation models. The MM/PBSA and MM/GBSA are more computationally effective when compared to rigorous approaches like the free energy perturbation (FEP) and thermodynamic integration (TI) methods. The linear interaction energy (LIE) method is a related strategy that estimates the absolute binding free energy by averaging interaction energy from MD simulations. LIE limits the simulations to the two endpoints of ligand binding, just like MM/PBSA and MM/GBSA. MM/PBSA and MM/GBSA do not require a huge training set to fit distinct parameters for each energy

component, in contrast to the majority of empirical scoring systems used in molecular docking.

The binding free energy ( $\Delta G_{\text{bind}}$ ) between a ligand (L) and a receptor (R) to form a complex RL is calculated as

$$\Delta G_{\text{bind}} = \Delta H - T\Delta S \approx \Delta E_{\text{MM}} + \Delta G_{\text{sol}} - T\Delta S$$

$$\Delta E_{\text{MM}} = \Delta E_{\text{internal}} + \Delta E_{\text{electrostatic}} + \Delta E_{\text{vdw}}$$

$$\Delta G_{\text{sol}} = \Delta G_{\text{PB/GB}} + \Delta G_{\text{SA}}$$

where  $\Delta E_{\text{MM}}$ ,  $\Delta G_{\text{sol}}$  and  $-T\Delta S$  are the changes of the gas phase MM energy, the solvation free energy, and the conformational entropy upon binding, respectively.  $\Delta E_{\text{MM}}$  includes  $\Delta E_{\text{internal}}$  (bond, angle, and dihedral energies),  $\Delta E_{\text{electrostatic}}$  (electrostatic), and  $\Delta E_{\text{vdw}}$  (van der Waals) energies.  $\Delta G_{\text{sol}}$  is the sum of electrostatic solvation energy (polar contribution),  $\Delta G_{\text{PB/GB}}$ , and the nonelectrostatic solvation component (nonpolar contribution),  $\Delta G_{\text{SA}}$ .

While the nonpolar energy is determined using the GB or PB model, solvent accessible surface area (SASA) is used to estimate the polar contribution. Typically, a set of conformational snapshots obtained from an MD simulations are used in normal-mode analysis to calculate the conformational entropy change  $-TS$ . Additionally, both MM/PBSA and MM/GBSA permit thorough free energy decomposition into contributions coming from various atom groups or kinds of interactions [150].

For the Molecular Dynamics (MD) simulations, Gromacs 2023.1 version was used in an Ubuntu Linux operating system based computer [148]. The same HDAC6 protein with PDB ID 5EDU was used. The best active molecule of the dataset (cpd 062) was used for the MD simulation. 5EDU represents the CD2 of the HDAC6 protein, its chain A was used for the experiment. Pose number 07 ligand the molecule, that is the best docking pose with minimal distance from the active zinc site was used. CHARMM36 force field [151] was used for generating parameters and topology for the protein. For generating the ligand topology from mol2 file, the SWISSPARAM webserver was used. MD simulations system was solvated with the Three-site (TIP3P) water model, with a triclinical box configuration with a distance of 1nm from all the directions. The prepared system was then neutralized with sufficient numbers of counter ions in the form of  $\text{Na}^+/\text{Cl}^-$  ions. Energy minimisation was performed on the system with the steepest descent algorithm. Post energy minimisation, a step called

position restraint was carried out under NVT and NPT conditions for 1 ns each. The system was kept at a constant volume (100 ps) and temperature (300 K) during NVT equilibration using the Berendsen thermostat algorithm. Additionally, NPT equilibration was carried out using a Parrinello-Rahman barostat to maintain a constant pressure of 1 bar for 100 ps. Finally MD simulation of 100 ns was carried out with the in-built gmx MD run command with coordinates saved at every 100 ps. For the visualisation of the system, the VMD program was used and post-simulation graphs were made with plotting tool GRACE [154].

## **Chapter 6: Result and Discussion**



## 6.1 Result and Validation

After completing the classification based models different predictions were observed it as given in Tables 6-10.

**Table 6: Internal and external parameters of LDA SARpy and Bayesian classification**

Method	Dataset	True positive	True Negative	False Positive	False Negative
<b>LDA</b>	Train	46	25	3	6
	Test	10	7	4	4
<b>SARpy</b>	Train	44	24	1	14
	Test	14	3	3	0
<b>Bayesian</b>	Train	57	19	6	3
	Test	12	3	3	2
<b>RP</b>	Train	44	21	4	16
	Test	14	2	4	0

### 6.1.2 SARpy Analysis

In the SARpy analysis an active ruleset with 8 substructural features was obtained, they are given in table 7 on the next page. Out of all the molecules in the training set, 51 structures matched by the application of 8 rules obtained through mining the structural alerts, after applying the ruleset from the training data in the test set 15 structures matched from the test set.

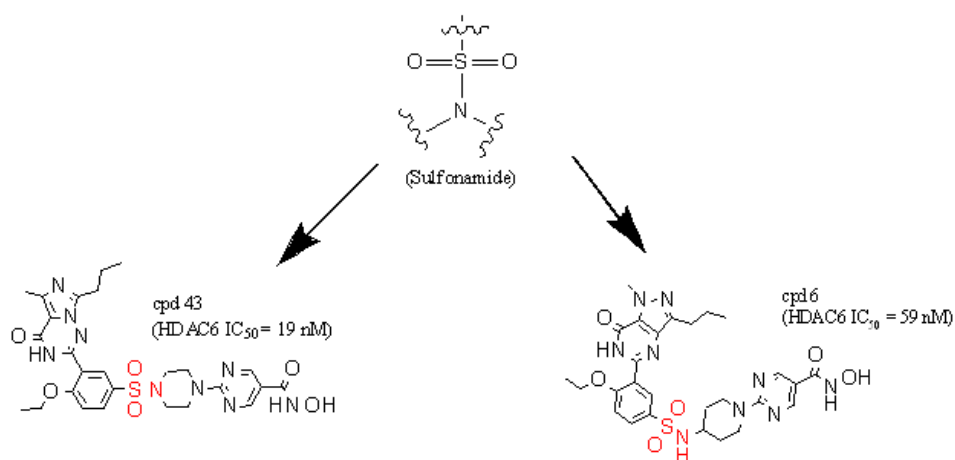


**Figure 13: Presence of substructure Sulfonamide (LR 5.29) in compound 43 and 6**

**Table 7: Active Ruleset of SARpy analysis**

Active Ruleset	Substructure	LR
<chem>1ccc(cc1)C(=O)NO</chem>	N-Hydroxy-4-methylbenzamide	Infinite
<chem>S(=O)(=O)N</chem>	Sulfonamide	5.29
<chem>c1ccc(cc1)C(=O)NO</chem>	N-Hydroxybenzamide	9.41
<chem>C1CCCC1</chem>	Cyclopentane	5.29
<chem>c1ccc(C(=O)NO)s1</chem>	2-Thiophenehydroxamic acid	2.94
<chem>O(c1ccc(cc1)C=CC)</chem>	p-Hydroxypropenylbenzene	Infinite
<chem>N1CCN(CC1)CCC</chem>	1-Propylpiperzine	2.94
<chem>c1ncc(cn1)C(=O)NO</chem>	N-Hydroxy-5-pyrimidinecarboxamide	1.76

Structural alert 1ccc(cc1)C(=O)NO or N-Hydroxy-4-methylbenzamide is present among compound number 73, 86 in the training set and 78,93 and 104 of the test set. S(=O)(=O)N alert is present in the compound number 2-7, 42-45 of the training set and compound no 1 of the test set. Presence of phenyl and heterocyclic rings as linker group increases the activity as seen in case of compound number 6 and 43 (Figure 13). c1ncc(cn1)C(=O)NO as structural alert represent N-Hydroxy-5-pyrimidinecarboxamide. The linker and zinc binding group, pyrimidine and hydroxamic acid respectively are present together in this SA. Compounds 82, 53 with the same structural alert show good potency against HDAC6. The validation matrices are given in the Table 9.

**Table 9: SARpy validation matrices value**

Parameter	Train	Test
Sensitivity	0.84	0.75
Accuracy	0.80	0.73
Specificity	0.73	0.70
F1	0.84	0.77
MCC	0.57	0.44

### **6.1.3 Linear Discriminant Analysis (LDA)**

LDA was performed as a part of the classification based modelling to separate the higher active molecules from the lower active ones in a binary fashion.  $pIC_{50}$  value of 6.30 was taken as the threshold value, molecules above this value was considered to be active and value below were considered to be inactive.

The LDA-QSAR model is described below:

$$\Delta P = -7.802 + 10.684 * KRFP3943 + 8.637 * KRFP3295 + 14.328 * KRFP4498 + 4.799 * KRFP4521 + 14.101 * KRFP3104 - 5.735 * KRFP3712 - 5.458 * AD2D102 + 5.350 * AD2D560$$

$$N_{Train} = 80 \quad \lambda = 0.36 \quad F(8,71) = 15.728 \quad p < 0.000 \quad R_c = 0.799 \quad \text{Squared Mahalanobis Distance} = 7.595 \quad MCC_{train} = 0.761 \quad N_{Test} = 27 \quad MCC_{Test} = 0.25.$$

Different validation matrices are used to assess the quality and fitness of the classification-based QSAR models. Wilk's lambda ( $\lambda$ ) is a distance based parameter for testing the significance of the discriminant function [143].

The ROC was plotted by taking the (1-specificity) along the x-axis and sensitivity along the Y-axis. ROC graph Euclidean distance (ROCED) and ROCED corrected with Fitness ( $\lambda$ ) function (ROCFIT) were calculated as 3.353 and 9.313, respectively. ROCED value greater than 4 is considered as a bad classifier, value above 2.5 as random classifier and for a perfect classifier the value should be 0. [144]

Youden's index ( $\gamma$ ), and likelihoods [both positive ( $p_+$ ) and negative likelihoods ( $p_-$ )] were calculated. To avoid failure of the model a higher value of Youden's index is desirable. The values are provided in table 10 [144]. Eight fingerprint descriptors in the final model were identified as significant contributing factors of the LDA model. Six descriptors among them contributed positively in the activity of our dataset while two descriptors contributed negatively. The positive contributions were KRFP3943 (compound that showed activity- cpd11), KRFP3295 (compounds that showed positive activity- cpd2, 4, 5, 7, 8, 28, 30-32, 36, 42, 45, 56, 51-53, 55, 65, 68, 69, 71, 72, 77, 89, 96, 100) , KRFP4498 ( compounds with the presence of substructure- cpd40,84), KRFP4521 (compounds with the presence of the substructure cpd22,23,37), KRFP3104 (compounds that showed activity were 49,71), AD2D560 ( compounds that were active cpd2-7, 20, 21, 39, 42, 43, 45, 51-53, 61, 79, 80, 82, 83, 85, 87-89, 92, 94, 98, 99). Two descriptors contributed negatively in our model, KRFP3712 (inactive compounds are cpd 15-17, 49, 71) and AD2D102 (compounds that were inactive in the training set - cpd44, 50). Compounds with fingerprint KRFP4521 showing positive activity are given in Figure 14. The descriptors with positive and negative contribution as per the LDA model are given in table 9 and the validation matrices are given in table 10.

**Table 9: Descriptors used in the LDA-QSAR Model:**

Descriptor	Definition	Contribution
KRFP3943	Presence of N-methylaniline group	Positive
KRFP3295	Presence of acetamide group	Positive
KRFP4498	Presence of 2-formylpyridine group	Positive
KRFP4521	Presence of 3-phenylpropanal group	Positive
KRFP3104	Presence of cyclohexylbenzene group	Positive
KRFP3712	Presence of hexane group	Negative
AD2D102	Presence of O-O at topological distance 2	Negative
AD2D560	Presence of N-O at topological distance 8	Positive

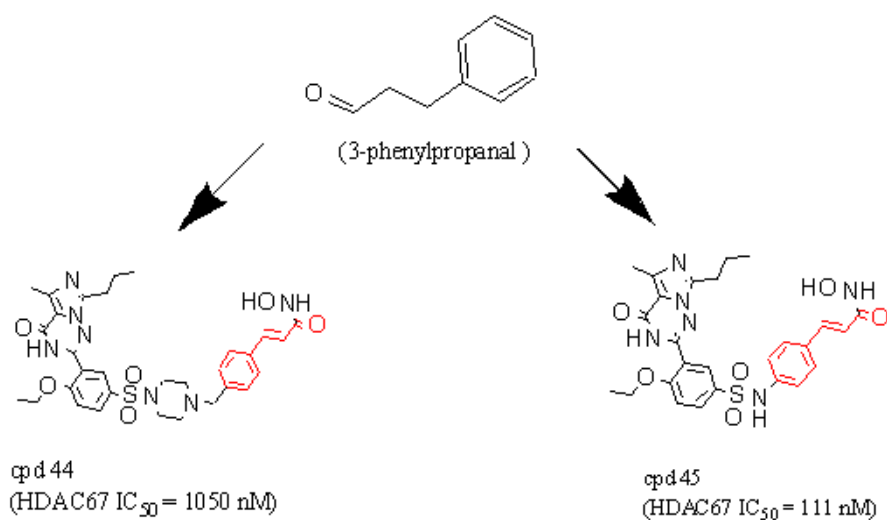
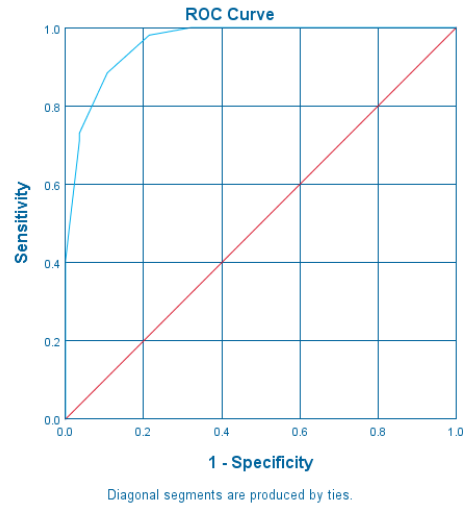


**Figure 14: Presence of fingerprint KRFP4521 in compound 44 and 45**

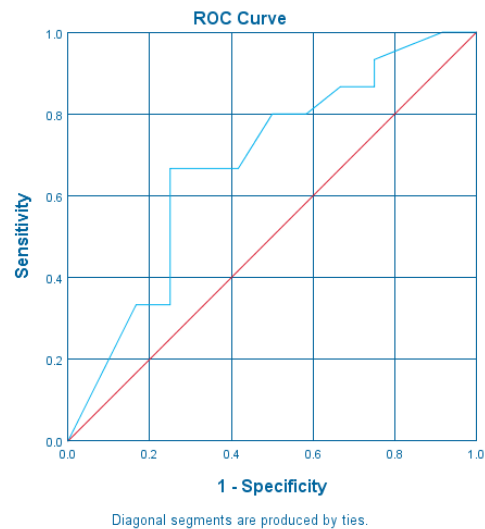
**Table 10: LDA validation matrices value**

Dataset	Se	Sp	Pr	Acc	MCC	F1	AUC <sub>b</sub>	$\gamma$	$\rho_+$	$\rho_-$
<b>Train</b>	0.884	0.892	0.938	0.887	0.761	0.91	0.88	0.776	8.18	0.13
<b>Test</b>	0.667	0.583	0.667	0.629	0.25	0.667	0.625	0.25	1.56	0.571

The calculated area under the ROC curve (AUROC) (Figure 15) for the training set was 0.962 and for the test set it was 0.681. The acceptable value for the AUROC must be above 0.5, so both of our training and test sets passed the acceptable range and they support the reliability of our calculated equation [144].



(A)



(B)

**Figure 15: The ROC curve of the LDA model: (A) Training set and (B) Test set**

#### **6.1.4 Bayesian Classification Analysis**

The training set showed a leave-five-out cross-validated ROC score ( $ROC_{5CV}$ ) of 0.665 it also showed accuracy(acc) of 0.894, sensitivity(se) of 0.950, Specificity(sp) of 0.760, and concordance of 0.894.

The test set used for external validation showed a cross-validation ROC value of 0.750, the value of Specificity is 0.500, value of Sensitivity came out as 0.857 and Concordance value was 0.750 and Accuracy came out as 0.750. The ROC plot is shown in Figure 19. The ECFP\_6 fingerprint selected the 20 most favourable fingerprints which are favourable for HDAC6 inhibition and 20 bad fingerprints detrimental to the inhibition activity (Figure 16 & 18, respectively). Favourable good features include chemical structures like branched aliphatic chains, aromatic ring derivatives, nitro cyclopentane, pyrazole derivatives shown in Figure 16. Compounds with high HDAC6 inhibitory activity and with the presence of Sulphur atom (Bayesian fingerprint G12), 2-Thiophene hydroxamic acid (Bayesian fingerprint G11), Thiophene group and its derivatives (Bayesian fingerprint G15, G17) are shown in Figure 17.

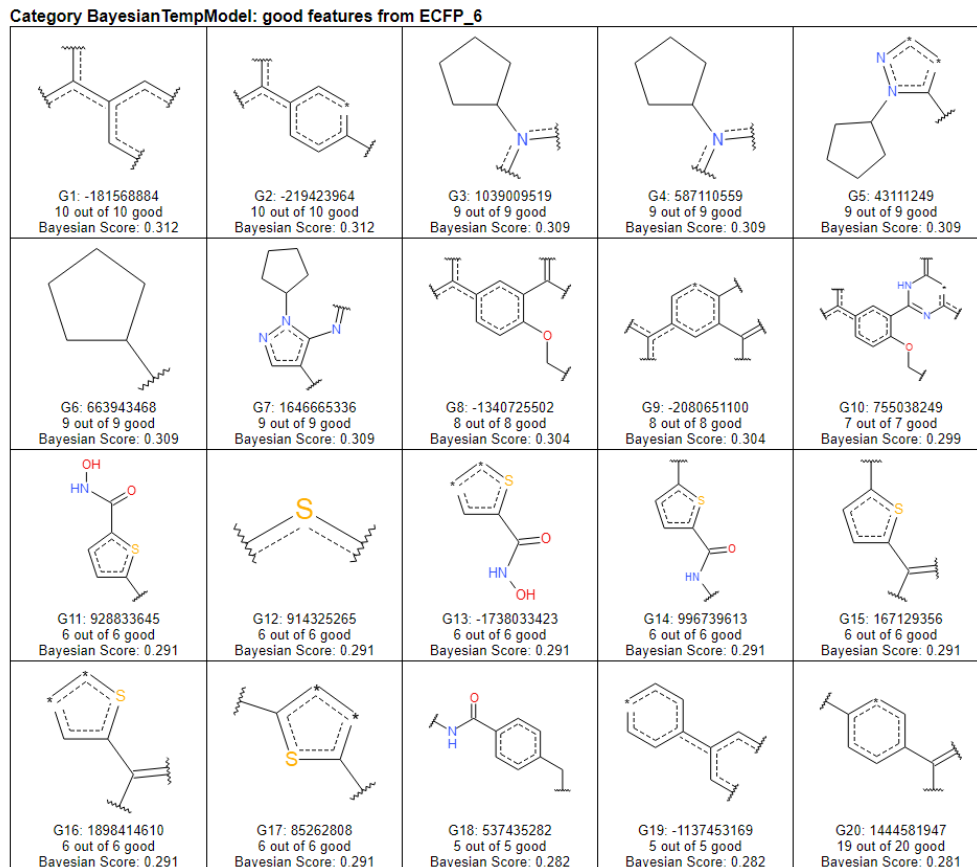


**Figure 16: Good fingerprints generated in the Bayesian Model**

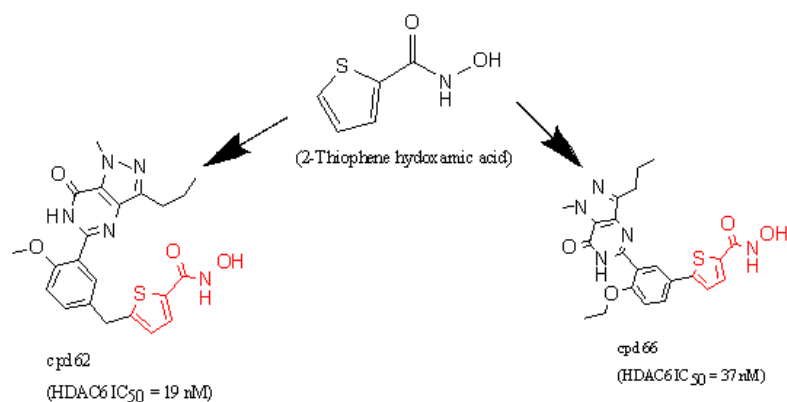


**Figure 17: Presence of 2-Thiophene hydroxamic acid (Bayesian fingerprint G11) in compound 62 and 66**

**Category BayesianTempModel: bad features from ECFP\_6**

 B1: -2137232509 0 out of 7 good Bayesian Score: -1.781	 B2: -175021654 0 out of 7 good Bayesian Score: -1.781	 B3: 296507651 0 out of 5 good Bayesian Score: -1.510	 B4: 2033861942 0 out of 5 good Bayesian Score: -1.510	 B5: -180013187 0 out of 5 good Bayesian Score: -1.510
 B6: -98352723 0 out of 5 good Bayesian Score: -1.510	 B7: -1625612070 0 out of 5 good Bayesian Score: -1.510	 B8: 1020564572 0 out of 5 good Bayesian Score: -1.510	 B9: -1747928788 0 out of 5 good Bayesian Score: -1.510	 B10: 412256466 0 out of 3 good Bayesian Score: -1.136
 B11: 408216150 0 out of 3 good Bayesian Score: -1.136	 B12: 215529134 0 out of 3 good Bayesian Score: -1.136	 B13: -1106731637 0 out of 3 good Bayesian Score: -1.136	 B14: 716757593 0 out of 3 good Bayesian Score: -1.136	 B15: -337325387 2 out of 9 good Bayesian Score: -0.895
 B16: 1991693541 2 out of 9 good Bayesian Score: -0.895	 B17: -1208463514 0 out of 2 good Bayesian Score: -0.880	 B18: 357764963 0 out of 2 good Bayesian Score: -0.880	 B19: -1385898624 0 out of 2 good Bayesian Score: -0.880	 B20: 1591615568 0 out of 2 good Bayesian Score: -0.880

**Figure 18: Bad fingerprints generated in the Bayesian Model**



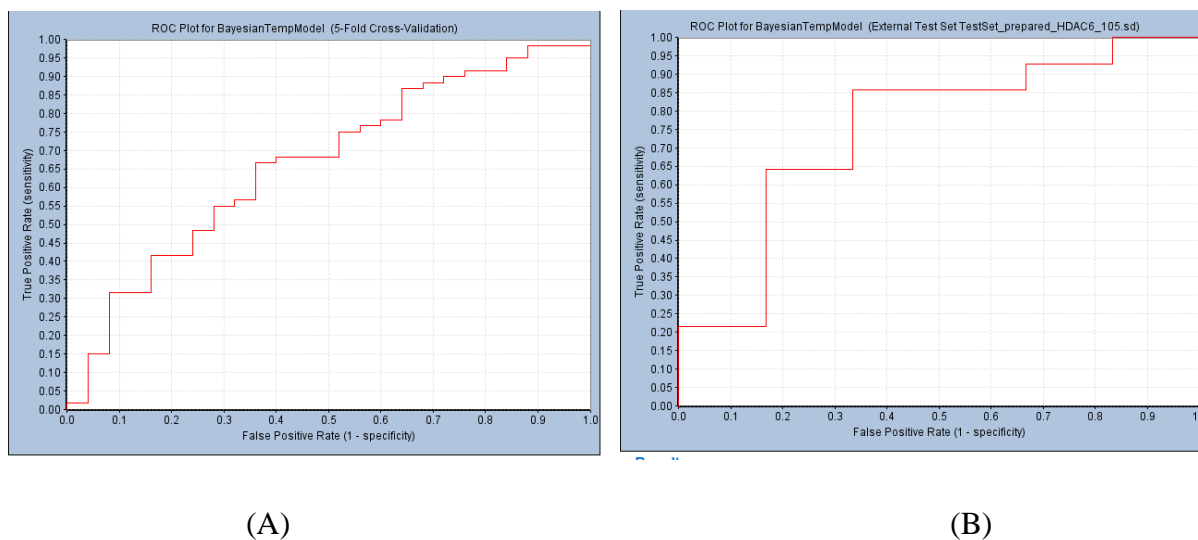


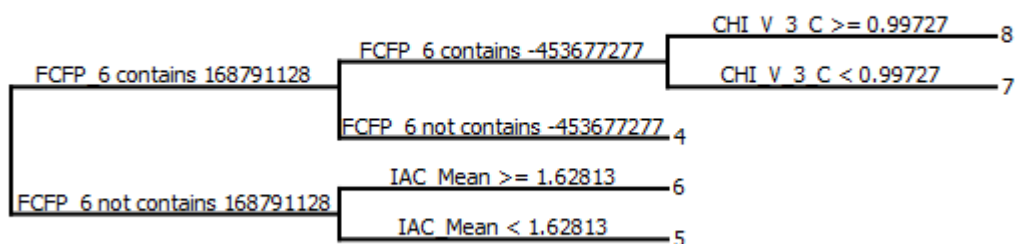
**Figure 19: The ROC plot of the training set (A) and test set (B) of the Bayesian model**

**Table 11: Bayesian and RP matrices value**

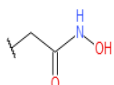
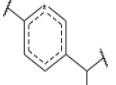
Model	Set	Acc	Sp	Se	MCC
<b>Bayesian</b>	Train	0.894	0.760	0.950	0.738
	Test	0.75	0.500	0.857	0.308
<b>RP</b>	Train	0.764	0.840	0.733	0.526
	Test	0.800	0.333	1.00	0.509

### **6.1.5 Recursive Partitioning (RP) Analysis**

Three different decision trees were constructed based on molecular properties (MP) and FCFP<sub>6</sub>. The model was built with molecular properties; AlogP, MW, nHBD, nHBA, nHBD, nRB, nR, nAR, and Molecular Fraction Polar Surface Area (MFPSA). Tree 1 with 5 (Figure 20) leaves was chosen as the best tree based on cross-validated ROC performed on the test set containing 20 molecules, the (ROC<sub>CV</sub>) score of 0.761 legitimates the model. Based on this tree FCFP<sub>6</sub> was chosen as the best descriptor to describe the activity against HDAC6. The model was further validated by the same external test set with a ROC score of 0.642. The fingerprints obtained from the model are given in Figure 21 and compounds showing good inhibitory activity with the fingerprint hydroxamate are given in Figure 22.



**Figure 20: TREE-1 of the RP prediction for the Training Set**

Fingerprint Features Used in Splitting Trees				
				
FCFP_6 168791128	FCFP_6 -453677277			

**Figure 21: Fingerprint features generated in the recursive Partitioning model**

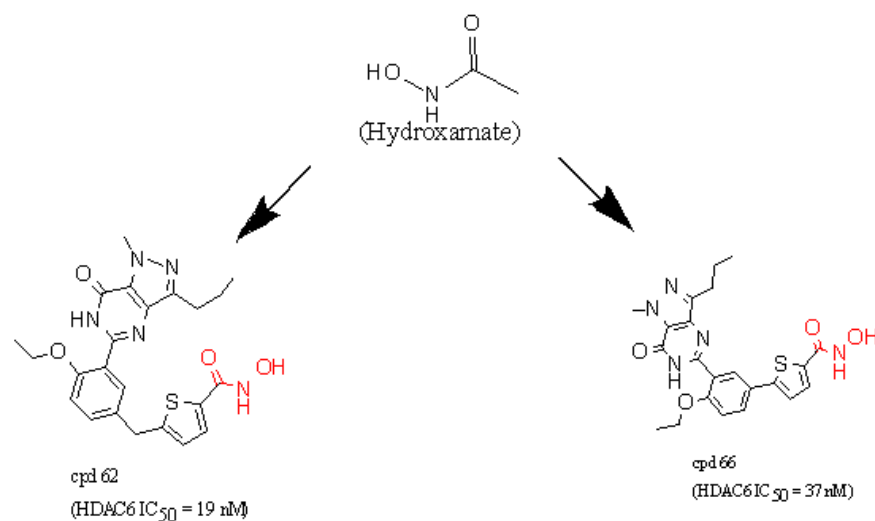


**Figure 22: Presence of hydroxamate in compound 62 and 66**

Results were analysed with tools like Pymol and GRACE by visualisation of protein-ligand complex and plotting subsequent graphs.

#### **6.1.6 Molecular Docking**

The docking scores of all the 20 poses of the compound 62 are given in table 12. Docking pose number 7 was used as the best conformation based on observation of its interaction with the protein (Figure 24, 25). The oxygen atom of the hydroxamate group formed a Zn-O bond with the zinc atom of the protein chain. It's interesting to note that His651 and this oxygen atom also create a hydrogen bond. This pairing is remarkably stable. It's also important to point out that the hydroxamate group creates two hydrogen bonds with Gly619 and His610. In addition, compound 62 and HDAC6 have a robust hydrophobic contact. Between Phe680 and the hydroxamate group-containing benzene ring, Phe620, and a five-membered ring, there is a pi-pi interaction contact. Additionally, Pro748, Pro501, and the compound benzene ring with  $-NH_2$  interact hydrophobically. When ligands attach to receptors, strong hydrophobic interactions and hydrogen bonds are crucial. They could improve the stability of chemical binding to receptors. Polar bonds were established in between the two oxygen atoms of the hydroxamate oxygen atoms and amino acid Tyr782, As742, and Asp649 residues.

**Table 12: Docking Score of different poses of the compound 62**

Mode	Affinity (kcal/mol)	Dist from Best Mode	
		RMSD L.B.	RMSD U.B.
1	-8.504	0	0
2	-8.411	1.512	2.158
3	-8.251	3.247	5.103
4	-8.237	2.322	3.897
5	-8.235	1.942	3.296
6	-8.042	3.669	5.69
7	-7.818	1.541	1.945
8	-7.76	2.962	4.322
9	-7.704	2	3.51
10	-7.678	1.748	3.103
11	-7.588	2.322	3.183
12	-7.515	3.66	4.545
13	-7.492	2.37	4.425
14	-6.923	1.855	4.654
15	-6.84	3.299	4.545
16	-6.807	1.797	3.553
17	-6.34	4.736	8.07
18	-6.074	4.281	8.551
19	-5.604	4.268	8.38
20	-5.389	2.145	3.209

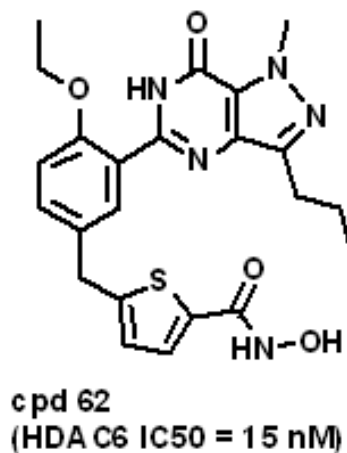


**Figure 23: structure of compound number 62, the most active compound of the dataset**

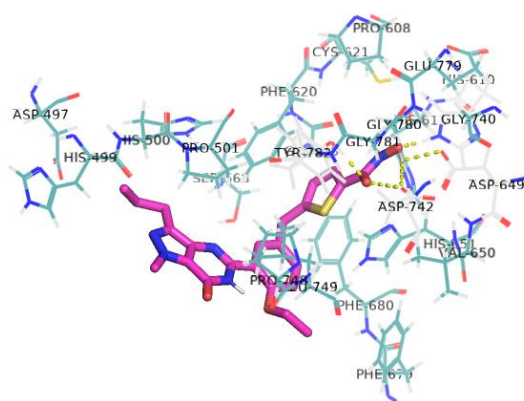


**Figure 24: Best active molecule cpd62 (magenta) interaction with the amino acid residues(light blue) of HDAC6 CD2. The polar contacts are showed with dotted yellow lines.**

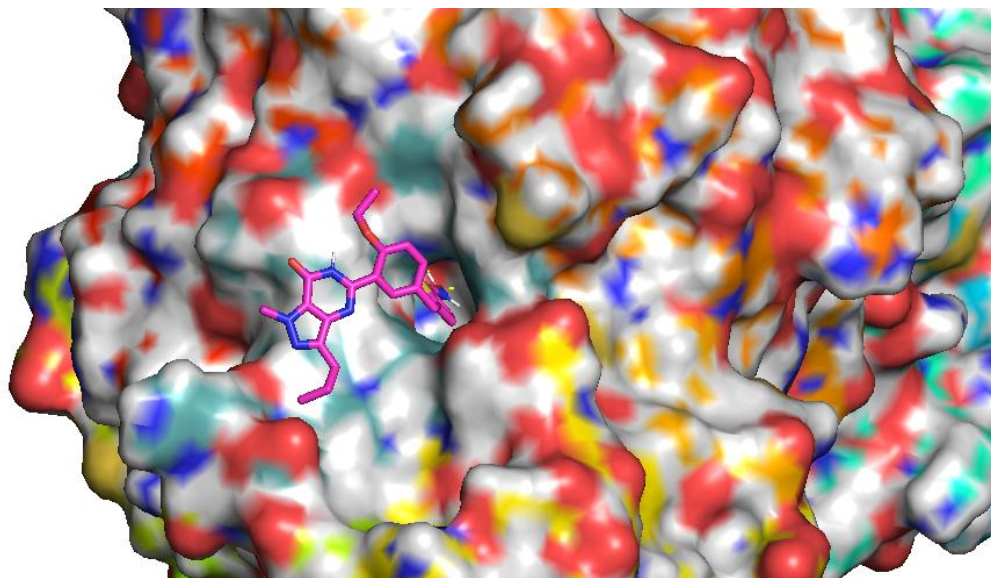


**Figure 25: Compound 62 in the binding pocket of HDAC6 CD2**

#### **6.1.7 Molecular Dynamics Simulation**

The protein RMSD (Figure 26, 27) values provide information about the structural conformation of the protein throughout the simulation, whereas the ligand RMSD values suggest that the ligand is more stable than the protein. The simulation system's improved stability was evidenced by the lower RMSD values. The 100 ns MD simulation was done to observe the stability of the protein-ligand complex stability. As observed from the graph of Figure 32, the system converged after 40 ns. The RMSD of the compound 62 fluctuates around 1 nm and that of the protein backbone around 0.8 nm. At 65 ns the RMSD of the protein backbone increases but then comes back at 80 ns. This phenomenon indicates the compound 62 (Figure 23) flips and goes out of the active site but then comes back again and stabilised.

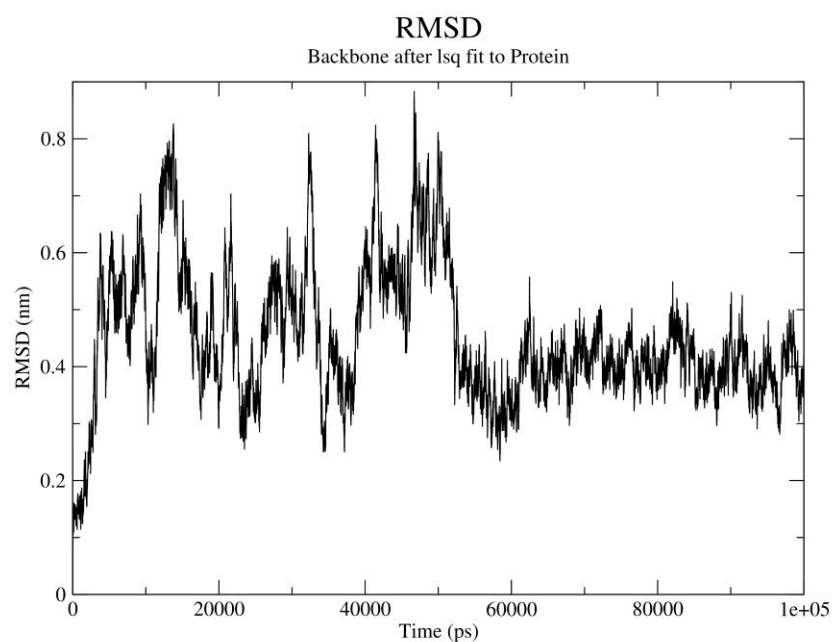


**Figure 26: RMSD of the ligand of the MD simulation of compound 62 with HDAC6**

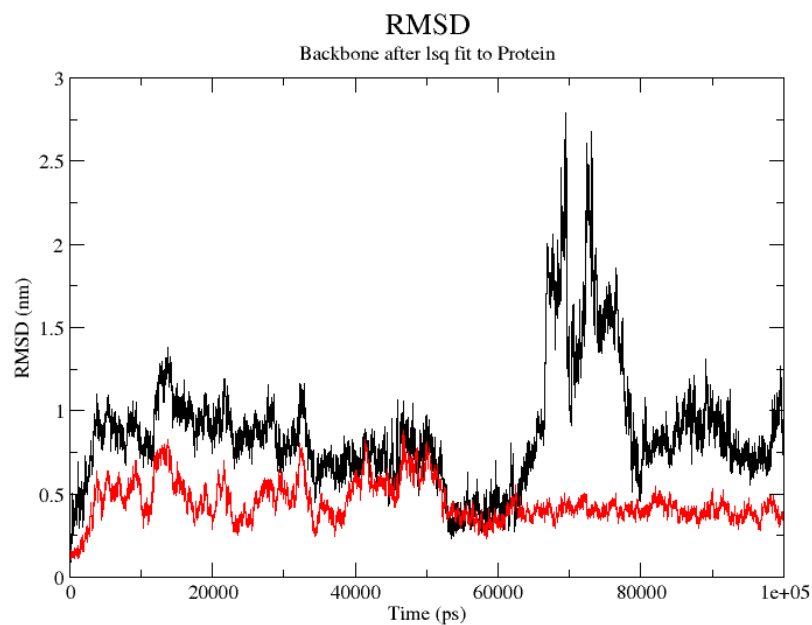


**Figure 27: RMSD of protein backbone shown in red colour while RMSD of the ligand (compound 62) is shown in black colour.**

## **Chapter 7: Conclusion & Future Aspects**



## **7.1 Conclusion:**

The molecular docking and MD simulations studies further supported the stability of the HDAC6 inhibitor of the dataset. Certain structural features that were highlighted through the QSAR/SAR models were present in the compound of the dataset. Good fingerprints obtained through the Bayesian model like G12, G13, G14, G15, G16, and G17 were present in highly active compounds of the dataset; for example compound numbers 62, 63, 66 and 72 with HDAC6 *IC*<sub>50</sub> values of 15, 192, 37, and 98 respectively. The same structural features like the presence of sulphur atom and thiophene with hydroxamic acid also validated by the presence of 2-Thiophenehydroxamic acid in the SARpy active rule set. The Recursive partitioning model came up with the hydroxamate group and aromatic ring as good features, further stressing on the importance of the hydroxamate group as a good ZBG and presence of the bulky aromatic linkers. Presence of bulky linkers such as substituted phenyl and benzene groups were also validated through LDA study, fingerprint KRFP4521, and KRFP3104 (3-phenylpropanal and cyclohexylbenzene respectively). The SARpy model pointed out the presence of piperazine in its active ruleset, in compound like 43 the presence of such structural alerts resulted in good inhibition activity (HDAC6 *IC*<sub>50</sub> 19 nM). Docking results showed the binding of the zinc atom with the electronegative oxygen atom of the hydroxamate group. The zinc atom is vital for the activities of zinc metalloprotein such as HDAC6, this interaction of the zinc atom is crucial for the inhibitory activity. In correlation with the ligand based models, the structure based models showed that Oxygen atoms of the hydroxamate group formed polar interactions and the presence of aromatic phenyl ring and heterocyclic aromatic rings like pyrimidine and pyrazole took part in pi-pi stacking interactions. The hydroxamate group and phenyl moiety of the compound interact with key HDAC6 amino acid residues such as His610, Pro748, and Tyr782, and molecular dynamics studies have further shown the interaction of the inhibitor molecule with the HDAC6 protein. These residues have been found by other researchers as key interaction parts of the HDAC6 structures with its inhibitors [5][155].

## **7.2 Future Aspect:**

In this age of artificial intelligence implementation of techniques like advanced machine learning and deep learning models could provide better results in a shorter time. This study helped to find out important structural characteristics of HDAC6 inhibitors that will be helpful in designing anti-cancer therapy and in neurodegenerative diseases. Further studies like the QM/MM model of MD studies would provide with better explanation of the inhibitory activity. Using artificial intelligence and modern computational power will cut down the time to search for a lead drug molecule.

## **References:**

- [1] Shi, W. and Chance, M.R., 2008. Metallomics and metalloproteomics. *Cellular and Molecular Life Sciences*, 65, pp.3040-3048.
- [2] Szpunar, J., 2005. Advances in analytical methodology for bioinorganic speciation analysis: metallomics, metalloproteomics and heteroatom-tagged proteomics and metabolomics. *Analyst*, 130(4), pp.442-465.
- [3] Seyfried, T.N. and Huysentruyt, L.C., 2013. On the origin of cancer metastasis. *Critical Reviews™ in Oncogenesis*, 18(1-2).DOI: 10.1615/CritRevOncog.v18.i1-2.40
- [4] Pulya, S., Amin, S.A., Adhikari, N., Biswas, S., Jha, T. and Ghosh, B., 2021. HDAC6 as privileged target in drug discovery: A perspective. *Pharmacological research*, 163, p.105274. DOI 10.1016/j.phrs.2020.105274
- [5] Hai, Y. and Christianson, D.W., 2016. Histone deacetylase 6 structure and molecular basis of catalysis and inhibition. *Nature chemical biology*, 12(9), pp.741-747
- [6] Rabal, O., Sánchez-Arias, J.A., Cuadrado-Tejedor, M., de Miguel, I., Pérez-González, M., García-Barroso, C., Ugarte, A., de Mendoza, A.E.H., Sáez, E., Espelosin, M. and Ursua, S., 2018. Design, synthesis, biological evaluation and in vivo testing of dual phosphodiesterase 5 (PDE5) and histone deacetylase 6 (HDAC6)-selective inhibitors for the treatment of Alzheimer's disease. *European Journal of Medicinal Chemistry*, 150, pp.506-524.
- [7] Amin, A., Adhikari, N., Bhargava, S., Jha, T. and Gayen, S., 2017. Designing potential antitrypanosomal thiazol-2-ethylamines through predictive regression based and classification based QSAR analyses. *Current Drug Discovery Technologies*, 14(1), pp.39-52.
- [8] Zhang, G. and Pradhan, S., 2014. Mammalian epigenetic mechanisms. *IUBMB life*, 66(4), pp.240-256. DOI 10.1002/iub.1264
- [9] Moore, L.D., Le, T. and Fan, G., 2013. DNA methylation and its basic function. *Neuropsychopharmacology*, 38(1), pp.23-38.

- [10] Miyake, Y., Keusch, J.J., Wang, L., Saito, M., Hess, D., Wang, X., Melancon, B.J., Helquist, P., Gut, H. and Matthias, P., 2016. Structural insights into HDAC6 tubulin deacetylation and its selective inhibition. *Nature chemical biology*, 12(9), pp.748-754. DOI 10.1038/nchembio.2140
- [11] Batchu, S.N., Brijmohan, A.S. and Advani, A., 2016. The therapeutic hope for HDAC6 inhibitors in malignancy and chronic disease. *Clinical science*, 130(12), pp.987-1003. DOI 10.1042/CS20160084
- [12] Zhang, Y., Gilquin, B., Khochbin, S. and Matthias, P., 2006. Two catalytic domains are required for protein deacetylation. *Journal of Biological Chemistry*, 281(5), pp.2401-2404. DOI 10.1074/jbc.C500241200
- [13] Zou, H., Wu, Y., Navre, M. and Sang, B.C., 2006. Characterization of the two catalytic domains in histone deacetylase 6. *Biochemical and biophysical research communications*, 341(1), pp.45-50. DOI 10.1016/j.bbrc.2005.12.144
- [14] Williams, K.A., Zhang, M., Xiang, S., Hu, C., Wu, J.Y., Zhang, S., Ryan, M., Cox, A.D., Der, C.J., Fang, B. and Koomen, J., 2013. Extracellular signal-regulated kinase (ERK) phosphorylates histone deacetylase 6 (HDAC6) at serine 1035 to stimulate cell migration. *Journal of Biological Chemistry*, 288(46), pp.33156-33170. DOI 10.1074/jbc.M113.472506
- [15] Liu, Y., Peng, L., Seto, E., Huang, S. and Qiu, Y., 2012. Modulation of histone deacetylase 6 (HDAC6) nuclear import and tubulin deacetylase activity through acetylation. *Journal of Biological Chemistry*, 287(34), pp.29168-29174. DOI 10.1074/jbc.M112.371120
- [16] Bertos, N.R., Gilquin, B., Chan, G.K., Yen, T.J., Khochbin, S. and Yang, X.J., 2004. Role of the tetradecapeptide repeat domain of human histone deacetylase 6 in cytoplasmic retention. *Journal of Biological Chemistry*, 279(46), pp.48246-48254. DOI 10.1074/jbc.M408583200
- [17] Watabe, M. and Nakaki, T., 2011. Protein kinase CK2 regulates the formation and clearance of aggresomes in response to stress. *Journal of cell science*, 124(9), pp.1519-1532. DOI 10.1242/jcs.081778

- [18] Zhang, M., Xiang, S., Joo, H.Y., Wang, L., Williams, K.A., Liu, W., Hu, C., Tong, D., Haakenson, J., Wang, C. and Zhang, S., 2014. HDAC6 deacetylates and ubiquitinates MSH2 to maintain proper levels of MutS $\alpha$ . *Molecular cell*, 55(1), pp.31-46. DOI 10.1016/j.molcel.2014.04.028
- [19] Lee, D.H., Won, H.R., Ryu, H.W., Han, J.M. and Kwon, S.H., 2018. The HDAC6 inhibitor ACY-1215 enhances the anticancer activity of oxaliplatin in colorectal cancer cells. *International journal of oncology*, 53(2), pp.844-854. DOI 10.3892/ijo.2018.4405
- [20] Lv, Z., Weng, X., Du, C., Zhang, C., Xiao, H., Cai, X., Ye, S., Cheng, J., Ding, C., Xie, H. and Zhou, L., 2016. Downregulation of HDAC6 promotes angiogenesis in hepatocellular carcinoma cells and predicts poor prognosis in liver transplantation patients. *Molecular carcinogenesis*, 55(5), pp.1024-1033. DOI 10.1002/mc.22345
- [21] Ding, G., Liu, H.D., Huang, Q., Liang, H.X., Ding, Z.H., Liao, Z.J. and Huang, G., 2013. HDAC6 promotes hepatocellular carcinoma progression by inhibiting P53 transcriptional activity. *FEBS letters*, 587(7), pp.880-886. DOI 10.1016/j.febslet.2013.02.001
- [22] Chang, Y.W., Tseng, C.F., Wang, M.Y., Chang, W.C., Lee, C.C., Chen, L.T., Hung, M.C. and Su, J.L., 2016. Deacetylation of HSPA5 by HDAC6 leads to GP78-mediated HSPA5 ubiquitination at K447 and suppresses metastasis of breast cancer. *Oncogene*, 35(12), pp.1517-1528. DOI 10.1038/onc.2015.214
- [23] Saji, S., Kawakami, M., Hayashi, S.I., Yoshida, N., Hirose, M., Horiguchi, S.I., Itoh, A., Funata, N., Schreiber, S.L., Yoshida, M. and Toi, M., 2005. Significance of HDAC6 regulation via estrogen signaling for cell motility and prognosis in estrogen receptor-positive breast cancer. *Oncogene*, 24(28), pp.4531-4539.
- [24] Chen, P.B., Hung, J.H., Hickman, T.L., Coles, A.H., Carey, J.F., Weng, Z., Chu, F. and Fazzio, T.G., 2013. Hdac6 regulates Tip60-p400 function in stem cells. *Elife*, 2, p.e01557. DOI: 10.7554/eLife.01557
- [25] Mak, A.B., Nixon, A.M., Kittanakom, S., Stewart, J.M., Chen, G.I., Curak, J., Gingras, A.C., Mazitschek, R., Neel, B.G., Stagljar, I. and Moffat, J., 2012. Regulation of CD133 by

HDAC6 promotes  $\beta$ -catenin signaling to suppress cancer cell differentiation. *Cell reports*, 2(4), pp.951-963.DOI10.1016/j.celrep.2012.09.016

[26] Li, L., Fang, R., Liu, B., Shi, H., Wang, Y., Zhang, W., Zhang, X. and Ye, L., 2016. Deacetylation of tumor-suppressor MST1 in Hippo pathway induces its degradation through HBXIP-elevated HDAC6 in promotion of breast cancer growth. *Oncogene*, 35(31), pp.4048-4057.DOI 10.1038/onc.2015.476

[27] Li, L., Fang, R., Liu, B., Shi, H., Wang, Y., Zhang, W., Zhang, X. and Ye, L., 2016. Deacetylation of tumor-suppressor MST1 in Hippo pathway induces its degradation through HBXIP-elevated HDAC6 in promotion of breast cancer growth. *Oncogene*, 35(31), pp.4048-4057.DOI 10.1038/onc.2015.476

[28] Yang, F., Wang, F., Liu, Y., Wang, S., Li, X., Huang, Y., Xia, Y. and Cao, C., 2018. Sulforaphane induces autophagy by inhibition of HDAC6-mediated PTEN activation in triple negative breast cancer cells. *Life Sciences*, 213, pp.149-157.DOI 10.1016/j.lfs.2018.10.034

[29] Hsieh, T.H., Tsai, C.F., Hsu, C.Y., Kuo, P.L., Lee, J.N., Chai, C.Y., Wang, S.C. and Tsai, E.M., 2012. Phthalates induce proliferation and invasiveness of estrogen receptor-negative breast cancer through the AhR/HDAC6/c-Myc signaling pathway. *The FASEB Journal*, 26(2), pp.778-787. DOI 10.1096/fj.11-191742

[30] Hsieh, Y.L., Tu, H.J., Pan, S.L., Liou, J.P. and Yang, C.R., 2019. Anti-metastatic activity of MPT0G211, a novel HDAC6 inhibitor, in human breast cancer cells in vitro and in vivo. *Biochimica et Biophysica Acta (BBA)-Molecular Cell Research*, 1866(6), pp.992-1003.DOI 10.1016/j.bbamcr.2019.03.003

[31] Li, Z.Y., Zhang, C., Zhang, Y., Chen, L., Chen, B.D., Li, Q.Z., Zhang, X.J. and Li, W.P., 2017. A novel HDAC6 inhibitor Tubastatin A: Controls HDAC6-p97/VCP-mediated ubiquitination-autophagy turnover and reverses Temozolomide-induced ER stress-tolerance in GBM cells. *Cancer letters*, 391, pp.89-99.DOI 10.1016/j.canlet.2017.01.025

[32] Gradilone, S.A., Radtke, B.N., Bogert, P.S., Huang, B.Q., Gajdos, G.B. and LaRusso, N.F., 2013. HDAC6 inhibition restores ciliary expression and decreases tumor growth. *Cancer research*, 73(7), pp.2259-2270.DOI 10.1158/0008-5472.CAN-12-2938

- [33] Dai, H.Y., Chang, L.S., Yang, S.F., Wang, S.N., Su, S.J. and Yeh, Y.T., 2023. HDAC6 promotes aggressive development of liver cancer by improving egfr mRNA stability. *Neoplasia* (New York, NY), 35.DOI doi.org/10.1016/j.neo.2022.100845
- [34] Deskin, B., Lasky, J., Zhuang, Y. and Shan, B., 2016. Requirement of HDAC6 for activation of Notch1 by TGF- $\beta$ 1. *Scientific Reports*, 6(1), p.31086.DOI 10.1038/srep31086
- [35] Wang, L., Xiang, S., Williams, K.A., Dong, H., Bai, W., Nicosia, S.V., Khochbin, S., Bepler, G. and Zhang, X., 2012. Depletion of HDAC6 enhances cisplatin-induced DNA damage and apoptosis in non-small cell lung cancer cells.DOI 10.1371/journal.pone.0044265
- [36] Yang, M.H., Laurent, G., Bause, A.S., Spang, R., German, N., Haigis, M.C. and Haigis, K.M., 2013. HDAC6 and SIRT2 regulate the acetylation state and oncogenic activity of mutant K-RAS. *Molecular Cancer Research*, 11(9), pp.1072-1077.1-7786.MCR-13-0040-TDOI 10.1158/1541-7786.MCR-13-0040-T
- [37] Hackanson, B., Rimmele, L., Benkíßer, M., Abdelkarim, M., Fliegeauf, M., Jung, M. and Lübbert, M., 2012. HDAC6 as a target for antileukemic drugs in acute myeloid leukemia. *Leukemia research*, 36(8), pp.1055-1062.DOI 10.1016/j.leukres.2012.02.026
- [38] Asthana, J., Kapoor, S., Mohan, R. and Panda, D., 2013. Inhibition of HDAC6 deacetylase activity increases its binding with microtubules and suppresses microtubule dynamic instability in MCF-7 cells. *Journal of Biological Chemistry*, 288(31), pp.22516-22526.DOI 10.1074/jbc.M113.489328
- [39] Hsieh, T.H., Hsu, C.Y., Wu, C.W., Wang, S.H., Yeh, C.H., Cheng, K.H. and Tsai, E.M., 2023. Vorinostat decrease M2 macrophage polarization through ARID1A6488delG/HDAC6/IL-10 signaling pathway in endometriosis-associated ovarian carcinoma. *Biomedicine & Pharmacotherapy*, 161, p.114500.DOI 10.1016/j.biopha.2023.114500
- [40] Fukumoto, T., Fatkhutdinov, N., Zundell, J.A., Tcyganov, E.N., Nacarelli, T., Karakashev, S., Wu, S., Liu, Q., Gabrilovich, D.I. and Zhang, R., 2019. HDAC6 inhibition synergizes with anti-PD-L1 therapy in ARID1A-inactivated ovarian cancer. *Cancer research*, 79(21), pp.5482-5489.DOI 10.1158/0008-5472.CAN-19-1302

- [41] Wang, Z., Hu, P., Tang, F., Lian, H., Chen, X., Zhang, Y., He, X., Liu, W. and Xie, C., 2016. HDAC6 promotes cell proliferation and confers resistance to temozolomide in glioblastoma. *Cancer letters*, 379(1), pp.134-142.DOI 10.1016/j.canlet.2016.06.001
- [42] Cao, J., Lv, W., Wang, L., Xu, J., Yuan, P., Huang, S., He, Z. and Hu, J., 2018. Ricolinostat (ACY-1215) suppresses proliferation and promotes apoptosis in esophageal squamous cell carcinoma via miR-30d/PI3K/AKT/mTOR and ERK pathways. *Cell death & disease*, 9(8), p.817.DOI 10.1038/s41419-018-0788-2
- [43] Liu, J.R., Yu, C.W., Hung, P.Y., Hsin, L.W. and Chern, J.W., 2019. High-selective HDAC6 inhibitor promotes HDAC6 degradation following autophagy modulation and enhanced antitumor immunity in glioblastoma. *Biochemical pharmacology*, 163, pp.458-471.DOI 10.1016/j.bcp.2019.03.023
- [44] Munoz, J.L., Rodriguez-Cruz, V., Greco, S.J., Ramkissoon, S.H., Ligon, K.L. and Rameshwar, P., 2014. Temozolomide resistance in glioblastoma cells occurs partly through epidermal growth factor receptor-mediated induction of connexin 43. *Cell death & disease*, 5(3), pp.e1145-e1145.DOI 10.1038/cddis.2014.111
- [45] Li, Z.Y., Zhang, C., Zhang, Y., Chen, L., Chen, B.D., Li, Q.Z., Zhang, X.J. and Li, W.P., 2017. A novel HDAC6 inhibitor Tubastatin A: Controls HDAC6-p97/VCP-mediated ubiquitination-autophagy turnover and reverses Temozolomide-induced ER stress-tolerance in GBM cells. *Cancer letters*, 391, pp.89-99.DOI 10.1016/j.canlet.2017.01.025
- [46] Subramanian, C., Jarzembowski, J.A., Opiari Jr, A.W., Castle, V.P. and Kwok, R.P., 2011. HDAC6 deacetylates Ku70 and regulates Ku70-Bax binding in neuroblastoma. *Neoplasia*, 13(8), pp.726-734.DOI 10.1593/neo.11558
- [47] Cao, J., Lv, W., Wang, L., Xu, J., Yuan, P., Huang, S., He, Z. and Hu, J., 2018. Ricolinostat (ACY-1215) suppresses proliferation and promotes apoptosis in esophageal squamous cell carcinoma via miR-30d/PI3K/AKT/mTOR and ERK pathways. *Cell death & disease*, 9(8), p.817.DOI 10.1038/s41419-018-0788-2



- [48] Wang, Z., Tang, F., Hu, P., Wang, Y., Gong, J., Sun, S. and Xie, C., 2016. HDAC6 promotes cell proliferation and confers resistance to gefitinib in lung adenocarcinoma. *Oncology reports*, 36(1), pp.589-597.DOI 10.3892/or.2016.4811
- [49] Lwin, T., Zhao, X., Cheng, F., Zhang, X., Huang, A., Shah, B., Zhang, Y., Moscinski, L.C., Choi, Y.S., Kozikowski, A.P. and Bradner, J.E., 2013. A microenvironment-mediated c-Myc/miR-548m/HDAC6 amplification loop in non-Hodgkin B cell lymphomas. *The Journal of clinical investigation*, 123(11), pp.4612-4626.DOI 10.1172/JCI64210
- [50] Wu, Y.W., Hsu, K.C., Lee, H.Y., Huang, T.C., Lin, T.E., Chen, Y.L., Sung, T.Y., Liou, J.P., Hwang-Verslues, W.W., Pan, S.L. and HuangFu, W.C., 2018. A novel dual HDAC6 and tubulin inhibitor, MPT0B451, displays anti-tumor ability in human cancer cells in vitro and in vivo. *Frontiers in Pharmacology*, 9, p.205.DOI 10.3389/fphar.2018.00205
- [51] Sarkar, R., Mukherjee, A., Mukherjee, S., Biswas, R., Biswas, J. and Roy, M., 2014. Curcumin augments the efficacy of antitumor drugs used in leukemia by modulation of heat shock proteins via HDAC6. *Journal of Environmental Pathology, Toxicology and Oncology*, 33(3).DOI 10.1615/jenvironpatholtoxicoloncol.2014010913
- [52] Liu, J., Gu, J., Feng, Z., Yang, Y., Zhu, N., Lu, W. and Qi, F., 2016. Both HDAC5 and HDAC6 are required for the proliferation and metastasis of melanoma cells. *Journal of translational medicine*, 14(1), pp.1-13.DOI 10.1186/s12967-015-0753-0
- [53] Santo, L., Hideshima, T., Kung, A.L., Tseng, J.C., Tamang, D., Yang, M., Jarpe, M., van Duzer, J.H., Mazitschek, R., Ogier, W.C. and Cirstea, D., 2012. Preclinical activity, pharmacodynamic, and pharmacokinetic properties of a selective HDAC6 inhibitor, ACY-1215, in combination with bortezomib in multiple myeloma. *Blood, The Journal of the American Society of Hematology*, 119(11), pp.2579-2589.DOI 10.1182/blood-2011-10-387365
- [54] Hideshima, T., Bradner, J.E., Wong, J., Chauhan, D., Richardson, P., Schreiber, S.L. and Anderson, K.C., 2005. Small-molecule inhibition of proteasome and aggresome function induces synergistic antitumor activity in multiple myeloma. *Proceedings of the National Academy of Sciences*, 102(24), pp.8567-8572.DOI 10.1073 pnas.0503221102

- [55] Hideshima, T., Qi, J., Paranal, R.M., Tang, W., Greenberg, E., West, N., Colling, M.E., Estiu, G., Mazitschek, R., Perry, J.A. and Ohguchi, H., 2016. Discovery of selective small-molecule HDAC6 inhibitor for overcoming proteasome inhibitor resistance in multiple myeloma. *Proceedings of the National Academy of Sciences*, 113(46), pp.13162-13167. DOI 10.1073/pnas.1608067113
- [56] New, M., Olzscha, H., Liu, G., Khan, O., Stimson, L., McGouran, J., Kerr, D., Coutts, A., Kessler, B., Middleton, M. and La Thangue, N.B., 2013. A regulatory circuit that involves HR23B and HDAC6 governs the biological response to HDAC inhibitors. *Cell Death & Differentiation*, 20(10), pp.1306-1316. DOI 10.1038/cdd.2013.47
- [57] Wickström, S.A., Masoumi, K.C., Khochbin, S., Fässler, R. and Massoumi, R., 2010. CYLD negatively regulates cell-cycle progression by inactivating HDAC6 and increasing the levels of acetylated tubulin. *The EMBO Journal*, 29(1), pp.131-144. DOI 10.1038/emboj.2009.317
- [58] Rathje, L.S.Z., Nordgren, N., Pettersson, T., Rönnlund, D., Widengren, J., Aspenström, P. and Gad, A.K., 2014. Oncogenes induce a vimentin filament collapse mediated by HDAC6 that is linked to cell stiffness. *Proceedings of the National Academy of Sciences*, 111(4), pp.1515-1520. DOI 1073/pnas.1300238111
- [59] Lee, Y.S., Lim, K.H., Guo, X., Kawaguchi, Y., Gao, Y., Barrientos, T., Ordentlich, P., Wang, X.F., Counter, C.M. and Yao, T.P., 2008. The cytoplasmic deacetylase HDAC6 is required for efficient oncogenic tumorigenesis. *Cancer research*, 68(18), pp.7561-7569. DOI 10.1158/0008-5472.CAN-08-0188
- [60] Sharif, T., Martell, E., Dai, C., Ghassemi-Rad, M.S., Hanes, M.R., Murphy, P.J., Margam, N.N., Parmar, H.B., Giacomantonio, C.A., Duncan, R. and Lee, P.W., 2019. HDAC6 differentially regulates autophagy in stem-like versus differentiated cancer cells. *Autophagy*, 15(4), pp.686-706. DOI 10.1080/15548627.2018.1548547
- [61] Kim, H.J., Nagano, Y., Choi, S.J., Park, S.Y., Kim, H., Yao, T.P. and Lee, J.Y., 2015. HDAC6 maintains mitochondrial connectivity under hypoxic stress by suppressing

MARCH5/MITOL dependent MFN2 degradation. Biochemical and biophysical research communications, 464(4), pp.1235-1240.DOI 10.1016/j.bbrc.2015.07.111

[62] Su, M., Shi, J.J., Yang, Y.P., Li, J., Zhang, Y.L., Chen, J., Hu, L.F. and Liu, C.F., 2011. HDAC6 regulates aggresome-autophagy degradation pathway of  $\alpha$ -synuclein in response to MPP<sup>+</sup>-induced stress. Journal of neurochemistry, 117(1), pp.112-120.DOI 10.1111/j.1471-4159.2011.07180.x

[63] Fan, S.J., Huang, F.I., Liou, J.P. and Yang, C.R., 2018. The novel histone de acetylase 6 inhibitor, MPT0G211, ameliorates tau phosphorylation and cognitive deficits in an Alzheimer's disease model. Cell death & disease, 9(6), p.655.DOI 10.1038/s41419-018-0688-5

[64] Noack, M., Leyk, J. and Richter-Landsberg, C., 2014. HDAC6 inhibition results in tau acetylation and modulates tau phosphorylation and degradation in oligodendrocytes. Glia, 62(4), pp.535-547.DOI 10.1002/glia.22624

[65] Govindarajan, N., Rao, P., Burkhardt, S., Sananbenesi, F., Schlüter, O.M., Bradke, F., Lu, J. and Fischer, A., 2013. Reducing HDAC6 ameliorates cognitive deficits in a mouse model for Alzheimer's disease. EMBO molecular medicine, 5(1), pp.52-63.DOI 10.1002/emmm.201201923

[66] Tapia, M., Wandosell, F. and Garrido, J.J., 2010. Impaired function of HDAC6 slows down axonal growth and interferes with axon initial segment development. PloS one, 5(9), p.e12908.DOI 10.1371/journal.pone.0012908

[67] Choi, H., Kim, H.J., Kim, J., Kim, S., Yang, J., Lee, W., Park, Y., Hyeon, S.J., Lee, D.S., Ryu, H. and Chung, J., 2017. Increased acetylation of Peroxiredoxin1 by HDAC6 inhibition leads to recovery of A $\beta$ -induced impaired axonal transport. Molecular neurodegeneration, 12, pp.1-14.DOI 10.1186/s13024-017-0164-1

[68] Cook, C., Gendron, T.F., Scheffel, K., Carlomagno, Y., Dunmore, J., DeTure, M. and Petrucelli, L., 2012. Loss of HDAC6, a novel CHIP substrate, alleviates abnormal tau accumulation. Human molecular genetics, 21(13), pp.2936-2945. DOI 10.1093/hmg/dds125

- [69] Tsushima, H., Emanuele, M., Polenghi, A., Esposito, A., Vassalli, M., Barberis, A., Difato, F. and Chierigatti, E., 2015. HDAC6 and RhoA are novel players in Abeta-driven disruption of neuronal polarity. *Nature communications*, 6(1), p.7781.DOI 10.1038/ncomms8781
- [70] Balmik, A.A., Sonawane, S.K. and Chinnathambi, S., 2021. The extracellular HDAC6 ZnF UBP domain modulates the actin network and post-translational modifications of Tau. *Cell Communication and Signaling*, 19(1), pp.1-17.DOI 10.1186/s12964-021-00736-9
- [71] Xiong, Y., Zhao, K., Wu, J., Xu, Z., Jin, S. and Zhang, Y.Q., 2013. HDAC6 mutations rescue human tau-induced microtubule defects in *Drosophila*. *Proceedings of the National Academy of Sciences*, 110(12), pp.4604-4609.DOI 10.1073/pnas.1207586110
- [72] d'Ydewalle, C., Krishnan, J., Chiheb, D.M., Van Damme, P., Irobi, J., Kozikowski, A.P., Berghe, P.V., Timmerman, V., Robberecht, W. and Van Den Bosch, L., 2011. HDAC6 inhibitors reverse axonal loss in a mouse model of mutant HSPB1–induced Charcot-Marie-Tooth disease. *Nature medicine*, 17(8), pp.968-974.DOI 10.1038/nm.2396
- [73] Espallergues, J., Teegarden, S.L., Veerakumar, A., Boulden, J., Challis, C., Jochems, J., Chan, M., Petersen, T., Deneris, E., Matthias, P. and Hahn, C.G., 2012. HDAC6 regulates glucocorticoid receptor signaling in serotonin pathways with critical impact on stress resilience. *Journal of Neuroscience*, 32(13), pp.4400-4416.DOI 10.1523/JNEUROSCI.5634-11.2012
- [74] Jochems, J., Boulden, J., Lee, B.G., Blendy, J.A., Jarpe, M., Mazitschek, R., Van Duzer, J.H., Jones, S. and Berton, O., 2014. Antidepressant-like properties of novel HDAC6-selective inhibitors with improved brain bioavailability. *Neuropsychopharmacology*, 39(2), pp.389-400.
- [75] Guthrie, C.R. and Kraemer, B.C., 2011. Proteasome inhibition drives HDAC6-dependent recruitment of tau to aggresomes. *Journal of Molecular Neuroscience*, 45, pp.32-41.DOI 10.1007/s12031-011-9502-x
- [76] Wang, Z., Leng, Y., Wang, J., Liao, H.M., Bergman, J., Leeds, P., Kozikowski, A. and Chuang, D.M., 2016. Tubastatin A, an HDAC6 inhibitor, alleviates stroke-induced brain infarction and functional deficits: potential roles of  $\alpha$ -tubulin acetylation and FGF-21 up-regulation. *Scientific Reports*, 6(1), p.19626.DOI 10.1038/serp19626

- [77] Pinho, B.R., Reis, S.D., Guedes-Dias, P., Leitão-Rocha, A., Quintas, C., Valentão, P., Andrade, P.B., Santos, M.M. and Oliveira, J.M., 2016. Pharmacological modulation of HDAC1 and HDAC6 in vivo in a zebrafish model: therapeutic implications for Parkinson's disease. *Pharmacological Research*, 103, pp.328-339. DOI 10.1016/j.phrs.2015.11.024
- [78] Kee, H.J., Bae, E.H., Park, S., Lee, K.E., Suh, S.H., Kim, S.W. and Jeong, M.H., 2013. HDAC inhibition suppresses cardiac hypertrophy and fibrosis in DOCA-salt hypertensive rats via regulation of HDAC6/HDAC8 enzyme activity. *Kidney and Blood Pressure Research*, 37(4-5), pp.229-239. DOI 10.1159/000350148
- [79] Su, M., Guan, H., Zhang, F., Gao, Y., Teng, X. and Yang, W., 2016. HDAC6 regulates the chaperone-mediated autophagy to prevent oxidative damage in injured neurons after experimental spinal cord injury. *Oxidative Medicine and Cellular Longevity*, 2016. DOI 10.1155/2016/7263736
- [80] Boucherat, O., Chabot, S., Paulin, R., Trinh, I., Bourgeois, A., Potus, F., Lampron, M.C., Lambert, C., Breuils-Bonnet, S., Nadeau, V. and Paradis, R., 2017. HDAC6: a novel histone deacetylase implicated in pulmonary arterial hypertension. *Scientific reports*, 7(1), p.4546. DOI 10.1038/s41598-017-04874-4
- [81] Demos-Davies, K.M., Ferguson, B.S., Cavasin, M.A., Mahaffey, J.H., Williams, S.M., Spiltoir, J.I., Schuetze, K.B., Horn, T.R., Chen, B., Ferrara, C. and Scellini, B., 2014. HDAC6 contributes to pathological responses of heart and skeletal muscle to chronic angiotensin-II signaling. *American Journal of Physiology-Heart and Circulatory Physiology*, 307(2), pp.H252-H258. DOI 10.1152/ajpheart.00149.2014.
- [82] Yang, Y., Ran, J., Liu, M., Li, D., Li, Y., Shi, X., Meng, D., Pan, J., Ou, G., Aneja, R. and Sun, S.C., 2014. CYLD mediates ciliogenesis in multiple organs by deubiquitinating Cep70 and inactivating HDAC6. *Cell Research*, 24(11), pp.1342-1353. DOI 10.1038/cr.2014.136
- [83] Cohen, H.Y., Lavu, S., Bitterman, K.J., Hekking, B., Imahiyerobo, T.A., Miller, C., Frye, R., Ploegh, H., Kessler, B.M. and Sinclair, D.A., 2004. Acetylation of the C terminus of Ku70 by CBP and PCAF controls Bax-mediated apoptosis. *Molecular cell*, 13(5), pp.627-638.

- [84] Boucherat, O., Chabot, S., Paulin, R., Trinh, I., Bourgeois, A., Potus, F., Lampron, M.C., Lambert, C., Breuils-Bonnet, S., Nadeau, V. and Paradis, R., 2017. HDAC6: a novel histone deacetylase implicated in pulmonary arterial hypertension. *Scientific reports*, 7(1), p.4546.DOI:10.1038/s41598-017-04874-4
- [85] Valera, M.S., de Armas-Rillo, L., Barroso-González, J., Ziglio, S., Batisse, J., Dubois, N., Marrero-Hernandez, S., Borel, S., García-Expósito, L., Biard-Piechaczyk, M. and Paillart, J.C., 2015. The HDAC6/APOBEC3G complex regulates HIV-1 infectiveness by inducing Vif autophagic degradation. *Retrovirology*, 12, pp.1-26.DOI 10.1186/s12977-015-0181-5
- [86] Tsujimoto, K., Jo, T., Nagira, D., Konaka, H., Park, J.H., Yoshimura, S.I., Ninomiya, A., Sugihara, F., Hirayama, T., Itotagawa, E. and Matsuzaki, Y., 2023. The lysosomal Ragulator complex activates NLRP3 inflammasome in vivo via HDAC6. *The EMBO Journal*, 42(1), p.e111389.DOI 10.15252/embj.2022111389
- [87] Beurel, E., 2011. HDAC6 regulates LPS-tolerance in astrocytes. *PLoS One*, 6(10), p.e25804.DOI 10.1371/journal.pone.0025804
- [88] Lienlaf, M., Perez-Villarroel, P., Knox, T., Pabon, M., Sahakian, E., Powers, J., Woan, K.V., Lee, C., Cheng, F., Deng, S. and Smalley, K.S.M., 2016. Essential role of HDAC6 in the regulation of PD-L1 in melanoma. *Molecular oncology*, 10(5), pp.735-750.DOI 10.1016/j.molonc.2015.12.012
- [89] Youn, G.S., Lee, K.W., Choi, S.Y. and Park, J., 2016. Overexpression of HDAC6 induces pro-inflammatory responses by regulating ROS-MAPK-NF- $\kappa$ B/AP-1 signaling pathways in macrophages. *Free Radical Biology and Medicine*, 97, pp.14-23.DOI 10.1016/j.freeradbiomed.2016.05.014
- [90] Yan, B., Xie, S., Liu, Z., Ran, J., Li, Y., Wang, J., Yang, Y., Zhou, J., Li, D. and Liu, M., 2014. HDAC6 deacetylase activity is critical for lipopolysaccharide-induced activation of macrophages. *PloS one*, 9(10), p.e110718.DOI 10.1371/journal.pone.0110718
- [91] Woan, K.V., Lienlaf, M., Perez-Villarroel, P., Lee, C., Cheng, F., Knox, T., Woods, D.M., Barrios, K., Powers, J., Sahakian, E. and Wang, H.W., 2015. Targeting histone deacetylase 6

mediates a dual anti-melanoma effect: Enhanced antitumor immunity and impaired cell proliferation. *Molecular oncology*, 9(7), pp.1447-1457.DOI 10.1016/j.molonc.2015.04.002

[92] Núñez-Andrade, N., Iborra, S., Trullo, A., Moreno-Gonzalo, O., Calvo, E., Catalán, E., Menasche, G., Sancho, D., Vázquez, J., Yao, T.P. and Martín-Cófreces, N.B., 2016. HDAC6 regulates the dynamics of lytic granules in cytotoxic T lymphocytes. *Journal of cell science*, 129(7), pp.1305-1311.DOI 10.1242/jcs.180885

[93] Gradilone, S.A., Habringer, S., Masyuk, T.V., Howard, B.N., Masyuk, A.I. and LaRusso, N.F., 2014. HDAC6 is overexpressed in cystic cholangiocytes and its inhibition reduces cystogenesis. *The American journal of pathology*, 184(3), pp.600-608.DOI 10.1016/j.ajpath.2013.11.027

[94] Liu, W., Fan, L.X., Zhou, X., Sweeney Jr, W.E., Avner, E.D. and Li, X., 2012. HDAC6 regulates epidermal growth factor receptor (EGFR) endocytic trafficking and degradation in renal epithelial cells. *PloS one*, 7(11), p.e49418.DOI 10.1371/journal.pone.0049418

[95] Gal, J., Chen, J., Barnett, K.R., Yang, L., Brumley, E. and Zhu, H., 2013. HDAC6 regulates mutant SOD1 aggregation through two SMIR motifs and tubulin acetylation. *Journal of Biological Chemistry*, 288(21), pp.15035-15045.DOI 10.1074/jbc.M112.431957

[96] Sadoul, K., Wang, J., Diagouraga, B., Vitte, A.L., Buchou, T., Rossini, T., Polack, B., Xi, X., Matthias, P. and Khochbin, S., 2012. HDAC6 controls the kinetics of platelet activation. *Blood, The Journal of the American Society of Hematology*, 120(20), pp.4215-4218.DOI 10.1182/blood-2012-05-428011

[97] De Diego, A.S., Alonso Guerrero, A., Martínez-a, C. and Van Wely, K.H., 2014. Dido3-dependent HDAC6 targeting controls cilium size. *Nature communications*, 5(1), p.3500.DOI 10.1038/ncomms4500

[98] Putcha, P., Yu, J., Rodriguez-Barrueco, R., Saucedo-Cuevas, L., Villagrasa, P., Murga-Penas, E., Quayle, S.N., Yang, M., Castro, V., Llobet-Navas, D. and Birnbaum, D., 2015. HDAC6 activity is a non-oncogene addiction hub for inflammatory breast cancers. *Breast Cancer Research*, 17(1), pp.1-14.DOI 10.1186/s13058-015-0658-0

- [99] Leyk, J., Goldbaum, O., Noack, M. and Richter-Landsberg, C., 2015. Inhibition of HDAC6 modifies tau inclusion body formation and impairs autophagic clearance. *Journal of Molecular Neuroscience*, 55, pp.1031-1046.DOI 10.1007/s12031-014-0460-y
- [100] Salemi, L.M., Almawi, A.W., Lefebvre, K.J. and Schild-Poulter, C., 2014. Aggresome formation is regulated by RanBPM through an interaction with HDAC6. *Biology open*, 3(6), pp.418-430.DOI 10.1242/bio.20147021
- [101] Lee, J.Y., Koga, H., Kawaguchi, Y., Tang, W., Wong, E., Gao, Y.S., Pandey, U.B., Kaushik, S., Tresse, E., Lu, J. and Taylor, J.P., 2010. HDAC6 controls autophagosome maturation essential for ubiquitin-selective quality-control autophagy. *The EMBO journal*, 29(5), pp.969-980.DOI 10.1038/emboj.2009.405
- [102] Ryu, H.W., Shin, D.H., Lee, D.H., Choi, J., Han, G., Lee, K.Y. and Kwon, S.H., 2017. HDAC6 deacetylates p53 at lysines 381/382 and differentially coordinates p53-induced apoptosis. *Cancer letters*, 391, pp.162-171.DOI 10.1016/j.canlet.2017.01.033
- [103] Boyault, C., Zhang, Y., Fritah, S., Caron, C., Gilquin, B., Kwon, S.H., Garrido, C., Yao, T.P., Vourc'h, C., Matthias, P. and Khochbin, S., 2007. HDAC6 controls major cell response pathways to cytotoxic accumulation of protein aggregates. *Genes & development*, 21(17), pp.2172-2181.DOI 10.1101/gad.436407
- [104] Boyault, C., Gilquin, B., Zhang, Y., Rybin, V., Garman, E., Meyer-Klaucke, W., Matthias, P., Müller, C.W. and Khochbin, S., 2006. HDAC6-p97/VCP controlled polyubiquitin chain turnover. *The EMBO journal*, 25(14), pp.3357-3366.DOI 10.1038/sj.emboj.7601210
- [105] Fusco, C., Micale, L., Egorov, M., Monti, M., D'Addetta, E.V., Augello, B., Cozzolino, F., Calcagni, A., Fontana, A., Polishchuk, R.S. and Didelot, G., 2012. The E3-ubiquitin ligase TRIM50 interacts with HDAC6 and p62, and promotes the sequestration and clearance of ubiquitinated proteins into the aggresome. *PLoS One*, 7(7), p.e40440.DOI 10.1371/journal.pone.0040440
- [106] Kim, C., Choi, H., Jung, E.S., Lee, W., Oh, S., Jeon, N.L. and Mook-Jung, I., 2012. HDAC6 inhibitor blocks amyloid beta-induced impairment of mitochondrial transport in hippocampal neurons.DOI 10.1371/journal.pone.0042983



- [107] Lafarga, V., Aymerich, I., Tapia, O., Mayor Jr, F. and Penela, P., 2012. A novel GRK2/HDAC6 interaction modulates cell spreading and motility. *The EMBO journal*, 31(4), pp.856-869.DOI 10.1038/emboj.2011.466
- [108] Parmigiani, R.B., Xu, W.S., Venta-Perez, G., Erdjument-Bromage, H., Yaneva, M., Tempst, P. and Marks, P.A., 2008. HDAC6 is a specific deacetylase of peroxiredoxins and is involved in redox regulation. *Proceedings of the National Academy of Sciences*, 105(28), pp.9633-9638DOI 10.1073/pnas.0803749105
- [109] Leng, Y., Wu, Y., Lei, S., Zhou, B., Qiu, Z., Wang, K. and Xia, Z., 2018. Inhibition of HDAC6 activity alleviates myocardial ischemia/reperfusion injury in diabetic rats: potential role of peroxiredoxin 1 acetylation and redox regulation. *Oxidative medicine and cellular longevity*, 2018.DOI 10.1155/2018/9494052
- [110] Pulya, S., Amin, S.A., Adhikari, N., Biswas, S., Jha, T. and Ghosh, B., 2021. HDAC6 as privileged target in drug discovery: A perspective. *Pharmacological research*, 163, p.105274.DOI 10.1016/j.phrs.2020.105274
- [111] Kozlov, M.V., Kleymenova, A.A., Konduktorov, K.A., Malikova, A.Z. and Kochetkov, S.N., 2014. Selective inhibitor of histone deacetylase 6 (tubastatin A) suppresses proliferation of hepatitis C virus replicon in culture of human hepatocytes. *Biochemistry (Moscow)*, 79, pp.637-642.DOI 10.1134/S0006297914070050
- [112] Saito, S., Zhuang, Y., Shan, B., Danchuk, S., Luo, F., Korfei, M., Guenther, A. and Lasky, J.A., 2017. Tubastatin ameliorates pulmonary fibrosis by targeting the TGF $\beta$ -PI3K-Akt pathway. *PLoS One*, 12(10), p.e0186615.DOI 10.1371/journal.pone.0186615 e0186615
- [113] Segretti, M.C., Vallerini, G.P., Brochier, C., Langley, B., Wang, L., Hancock, W.W. and Kozikowski, A.P., 2015. Thiol-based potent and selective HDAC6 inhibitors promote tubulin acetylation and T-regulatory cell suppressive function. *ACS medicinal chemistry letters*, 6(11), pp.1156-1161.DOI 10.1021/acsmedchemlett.5b00303
- [114] Mishima, Y., Santo, L., Eda, H., Cirstea, D., Nemani, N., Yee, A.J., O'Donnell, E., Selig, M.K., Quayle, S.N., Arastu-Kapur, S. and Kirk, C., 2015. Ricolinostat (ACY-1215) induced

inhibition of aggresome formation accelerates carfilzomib-induced multiple myeloma cell death. *British journal of haematology*, 169(3), pp.423-434. DOI 10.1111/bjh.13315

[115] Niesvizky, R., Richardson, P.G., Gabrail, N.Y., Madan, S., Yee, A.J., Quayle, S.N., Almeciga-Pinto, I., Jones, S.S., Houston, L., Hayes, D. and Van Duzer, J., 2015. ACY-241, a novel, HDAC6 selective inhibitor: synergy with immunomodulatory (IMiD®) drugs in multiple myeloma (MM) cells and early clinical results (ACE-MM-200 Study). DOI 10.1182/blood.V126.23.3040.3040

[116] Yee, A.J., Bensinger, W.I., Supko, J.G., Voorhees, P.M., Berdeja, J.G., Richardson, P.G., Libby, E.N., Wallace, E.E., Birrer, N.E., Burke, J.N. and Tamang, D.L., 2016. Ricolinostat plus lenalidomide, and dexamethasone in relapsed or refractory multiple myeloma: a multicentre phase 1b trial. *The Lancet Oncology*, 17(11), pp.1569-1578. DOI 10.1016/S1470-2045(16)30375-8

[117] Krukowski, K., Heijnen, C.J., Golonzhka, O., Gutti, T., Jarpe, M. and Kavelaars, A., 2015. An HDAC6 inhibitor for treatment of chemotherapy-induced peripheral numbness and pain in a mouse model. *Brain, Behavior, and Immunity*, 49, p.e28. DOI 10.1016/j.bbi.2015.06.114

[118] Porter, N.J., Mahendran, A., Breslow, R. and Christianson, D.W., 2017. Unusual zinc-binding mode of HDAC6-selective hydroxamate inhibitors. *Proceedings of the National Academy of Sciences*, 114(51), pp.13459-13464. DOI 10.1073/pnas.1718823114

[119] Yu, C.W., Hung, P.Y., Yang, H.T., Ho, Y.H., Lai, H.Y., Cheng, Y.S. and Chern, J.W., 2018. Quinazolin-2, 4-dione-based hydroxamic acids as selective histone deacetylase-6 inhibitors for treatment of non-small cell lung cancer. *Journal of Medicinal Chemistry*, 62(2), pp.857-874. DOI 10.1021/acs.jmedchem.8b01590

[120] Yu, C.W., Chang, P.T., Hsin, L.W. and Chern, J.W., 2013. Quinazolin-4-one derivatives as selective histone deacetylase-6 inhibitors for the treatment of Alzheimer's disease. *Journal of medicinal chemistry*, 56(17), pp.6775-6791. DOI 10.1021/jm400564j

[121] Chen, X., Chen, X., Steimbach, R.R., Wu, T., Li, H., Dan, W., Shi, P., Cao, C., Li, D., Miller, A.K. and Qiu, Z., 2020. Novel 2, 5-diketopiperazine derivatives as potent selective

histone deacetylase 6 inhibitors: Rational design, synthesis and antiproliferative activity. *European Journal of Medicinal Chemistry*, 187, p.111950. DOI 10.1016/j.ejmech.2019.111950

[122] Lv, W., Zhang, G., Barinka, C., Eubanks, J.H. and Kozikowski, A.P., 2017. Design and synthesis of mercaptoacetamides as potent, selective, and brain permeable histone deacetylase 6 inhibitors. *ACS Medicinal Chemistry Letters*, 8(5), pp.510-515. DOI 10.1021/acsmmedchemlett.7b00012

[123] Tang, G., Wong, J.C., Zhang, W., Wang, Z., Zhang, N., Peng, Z., Zhang, Z., Rong, Y., Li, S., Zhang, M. and Yu, L., 2014. Identification of a novel aminotetralin class of HDAC6 and HDAC8 selective inhibitors. *Journal of medicinal chemistry*, 57(19), pp.8026-8034. DOI 10.1021/jm5008962

[124] Tavares, M.T., Kozikowski, A.P. and Shen, S., 2021. Mercaptoacetamide: A promising zinc-binding group for the discovery of selective histone deacetylase 6 inhibitors. *European journal of medicinal chemistry*, 209, p.112887. DOI 10.1016/j.ejmech.2020.112887

[125] Rabal, Obdulia, Juan A. Sánchez-Arias, Mar Cuadrado-Tejedor, Irene de Miguel, Marta Pérez-González, Carolina García-Barroso, Ana Ugarte et al. "Design, synthesis, and biological evaluation of first-in-class dual acting histone deacetylases (HDACs) and phosphodiesterase 5 (PDE5) inhibitors for the treatment of Alzheimer's disease." *Journal of Medicinal Chemistry* 59, no. 19 (2016): 8967-9004.

[126] Sanchez-Arias, Juan A., Obdulia Rabal, Mar Cuadrado-Tejedor, Irene de Miguel, Marta Perez-Gonzalez, Ana Ugarte, Elena Saez et al. "Impact of scaffold exploration on novel dual-acting histone deacetylases and phosphodiesterase 5 inhibitors for the treatment of Alzheimer's disease." *ACS Chemical Neuroscience* 8, no. 3 (2017): 638-661.

[127] Rabal, Obdulia, Juan A. Sánchez-Arias, Mar Cuadrado-Tejedor, Irene de Miguel, Marta Pérez-González, Carolina García-Barroso, Ana Ugarte et al. "Design, synthesis, biological evaluation and in vivo testing of dual phosphodiesterase 5 (PDE5) and histone deacetylase 6 (HDAC6)-selective inhibitors for the treatment of Alzheimer's disease." *European Journal of Medicinal Chemistry* 150 (2018): 506-524.

[128] Rabal, Obdulia, Juan A. Sánchez-Arias, Mar Cuadrado -Tejedor, Irene de Miguel , Marta Pérez-González, Carolina García-Barroso, Ana Ugarte et al. "Discovery of in vivo chemical probes for treating Alzheimer's disease: dual phosphodiesterase 5 (PDE5) and class I histone deacetylase selective inhibitors." *ACS Chemical Neuroscience* 10, no. 3 (2018): 1765-1782.

[129] Rabal, Obdulia, Juan A. Sánchez-Arias, Mar Cuadrado -Tejedor, Irene de Miguel , Marta Pérez-González, Carolina García-Barroso, Ana Ugarte et al. "Multitarget approach for the treatment of Alzheimer's disease: Inhibition of Phosphodiesterase 9 (PDE9) and Histone Deacetylases (HDACs) covering diverse selectivity profiles." *ACS Chemical Neuroscience* 10, no. 9 (2019): 4076-4101.

[130] Chem 3D Pro Version 8.0 and Chem Draw Ultra Version 8.0 are software programs developed by Cambridge Soft Corporation, U. S. A.

[131] Discovery Studio 3.0, Accelrys Software Inc., San Diego, California, USA, 2011

[132] Yap, Chun Wei. "PaDEL-descriptor: An open source software to calculate molecular descriptors and fingerprints." *Journal of computational chemistry* 32, no. 7 (2011): 1466-1474.

[133] QSAR tools, DTC laboratory, India, 2015; Software available at <https://dtclab.webs.com/software-tools>.

[134] Baderna, Diego, Domenico Gadaleta, Eleonora Lostaglio, Gianluca Selvestrel, Giuseppa Raitano, Azadi Golbamaki, Anna Lombardo, and Emilio Benfenati. "New in silico models to predict in vitro micronucleus induction as marker of genotoxicity." *Journal of hazardous materials* 385 (2020): 121638.

[135] Gini, Giuseppina. "QSAR methods." In *In silico methods for predicting drug toxicity*, pp. 1-20. Humana Press, New York, NY, 2016.

[136] Ferrari, T., D. Cattaneo, G. Gini, N. Golbamaki Bakhtyari, A. Manganaro, and E. Benfenati. "Automatic knowledge extraction from chemical structures: the case of mutagenicity prediction." *SAR and QSAR in Environmental Research* 24, no. 5 (2013): 365-383.

- [137] Adhikari, N., Amin, S.A., Saha, A. *et al.* Exploring *in house* glutamate inhibitors of matrix metalloproteinase-2 through validated robust chemico-biological quantitative approaches. *Struct Chem* **29**, 285–297 (2018)
- [138] Jha, T., N. Adhikari, A. Saha, and S. A. Amin. "Multiple molecular modelling studies on some derivatives and analogues of glutamic acid as matrix metalloproteinase-2 inhibitors." *SAR and QSAR in Environmental Research* 29, no. 1 (2018): 43-68.
- [139] Banerjee, S., S. A. Amin, S. K. Baidya, N. Adhikari, and T. Jha. "Exploring the structural aspects of ureido-amino acid-based APN inhibitors: a validated comparative multi-QSAR modelling study." *SAR and QSAR in Environmental Research* 31, no. 5 (2020): 325-345.
- [140] Pérez-Garrido, Alfonso, Aliuska Morales Helguera, Fernanda Borges, M. Natália DS Cordeiro, Virginia Rivero, and Amalio Garrido Escudero. "Two new parameters based on distances in a receiver operating characteristic chart for the selection of classification models." *Journal of chemical information and modeling* 51, no. 10 (2011): 2746-2759.
- [141] Amin, Sk Abdul, Nilanjan Adhikari, Shovanlal Gayen, and Tarun Jha. "First report on the validated classification-based chemometric modeling of human rhinovirus 3C Protease (HRV3Cpro) inhibitors." *International Journal of Quantitative Structure-Property Relationships (IJQSPR)* 3, no. 2 (2018): 1-20.
- [142] Das, Rudra Narayan, and Kunal Roy. "Predictive in silico modeling of ionic liquids toward inhibition of the acetyl cholinesterase enzyme of *Electrophorus electricus*: a predictive toxicology approach." *Industrial & Engineering Chemistry Research* 53, no. 2 (2014): 1020-1032.
- [143] Amin, S.A., Adhikari, N. and Jha, T., 2020. Exploration of histone deacetylase 8 inhibitors through classification QSAR study: Part II. *Journal of Molecular Structure*, 1204, p.127529.
- [144] Stote, R. H.; Karplus, M. Zinc binding in proteins and solution: a simple but accurate nonbonded representation. *Proteins: Struct., Funct., Bioinf.* 1995, 23, 12–31.
- [145] Laitaoja, M.; Valjakka, J.; Jänis, J. Zinc Coordination Spheres in Protein Structures. *Inorg. Chem.* 2013, 52, 10983– 10991.

- [146] Huey, R.; Morris, G. M.; Olson, A. J.; Goodsell, D. S. A semiempirical free energy force field with charge-based desolvation. *J. Comput. Chem.* 2007, 28, 1145–1152.
- [147] Hansson, T., Oostenbrink, C. and van Gunsteren, W., 2002. Molecular dynamics simulations. *Current opinion in structural biology*, 12(2), pp.190-196. DOI 10.1016/S0959-440X(02)00308-1
- [148] Hollingsworth, S.A. and Dror, R.O., 2018. Molecular dynamics simulation for all. *Neuron*, 99(6), pp.1129-1143. DOI 10.1016/j.neuron.2018.08.011
- [149] Sargsyan, K., Grauffel, C. and Lim, C., 2017. How molecular size impacts RMSD applications in molecular dynamics simulations. *Journal of chemical theory and computation*, 13(4), pp.1518-1524. DOI 10.1021/acs.jctc.7b00028
- [150] Genheden, S. and Ryde, U., 2015. The MM/PBSA and MM/GBSA methods to estimate ligand-binding affinities. *Expert opinion on drug discovery*, 10(5), pp.449-461. DOI 10.1517/17460441.2015.1032936
- [151] Huang, J. and MacKerell Jr, A.D., 2013. CHARMM36 all-atom additive protein force field: Validation based on comparison to NMR data. *Journal of computational chemistry*, 34(25), pp.2135-2145. DOI 10.1002/jcc.23354
- [152] Humphrey, W., Dalke, A. and Schulten, K., 1996. VMD: visual molecular dynamics. *Journal of molecular graphics*, 14(1), pp.33-38.
- [153] Sixto-López, Y., Bello, M., Rodríguez-Fonseca, R.A., Rosales-Hernández, M.C., Martínez-Archundia, M., Gómez-Vidal, J.A. and Correa-Basurto, J., 2017. Searching the conformational complexity and binding properties of HDAC6 through docking and molecular dynamic simulations. *Journal of Biomolecular Structure and Dynamics*, 35(13), pp.2794-2814.
- [154] Wang, L., Chen, L., Liu, Z., Zheng, M., Gu, Q. and Xu, J., 2014. Predicting mTOR inhibitors with a classifier using recursive partitioning and naive Bayesian approaches. *PLoS One*, 9(5), p.e95221.

[155] Chen, L., Li, Y., Zhao, Q., Peng, H. and Hou, T., 2011. ADME evaluation in drug discovery. 10. Predictions of P-glycoprotein inhibitors using recursive partitioning and naive Bayesian classification techniques. *Molecular Pharmaceutics*, 8(3), pp.889-900.

[156] PDB DOI: <https://doi.org/10.2210/pdb5EDU/pdb>